Development and Characterization of Termite Mound Clay Reinforced HDPE Composite Under Low Strain Rate

By

Hintsa Gebreabezgi Gebremeskel

Under the Guidance of Dr Shishay Amare (PhD.)

A Thesis Submitted for the Requirements of Partial Fulfilment of the Master of Science Degree in Materials Science and Engineering

Faculty of Mechanical and Industrial Engineering

Ethiopian Institute of Technology – Mekelle

Mekelle University

Feb 2026.

Approval of Thesis Acceptance

This is issued to approve that *Hintsa Geberabezgi Geberemeskel* has included all the comments and feedback provided by both the internal and external examiners, as well as the chairperson, during the thesis defense.

Members of the Examination Board

Mr. Redae Alemayoh		March 17/2026
Chairman Name	Signature	Date
Dr. Alula Gebresas		March 10/2026
Internal Examiner Name	Signature	Date
Dr. Desalegn Wogaso		March 10/2026
External Examiner Name	Signature	Date

Confirmation

Head of the Postgraduate and Research Office

Fana Filli		29/04/2026
Head Name	Signature	Date

Faculty of Mechanical and Industrial Engineering (FoMIE)

ሚካኤለ ገ/ኢየሱስ (ዶ/ር) የሜካኒካልና ኢንዱስትሪያል ምህንድስና ፋካሊቲ ገላፊ Michael G/yesus (PhD) Head Faculty of Mechanical & Industrial Engineering	for	29/04/2026
Dean Name	Signature	Date

የኢትዮጵያ ቴክኖሎጂ ኢንስቲትዩት-መቐለ
የሜካኒካልና ኢንዱስትሪያል ምህንድስና ፋካሊቲ
* Ethiopian Institute of Technology-Mekelle *
Faculty of Mechanical & Industrial Engineering

DECLARATION

I, Hintsa Gebreabezgi Gebremeskel, declare that this written submission represents my ideas in my own words and where others' ideas have been included; I have adequately cited and referenced the sources. I also assure that I have never adhered to all principles of academic honesty and integrity and have not misrepresented or fabricated any ideas in my submission. I understand that disciplinary action can be taken if any violation of the above happens.

Candidate: Hintsa Gebreabezgi Gebremeskel

Signature: _____ Date: 17/03/2026

ADVISOR'S DECLARATION

As an advisor, and to the best of my knowledge, this is to assure that the above declaration made by the candidate is correct. Therefore, as per the requirements for the award of the MSc in Materials Science and Engineering, this thesis work is complete.

Advisor: Dr. Shishay Amare (PhD)

Signature: _____ Date: 17/03/2026

ABSTRACT

In recent years, composite materials have gained significant attention due to their environmental sustainability, economic efficiency, durability, and enhanced mechanical performance. This study focuses on the development and characterisation of termite mound clay reinforced high-density polyethene (HDPE) composites aimed at improving resistance to low-strain-rate impacts.

Specimens were manufactured according to ASTM standards using a Design of Experiments (DOE) approach. Three variables were considered: plastic weight ratio (90%, 80%, 70%), mixing time (5, 15, 25 minutes), and clay particle size (63–90, 90–125, 125–150 μm). Nine experimental combinations with three replications were produced. Mechanical testing was conducted under low strain rate conditions, with tensile testing performed at 6.67×10^{-3} s^{-1} and flexural testing at 10^{-3} s^{-1} (20 mm/min cross head speed), alongside impact evaluation. Physical properties, including density and water absorption, were also assessed.

The results demonstrated improved mechanical performance, with maximum tensile, flexural, and impact strengths of 22.73 MPa, 90.65 MPa, and 15.67 kJ/m², respectively. The highest density recorded was 1.266 g/cm³, comparable to pure HDPE, while water absorption remained low at 0.28%. Statistical analysis using Minitab 19 indicated that plastic weight ratio significantly influenced flexural strength, whereas other factors showed limited statistical significance. Optimization identified 90% plastic content, approximately 7 minutes mixing time, and 90–125 μm particle size as the best-performing combination. Overall, termite mound clay reinforcement enhanced the physical and mechanical behaviour of recycled HDPE, indicating suitability for applications such as protective soft body Armor.

Keywords: Body Armour, DOE, HDPE, Polymer composite, strain rate, Termite mound clay

ACKNOWLDGEMENT

Above all, I am grateful to the Almighty God for giving me the ability, health and strength for completion of the study.

My gratitude also extends to my thesis advisor Dr. Shishay Amare, for his patience, motivation, interest, and immense knowledge. His guidance helped me throughout the time of research and writing of the thesis. You were devoting much time to reading my work over and over again and gave me a valuable comment, hence I would like to take this opportunity to thank you and let you know I have great respect.

I would also like to acknowledge staff members of the School of Mechanical and Industrial Engineering, especially the manufacturing engineering chair staffs for their valuable comments on my work.

Finally, I would like to express my sincere gratitude to my husband for his constant support, patience, and encouragement throughout my study. His understanding and motivation gave the strength to overcome challenges and successfully complete this work. And my family Thank you so much.

TABLE OF CONTENTS

List of Figures

List of Tables

CHAPTER-1

INTRODUCTION

1.1 Background and justification

Currently, thermoplastic matrix composites are widely selected for applications that require toughness, lightweight characteristics, and impact resistance. Compared to conventional engineering materials such as metals and alloys, polymer-based composites offer several advantages, including corrosion resistance, chemical stability, reduced weight, and relatively lower manufacturing cost. Metals and alloys often face limitations in achieving a good combination of toughness, corrosion resistance, chemical resistance, and high-temperature performance, and they may require expensive processing techniques. As a result, interest in composite materials has significantly increased due to their wide range of applications in construction, industrial components, military systems, spacecraft, automotive parts, packaging, and biomedical devices, mainly because of their excellent thermo-mechanical properties. (Sultana et al., 2013).

A composite material can be defined as a mixture of two or more physically distinct and mechanically separable materials combined in such a way that the dispersion of one material into another is controlled to achieve improved or optimised properties. The constituents retain their individual characteristics, but the resulting material exhibits enhanced mechanical, physical, or thermal performance compared to the individual components. Composites can be classified based on the size and shape of reinforcement (particulate, flake, and fibre) or based on the type of matrix phase (metal, ceramic, or polymer). Among these, polymer matrix composites are particularly attractive due to their ease of processing, low density, good impact resistance, and versatility.

In recent years, sustainability and environmental protection have become critical factors in material development. The increasing accumulation of plastic waste, especially polyethene-based materials, has created serious environmental challenges due to their non-biodegradable nature and long degradation time. Recycling thermoplastic polymers such as high-density polyethene (HDPE)

provides an effective strategy to reduce environmental pollution, conserve natural resources, and lower energy consumption compared to virgin polymer production (Hopewell et al., 2009). Therefore, utilizing recycled HDPE in composite development contributes directly to circular economy principles and sustainable material engineering.

Furthermore, the incorporation of naturally available fillers or mineral reinforcements into polymer matrices has gained attention as an environmentally friendly and cost-effective approach. Natural mineral fillers reduce reliance on synthetic reinforcements, decrease overall material cost, and improve stiffness and mechanical strength. (Pickering et al., 2016). Termite mound clay, a naturally occurring and locally available material, possesses a compact microstructure and mineral-rich composition. Its utilization as reinforcement not only adds value to locally sourced materials but also promotes sustainable resource utilisation.

The development of termite mound clay-reinforced HDPE composite, therefore, aligns with sustainable engineering objectives by combining recycled thermoplastic waste with naturally available clay reinforcement. This approach reduces environmental impact, promotes waste recycling, lowers production costs, and enhances material performance.

Characterization of the developed composite in terms of density, water absorption, tensile strength, flexural strength, and impact resistance is essential to evaluate its suitability for engineering applications. Through systematic development and characterisation, this study aims to contribute to sustainable composite material development while improving the physical and mechanical performance of HDPE-based systems.

1.2 Statement of the Problem

Conventional protective materials such as ceramics and metals are widely used in impact-resistant applications; however, their high density and weight significantly reduce mobility, flexibility, and comfort. (Bandaru et al., 2017). Although polymer composites offer improved specific strength and energy absorption with reduced weight, the search for low-cost, sustainable, and locally available reinforcement materials remains an ongoing challenge. At the same time, the growing accumulation of plastic waste, particularly High-Density Polyethene (HDPE), necessitates the development of value-added recycling approaches that align with sustainable material engineering. (Ragaert et al., 2017).

Natural mineral fillers have been investigated as alternatives to synthetic reinforcements due to their environmental compatibility and cost-effectiveness. However, despite the widespread availability and inherent structural stability of termite mound clay, there is limited scientific evidence regarding its effectiveness as a reinforcement in thermoplastic composites. In particular, insufficient research has been conducted to evaluate its influence on the physical and mechanical properties of HDPE under low-strain-rate loading conditions.

Therefore, a clear research gap exists in understanding whether termite mound clay can enhance the impact resistance and overall performance of recycled HDPE composites. This study addresses this gap by developing and characterizing termite mound clay-reinforced HDPE composite and experimentally investigating its physical properties and mechanical response.

1.3 Objective

1.3.1 General objective

The main objective of this thesis work was to develop and characterize termite mound clay reinforced high-density polyethene composite under low-strain-rate impact.

1.3.2 Specific objective

- Design and implement an appropriate Design of Experiment (DOE) methodology.
- Characterize composite's physical properties.
- Characterize composite's mechanical properties.
- Optimize mix ratio of termite mound clay and HDPE using the Taguchi Method combined with Grey Relational Analysis.

1.4 Significance of the study

By developing termite mound clay reinforced HDPE composites, this study seeks to provide a dual benefit, reducing the environmental burden of plastic waste and enhancing agricultural productivity through improved soil conditions. Additionally, the successful development and characterization of termite mound clay reinforced HDPE composites could lead to more sustainable and cost-effective materials with enhanced impact resistance. This would benefit industries seeking durable materials for applications that experience low strain rate impacts, while also promoting the use of environmentally friendly reinforcement materials.

Furthermore, it aims to create economic opportunities for farmers by using the potential of termite mound clay as a sustainable and profitable resource. This approach aligns with broader goals of environmental sustainability and economic development.

1.5 Scope of the Research

This research focused on the utilization of termite mound clay and High-Density Polyethylene (HDPE) plastic as composite materials. The study aimed to explore the potential of combining

these two materials for improved mechanical and physical properties. The investigation included low strain rate impact tests to evaluate how the composite material made from termite mound soil and HDPE behaved under sudden forces, simulating real-world applications and conditions. A thorough characterization of the physical properties (e.g., density, porosity) and mechanical properties (e.g., tensile strength, compressive strength, impact resistance) of the composite mixtures was conducted. Standard testing methods and protocols were employed to ensure data reliability. The study aimed to identify the optimal proportions of termite mound and HDPE plastic to maximize the desired mechanical properties while minimizing costs, waste, and environmental impact. Various mixture ratios were tested to find the best-performing composite.

1.6 Limitation of the study

The research was conducted in a specific geographic region (TiGrey, Central Zone, Tembien) where termite mounds were prevalent. All experiments were conducted under controlled laboratory conditions, environmental factors like moisture and microbial activities affect both the mechanical and physical properties of termite mound clay which influenced the outcomes of the study. Hence real-world applications exposed materials to varying conditions (e.g., temperature, humidity) that were not accounted for in the research.

The study focused solely on low strain rate impact testing; therefore, the behavior of the composite material under high strain rate impacts or other loading conditions was not evaluated. While various mechanical and physical properties were characterized, the study did not encompass all possible properties (e.g., thermal and chemical resistance), nor did it consider long-term durability under extended exposure to environmental conditions.

Due to limitations in time, funding and resources, the scope of testing was confined to a select range of mixtures and testing conditions, potentially leading to gaps in the overall understanding of composite performance. The effect and behavior of differing concentrations of HDPE plastic within the mixtures were monitored, but may not have fully accounted for all possible variations in proportion, limiting the breadth of optimization strategies derived from the findings.

CHAPTER-2

LITERATURE REVIEW

This chapter provides information related to the subject of this research, as explored by previous researchers. Its purpose is to outline the scope of the study, gather relevant data used in conducting this research, and identify any existing research gaps. Specifically, the chapter covers information on composite materials, the application area of termite mound clay, testing methods and procedures for composites. It also presents detailed information on critical properties that define body armor performance subjected to low strain impact, along with acceptable values based on standards. Additionally, the chapter discusses past studies related to the manufacturing of clay-reinforced composites, detailing their results and step-by-step procedures which serve as benchmarks for achieving the goals of this work.

2.1 What are Composites?

The material produced by combining two or more different property components to achieve a product exhibit more enhanced properties than the individual constituent's is termed as composites. Constituent elements blend on a molecular level, each material in a composite retains its individual physical, chemical, and mechanical characteristics.

A composite typically consists of two primary components as shown in Figure 1: the reinforcement and the matrix (Ngo, 2020).

(a) Reinforcement: This part adds strength and load-bearing capability to the composite. Reinforcement materials, such as fibres or particulates, are usually stronger and stiffer than the matrix. The effectiveness of the reinforcement is often determined by its ability to carry loads and enhance the mechanical performance of the final composite material.
(b) Matrix: The matrix binds the reinforcement materials together and is responsible for distributing loads among them. It also provides environmental protection to the fibers, shielding them from wear, moisture, and other damaging factors. The matrix is typically

less stiff and in terms of strength than the reinforcement but it contributes essential role in maintaining the integrity and shape of the composite structure.

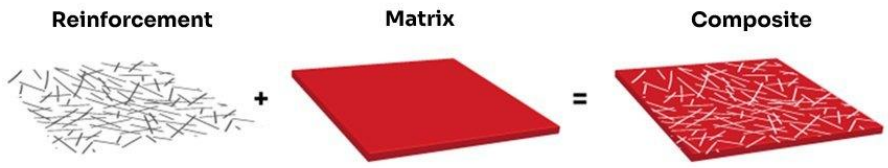

Figure 1 composite constituents (Source: https://romeorim.com/what-are-composites)

Performances of components highly depends on the interaction between the matrix and reinforcement materials. A strong bond at this interface allows for effective load transfer, which is essential for maximizing the composite's strength and overall durability. The combination of these components ensures that composites can be tailored for specific applications, leading to superior performance in various industries, including aerospace, automotive, and construction.

In general, to obtain improved properties of the composite material it mandatory to select the type of matrix, reinforcement and manufacturing. This approach enables engineers to customize materials for various applications, ensuring that they meet specific performance criteria and operational needs.

2.2 Plastic Types, Property and Applications

Synthetic polymers, particularly plastics, stand out as one of the most remarkable innovations of the past century, dramatically influencing various facets of modern life. Since their inception, these versatile materials have rapidly supplanted traditional substances such as metals, glass, natural fibres, and wood across a plethora of applications, fundamentally altering the landscape of daily living and industrial processes. Their production is attributed to several key advantages: low production costs, exceptional thermo-mechanical properties, heightened chemical resistance, and remarkable adaptability to diverse applications.

The properties and characteristics of synthetic polymers derive from a complex interplay of factors, predominantly the nature, quantity, and arrangement of their building blocks, the monomers. This molecular structure allows for the customization of polymers, enabling engineers and scientists to tailor these macromolecules for specific applications and performance requirements. (Callister & Rethwisch, 2020; Young, n.d.). For example, modifications at the molecular level can enhance elasticity, strength, or temperature stability, thereby expanding the utility of these materials.

Given the vast array of synthetic polymers available today, various classifications have been developed to simplify their study and usage by categorizing them into functional subgroups (Callister & Rethwisch, 2020). These classifications (Figure 2) are based on multiple criteria including:

- ✓ **Origin**: This classification differentiates between natural polymers (derived from natural sources) and synthetic ones (manufactured through chemical processes).
- ✓ **Thermal Properties**: Based on their thermal properties polymers can reshaped or not. Polymers which are capable of reshaped and recycled upon heating are termed as thermoplastics, whereas thermoset plastics, which harden permanently after curing hence does not allow recycling or reshaping.
- ✓ **Mechanical Properties**: This includes categorizing polymers based on their tensile strength, elasticity, and durability, which can be influenced by the polymer's chain structure and molecular configuration.
- ✓ **End-use**: Some polymers are designed for specific sectors, including packaging, automotive, medical, and construction industries.
- ✓ **Synthesis**: This reflects the method by which the polymer is created, leading to classifications such as addition or condensation polymers.
- ✓ **Chain Structure**: This encompasses linear, branched, or cross-linked structures that impact the material’s properties.
- ✓ **Molecular Structure and Configuration**: This involves the arrangement of atoms within the polymer and can influence properties such as crystallinity and optical characteristics.

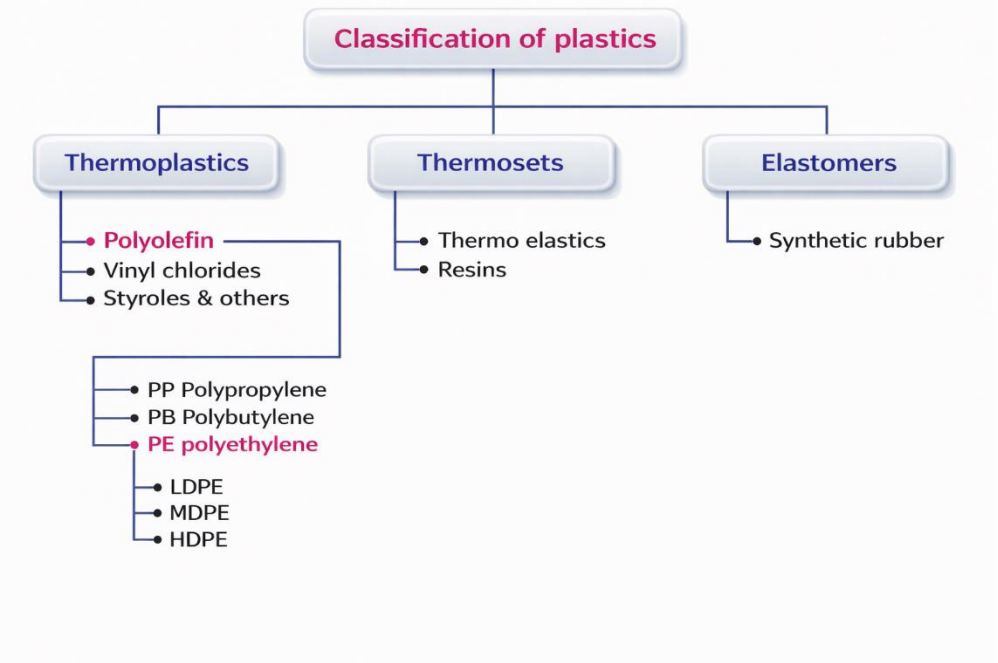

Figure 2 Classification of plastics (Source: researchgate.net)

These classifications encompass a wide variety of materials that find applications across numerous sectors, including packaging, construction, automotive, and consumer goods. Understanding these categories helps in studying their environmental impact and recycling processes, especially as concerns about plastic pollution continue to grow(Erni-Cassola et al., 2019). This article seeks to furnish a comprehensive overview of synthetic polymers and plastics, clarifying their primary types, classifications, applications, and inherent properties. Practical examples underscore their significance across various sectors, illustrating how polymers enhance functionalities and improve product longevity and efficiency.

Furthermore, the research investigates into the processing of polymeric materials, detailing the numerous techniques employed in the formation of plastics. These methods include injection molding, extrusion, and blow molding, each with unique advantages relevant to different applications(Polychronopoulos & Vlachopoulos, 2019).

Moreover, as the sustainability of synthetic materials comes under increasing scrutiny, this study emphasizes the routes available for recycling plastic materials. An exploration of current recycling

technologies, challenges, and innovations is offered, highlighting the importance of developing sustainable practices to mitigate environmental impact and promote a circular economy in the plastic industry.

In conclusion, synthetic polymers represent a cornerstone of modern material science, intimately woven into the fabric of daily life and industry. Understanding their properties, classifications, and processing techniques is crucial as we navigate the challenges and opportunities presented by these ubiquitous materials in the 21st century.

2.3 What is a Polymer Matrix Composite?

Irrespective of the type, size or shape of the reinforcement, composites prepared using polymer as matrix are referred to as polymer matrix composites (PMCs). As a result of their lightweight, high stiffness, high strength along the direction of their reinforcements, good abrasion resistance and good corrosion resistance, PMCs are the most common advanced composites. PMCs matrices are typically either thermosets (e.g. epoxies, polyesters, phenolic, and polyamide) or thermoplastics (polyethene, polystyrene, polypropylene) (Kaw & Group, 2006). There are increasing interest in using thermoplastics to replace thermosets for laminate fabrication due to their advantages, such as high toughness, high strength, shorter manufacturing cycles (Gabr et al., 2015). High-Density Polyethene (HDPE) is one of the classes of thermoplastics which is widely used in many applications as a result of its low weight, enhanced tensile strength, low cost of manufacturing, high impact strength, high recyclability and resistance to chemicals.

Many researchers have reported the modification of the HDPE by various fillers (Shebani et al., 2016). The purpose of adding inorganic fillers such as clay, talc, carbon black, graphene, and calcium carbonate to polymers is to reduce the production cost and to enhance thermal, barrier, physical and mechanical properties which result in the composite having superior properties to original polymer (Essabir, Boujmal, Bensalah, Rodrigue, & Bouhfid, 2016; Kusuktham & Teeranachaideekul, 2015) (Tanniru et al., 2006).

2.4 What is Termite mound clay?

Termite mound clay is one type of clay which occurs naturally through the prolonged activities of Termites[1]. The reason why termites construct mound is to protect themselves from predators, environmental hazards, and humidity. This mound is constructed by transporting and reworking of soils from lower part of ground to the upper surface of the earth.

Figure 3 (a): Termite mound clay in Palapye, Central Botswana (Source photo: Peter N. Eze), (b) : Termite clay in Tembien abiy adi.

Even though mounds are made up of sand, silt, and clay particles like other adjoining soils, studies indicated that the clay content of mounds is higher as compared to the surrounding ordinary soils.

[1] Termites are "eusocial insects that are classified at the taxonomic rank of infraorder Isoptera, or as epifamily Termitoidae within the order Blattodea (along with cockroaches)".

The study also proved that clay minerals enhance soil stability in a way that they form strong bonds between particles which hold them together (Mujinya et al., 2013).

Figure 4 Termites (Source: https://en.wikipedia.org/wiki/Termite)

Due to the enhanced bonding characteristics of termite mound clay arising from its unique mineralogy (kaolinite, quartz) and organic-mediated organo-mineral binding researchers are increasingly investigating its structural properties and potential reinforcement applications in polymer matrix composites, although comprehensive studies are still emerging. For instance, the study conducted on termite mound clay for construction application shows that termite mound material consists of minerals such as quartz and kaolinite, with termite saliva contributing organo-mineral complexes that act like natural binders and mortars, resulting in strong material cohesion and structural integrity (Millogo et al., 2011a).

Other researchers reported that as a result of the enhanced binding energy of termite mound clay they achieve composite of improved impact strength. It is known that impact property is one of the most essential mechanical properties and an important property of any material characterization for different applications. So addressing of impact response like energy absorption capability, energy dissipation and failure mode of composite structures is very important in order

to make proper decisions before or after impact occurs, and which leads to safer materials (Yigit & Christoforou, 2007).

Therefore, as mentioned above since termite mound clay are quite different in terms of all properties than ordinary clay, composites developed from these reinforcements coupled with thermoplastic matrix obviously will have different properties. Furthermore, their effect on physical, mechanical property, effect of their size and amount was not well studied, hence this research work intends to develop termite mound clay reinforced high density polyethylene composite for low strain rate impact behavior application purpose.

2.5 Method of mixing of clay and polymers

There are different methods and ways to mix clay and polymers, among theses the most common are

i. Solution intercalation
ii. Melt compounding
iii. In-situ polymerization

Each method has its advantages and is chosen based on the specific requirements of the composite material, the properties desired, and the compatibility of clay and polymer. Effective dispersion and intercalation of clay particles within the polymer matrix are crucial for maximizing the performance enhancements offered by clay-polymer nanocomposites.(Zeng et al., 2005) stated that due to the nature of clay and polymer mixing of both ingredients often causes a situation known as agglomeration of clay minerals.

It is obvious that agglomeration arises due to the inherent hydrophilic property of clay and hydrophobic nature of HDPEs. Adhesion capability and compatibility reduced as a result of this difference in properties of the clay particles and the polymer matrix in turn affects the overall performance of the composite. Here are the drawbacks and the methods used to address them.

Drawbacks

a) Poor Dispersion: Clay particles tend to agglomerate in the hydrophobic polymer matrix due to their hydrophilic nature, leading to uneven distribution and weakening of mechanical properties.
b) Reduced Mechanical Strength: Inadequate bonding between clay and polymer results in lower tensile strength, impact resistance, flexural strength.
c) Barrier Properties: The effectiveness of clay particles as barrier fillers against gases and moisture can be compromised if not properly dispersed and bonded within the polymer matrix.

Surface Modification Methods:

a) Silane Coupling Agent Treatment: The functional groups of silane coupling allows to react with both the hydrophilic clay surface and the hydrophobic polymer matrix. This treatment modifies the clay surface, making it more compatible with the polymer and improving adhesion (Xie et al., 2010).
b) Cation Exchange: This involves replacing the interlayer inorganic cations (typically sodium ions) of the clay with organic cations to make it polymer matrix compatible. This modification helps in reducing the hydrophilicity of the clay surface (Alexandre & Dubois, 2000a).
c) Interlayer Space Swelling: By swelling the interlayer space of clay with organic modifiers or surfactants, the clay particles become more dispersible in the polymer matrix. Therefore, compatibility and interaction between clay and polymer get enhanced, which in turn improves the composite's mechanical properties.
d) Preheating of termite mound clay: is one of the effective and cost minimized surface modification method for mixing termite mound clay and high-density polyethylene (HDPE) plastic is the preheating of the clay before mixing. Preheating the clay helps to reduce its moisture content and enhances its surface activity, promoting better interfacial bonding with the hydrophobic HDPE matrix (Millogo et al., 2011a). By driving off water and possibly activating reactive sites on the clay surface, preheating improves the

compatibility between the inorganic and organic phases. This thermal treatment can also reduce the viscosity mismatch during processing, leading to more uniform dispersion of the clay within the plastic and ultimately enhancing the mechanical and thermal properties of the resulting composite material.

These surface modification techniques aim to enhance the interfacial adhesion between clay and polymer, thereby optimizing the performance of clay-polymer composites despite the inherent differences in their surface properties.

2.6 Classification of strain Rates

Strain rate refers to the degree at which a material deforms/elongates under stress, typically defined as the change in strain per unit of time. It plays a crucial role in understanding and analyzing the mechanical behavior of materials, particularly when subjected to different loading conditions. Strain rate can be classified based on the speed or duration of the applied deformation (Callister & Rethwisch, 2020). Here below are discussed the four strain rates types with their respective duration of time based on the book mentioned above.

1. **Low Strain Rate (Quasi-static or Slow Strain Rate)**: This strain rate is slow, typically occurring over a longer period of time, with strain rates ranging from **10^{-6} to 10^{-3} s^{-1}**. It is observed in slow deformation processes, such as materials testing at room temperature or under low-speed loading conditions. Examples include tensile tests on metals at room temperature and concrete under slow compression. Under low strain rates, materials generally behave in a more ductile or elastic manner.
2. **Medium Strain Rate**: This strain rate falls between slow (quasi-static) and high strain rates, with a range from **10^{-3} to 10^{-1} s^{-1}**. It occurs in conditions such as machinery, automotive, or structural loading, where deformation happens at moderate speeds. Materials subjected to medium strain rates may experience a balance of elastic and plastic behavior, along with some strain hardening.
3. **High Strain Rate (Dynamic Strain Rate)**: High strain rate refers to rapid deformation, typically occurring over a very short period of time, with strain rates ranging from **10^{1} to**

10^3 s^{-1} and higher. This strain rate is seen in processes such as high-speed impact, explosions, or ballistic testing. Materials behave differently under high strain rates, often exhibiting more brittle behavior or significant strain rate sensitivity, where the material strength increases at higher rates of deformation. Examples include car crash tests, material testing under impact loading, and ballistic testing.

4. **Very High Strain Rate (Ultra-high Strain Rate)**: This refers to extremely rapid strain rates, typically associated with high-energy impacts or explosive events, with strain rates greater than **10^3 s^{-1}**. This category describes ultra-rapid events, such as explosive or hypervelocity impact testing. Materials subjected to very high strain rates undergo extreme changes in behavior due to the very short time frame of deformation, including significant rate-dependent effects like adiabatic heating and material failure modes, such as fragmentation.

2.7 Reinforcement particles of polymer composites

To create polymer composites, it is crucial to incorporate reinforcements, which can be either particles or fibers. However, past research and practical experiences suggest that fiber reinforcement is most effective when a cool liquid resin is used as the matrix. Conversely, using a matrix produced through melting can weaken the fibers due to the applied heat. As a result, researchers advocate for the use of particles rather than fibers. Commonly utilized particles include clay, glass, sand, sawdust, and nano-carbon, among others.

The paper focused on the development of clay-based polymer nanocomposites. It discussed several processing techniques essential for fabrication of clay reinforced polymer composites, such as in-situ polymerization, solution exfoliation, and melt intercalation (Zeng et al., 2005). These methods are crucial for achieving uniform dispersion of clay nanoparticles within the polymer matrix, where the addition of about 3–5 wt.% clay was reported to increase tensile strength by approximately 20–50% and Young's modulus by nearly 40–100% compared to neat polymers. The paper emphasizes that the application area of the composite determines its optimal characteristics. Therefore, nanocomposites should undergo thorough characterization for mechanical properties, thermal properties, barrier properties, electrical conductivity, and

biodegradability to ensure suitability for specific applications, as improvements of up to 50–60% reduction in gas permeability and 20–30°C increase in thermal degradation temperature were observed with proper clay dispersion.

The authors highlight the versatility of clay-reinforced nanocomposites, recommending their use across various industries. These include manufacturing automotive components, where weight reductions of approximately 10–20% can be achieved while maintaining strength, producing packaging materials with up to 50% improved barrier performance (Sinha Ray & Okamoto, 2003a). Developing nanocomposite coatings and pigments with enhanced scratch resistance by over 30%, facilitating drug delivery systems through controlled diffusion behavior, and creating sensors and medical devices (Alexandre & Dubois, 2000a). This broad application spectrum underscores the potential of clay-based polymer nanocomposites to enhance performance and functionality in diverse technological and industrial settings.

Reinforcements in high-density polyethylene (HDPE) polymer composites are critical for enhancing mechanical properties and expanding application range. Various studies have explored the use of different fillers and fibers as reinforcements to address the inherent limitations of HDPE, such as brittleness and lack of flexibility. For instance, rubber leaves have been investigated as natural filler, showing improved tensile strength by approximately 15–25% at optimized filler loading when combined with glycerol and citric acid (Shaari et al., 2021). Similarly, carbon nanotubes (CNTs) have been used to significantly enhance mechanical and tribological properties, where the incorporation of 1–3 wt.% CNTs increased tensile strength by about 30–45% and improved wear resistance by nearly 40% without affecting the melting point or oxidation temperature of HDPE (Kanagaraj et al., 2007). Leather buffing dust (BF), a tannery waste product, has also been utilized, demonstrating improved tensile strength by approximately 18–22% and Young's modulus by nearly 35–50%, with the added benefit of recyclability (Kiliç et al., 2020).

In addition to natural fillers, synthetic fibers like Kevlar have been employed, resulting in improved tensile strength by approximately 25–35%, flexural strength by 30–40%, and impact strength by nearly 20% when surface-grafted and mixed with wood flour in HDPE composites (Ou et al., 2010). Agro-residues such as wheat straw, cornstalk, and corncob have been considered as

alternative reinforcements, with wheat straw-HDPE composites exhibiting superior mechanical properties, including flexural modulus increases of up to 60% at 30 wt.% loading (Panthapulakkal & Sain, 2007a). Furthermore, the use of microcrystalline cellulose (MCC) and nutshell fibers has been shown to enhance tensile and flexural moduli by approximately 40–70%, although impact strength may decrease by about 10–20% (Boran, 2016).

Contradictions arise when considering the impact of fillers on water absorption and mechanical properties. While some reinforcements like BF and treated sawdust improve mechanical properties and reduce water absorption by approximately 15–25% (Akter et al., 2018) ; (Kiliç et al., 2020), others, such as agro-residues, increase water uptake to nearly 8–12% despite the presence of compatibilizer (Panthapulakkal & Sain, 2007b). Additionally, while some fillers improve tensile strength by nearly 20%, they may simultaneously reduce impact strength and elongation at break by approximately 30–50% (Rasib et al., 2021).

Generally, the development of HDPE polymer composites with various reinforcements has shown promising results in enhancing mechanical properties and utilizing waste materials. Natural fibers, synthetic fibers, and nanoparticles each contribute uniquely to the composite's performance, with trade-offs in properties such as water absorption and impact strength.

The literature on termite mound clay as a reinforcement for polymer composites suggests that the unique properties of termite mound soil, such as its mineral composition and structural stability, make it a promising material for enhancing the mechanical properties of composites (Claggett et al., 2018).

A study on termite mound clay (TMC) reinforced with high-density polyethylene (HDPE) composite for low strain rate applications shows a gap in the specific area of study. While there are studies on the use of TMC in various composite materials, none of the papers provided directly address the combination of TMC with HDPE.

However, some insights can be drawn from the related research. (Akinyemi et al., 2016) discusses the feasibility of using termite mound soil reinforced with coir fibers for construction materials, indicating that low fiber inclusion is viable for certain structural applications. (Saeed et al., 2021)

examines the stress relaxation behavior of glass fiber-reinforced HDPE composites, which could provide a comparative baseline for understanding how TMC might behave when used as reinforcement in HDPE composites. Lastly, (Li & Liu, 2015) discuss the characterization of carbon composites at low strain rates, which could offer methodological insights for testing TMC-reinforced HDPE composites under similar conditions.

Due to the availability, clay is most of the time applicable in developing enhanced polymer composites. Clay content of soils and quality of the clay varies from place to place. A research conducted in Nigeria showed that the amount of clay in a soil have termite mound is higher than normal soil (Adekayode & Ogunkoya, 2009). The researchers showed that a soil 10m apart from the place where termite mound is found, the amount of clay decreases by 21% furthermore as the distance increased to 30m the amount of clay decreased by 65%.

Termite mound clay is rich in minerals like quartz and kaolinite, which contribute to its strength and durability (Millogo et al., 2011b). The inclusion of termite mound soil particles in coir fiber–polyester composites has been shown to solve the problem of matrix cracking, which is a common failure mode in natural fiber reinforced polymer composites, by strengthening the matrix (Jayabal & Bharathiraja, 2016).

Mechanical properties of composites obviously improved as a result termite mound clay incorporation, however there are trade-offs to consider. For instance, the compressive strength of termite mound cement paste and concrete decreases with increased percentage replacement of cement with termite mound clay, although certain proportions can still yield good quality concrete (Elinwa, 2018). Additionally, the role of termite mound clay in soil structural stability is complex, with clay content influencing pore sizes and water diffusion rates, which in turn affect the mound's stability (Jouquet et al., 2004).

Thus it can be concluded that termite mound clay is a valuable natural resource for reinforcing polymer composites due to its inherent strength and mineralogical properties. However, the optimal use of this material requires careful consideration of its effects on the mechanical properties of the resulting composites. The literature indicates that while termite mound clay can

enhance certain properties, such as matrix strength, it may also lead to reductions in other properties, such as compressive strength, depending on the proportion used and the specific application (Jayabal & Bharathiraja, 2016).

Most literatures and researches indicated that the selection and distribution of reinforcement particles are critical for optimizing the performance of polymer composites. The effectiveness of these particles is influenced by their shape, size, and compatibility with the polymer matrix. Advanced techniques such as chemical functionalization and the use of compatibilizer are employed to improve interfacial bonding and dispersion, which are essential for realizing the full potential of the reinforcement (W. Wang et al., 2008).

In addition to this the type and size of reinforcement particles, as well as their distribution and alignment within the polymer matrix, are key factors influencing the performance of the composites. Future research may focus on optimizing these factors to develop advanced polymer composites with desired properties for various industrial applications (Panthapulakkal & Sain, 2007).

2.8 Nature of clay reinforced HDPE composites

As a result of their improved mechanical, physical and thermal properties, clay reinforced HDPE composites are suitable for a wide range of applications. Specifically, termite mound clay reinforced HDPE composites have gained attention due to the enhancement of properties imparted by the clay fillers. The Brazilian bentonite chocolate clay (smectite clay) is commonly used to produce nanocomposites and has been shown to improve the mechanical and thermo-mechanical properties of HDPE when used as reinforcement. For example, the incorporation of 3–5 wt.% organo-modified bentonite into HDPE resulted in an increase of tensile strength by approximately 15–25%, Young's modulus by 30–40%, and heat deflection temperature by nearly 10–20°C compared to neat HDPE (Ortiz et al., 2014). These improvements were attributed to better interfacial adhesion and improved dispersion of clay platelets within the polymer matrix.

Interestingly, thermal stability and cross-linking are also improved, although clay reinforcement generally aims to enhance mechanical properties of HDPE. For instance, electron-beam irradiation

of clay-reinforced HDPE composites has been reported to significantly increase the gel fraction (cross-linking degree) from below 10% in neat HDPE to above 60–70% in irradiated clay-filled systems, resulting in enhanced tensile modulus and thermal resistance (Ortiz et al., 2014). The onset degradation temperature was reported to increase by approximately 15–30°C after irradiation. This suggests that the interaction between HDPE and clay fillers, as well as post-processing treatments, can be crucial in determining the final characteristics of the composite.

Besides clay particulates, various other additives are incorporated into the composite to improve its properties. Key additives include compatibilizers, fibers, and surface modifiers. Research supports this approach, with studies on HDPE/clay composites indicating that tensile strength can increase by 10–35% and flexural modulus by up to 50% when maleic anhydride grafted polyethylene (MAPE) is used as a compatibilizer to enhance interfacial bonding (Guo et al., 2020; Han et al., 2008a). Thermal degradation temperatures were also reported to increase by 10–25°C depending on filler loading and compatibilizer content.

Natural fiber and particulate fillers incorporated into HDPE further enhance its performance for structural applications. The literature reveals that clay reinforced HDPE composites have been investigated for their potential use in load-bearing and thermally demanding applications due to their improved mechanical and thermal properties (Treesh et al., 2023). For instance, the addition of nano-clay (2–4 wt.%) and MAPE to HDPE/bamboo composites improved tensile strength by approximately 18–28% and bending modulus by nearly 35–60% compared to unfilled composites (Han et al., 2008b)). Moreover, thermogravimetric analysis showed an increase in initial degradation temperature by approximately 20°C and a shift in maximum degradation temperature by 15–25°C (Guo et al., 2020).

The literature also points to the potential of clay reinforced HDPE composites in the biomedical field. The development of hydroxyapatite (HAp)-filled HDPE composites has shown increases in compressive strength by 20–40% and elastic modulus by 30–50%, while maintaining biocompatibility and non-toxicity, indicating suitability for orthopedic and implant-related applications (Aiza Jaafar et al., 2022). This diversification in application areas underscores the versatility of clay reinforced HDPE composites.

2.9 Characterization of Particle reinforced polymer composites

(Sadik et al., 2021) studied the properties of HDPE and waste glass powder composite. In order to obtain a uniformly mixed, the authors added a compatibilizer known as malic anhydride-grafted polyethylene with five levels (0.5, 1.5, 2.5, 5 and 7.5% of weight). The prepared specimens were characterized for mechanical properties such as Tensile strength, strain and tensile modulus (Sadik et al., 2021). According to the results obtained the maximum tensile strength recorded when 20% and 1.5% of glass powder and compatibilizer respectively are used, on the other hand elongation at break decreases with an increase in amount of glass powder (reinforcement).

(A. S. Alghamdi, 2018) conducted a research to synthesis and characterize Graphene reinforced HDPE Nano-composite. Specimens were prepared at various HDPE weight to Graphene ratio. The amount of plastics varies from 0.1-0.5% by weight ratio. The prepared specimens were characterized for their mechanical properties such as hardness, Elastic modulus and strain at break as well physical property and thermal resistance. Though, like to other study results, the mechanical property especially tensile strength and modulus of elasticity increases with an increasing amount of graphene, but as the amount of graphene increases more than 0.4% the mechanical properties diminished. Unlike to tensile strength and modulus of elasticity, the strain at break decreased with an increasing graphene weight ratio.

(Essabir, Boujmal, Bensalah, Rodrigue, Bouhfid, et al., 2016) stated that hybrid composite developed from oil-palm and clay reinforced HDPE gave enhanced mechanical and thermal property. Injection molding was used to prepare specimens following to twin-screw extrusion on the presence of compatibilizer. Based on the results presented maximum tensile properties hybrid composite was recorded while 12.5:12.5 of both reinforcements implemented. Both young's modulus and tensile strength showed 49% and 11% increment respectively. The authors recommended that use of fibers and particles to develop hybrid composite is viable.

(Sultana et al., 2013) the paper presented a composite of sand reinforced polyester resin, amount of sand varying from 10% to 60% to study physico-mechanical properties. Experiments were conducted based on the principle that a specified amount of sand and polyester resin was mixed in

a bowl very carefully with a stirrer for about half an hour. The composite was prepared using compression molding. The effects of amount of sand in SPCs on different mechanical and thermal properties of SPCs were studied in detail and results indicated that amount of reinforcing agent plays a vital role in the properties of SPCs.

(Ganesh et al.) The impact performance of composite materials incorporating termite mound particulates with natural fiber-polymer matrices was investigated. Ratios of termite mound clay ranged from 10% to 30%. At a 20% particulate content, coir fiber-reinforced composites showed impact strength of 45.35 kJ/m^3. The study noted that integrating termite mound particulates into natural fibers enhances strength and enables better resistance to impact load.

(Gabr et al., 2015) investigated the effect of organoclay on the mechanical and thermal properties of woven carbon fiber (CF)/compatibilized polypropylene (PP) composites. A compatibilizer known as maleic anhydride-modified PP oligomer (PP-g-MA) were used to manufacture the hybrid composites. The constituents were first dry blended then followed by melt-blending on a twin-screw extruder to ensure even mixing. To characterize the nanocomposite specimens using dynamic mechanical analysis (DMA), fracture toughness and scanning electron microscope, the authors use compression molding to manufacture them. Results published indicate initiation and propagation interlaminar fracture toughness in mode-1 increases by 64% and 67% respectively at organoclay weight ratio of 3%. In addition to this the glass transition temperature increased by about 6^{o}C for 3 wt. % organoclay compared to neat CF/PP composite indicating better heat resistance.

(Kusuktham & Teeranachaideekul, 2015) investigated the thermal and mechanical properties of High density polyethylene (HDPE) and Calcium silicate (CS) composites containing vinyl triethoxysilanetreated calcium silicate. The mixing ratio ranges in between 2.5%-10% by weight of HDPE and constituents initially mixed mechanically then followed by heat blending at temperature of 150 $^{\circ}$C in a mixer. Injection molding is used to manufacture specimens.. A result was found that the incorporation of the calcium silicate into high density polyethylene resulted in a slight increase in the yield stress (6.85–11.76 %) as well as tensile strength (7.02–12.84 %).

(Essabir, Boujmal, Bensalah, Rodrigue, & Bouhfid, 2016) studied the thermal, mechanical, and dynamic mechanical performances of the hybrid composites as a function of filler content . The hybrid composite consists of oil palm fibers (OPF) and clay particles which were modified and then incorporated to Reinforce high density polyethylene (HDPE). Injection molding was used to manufacture the testing specimen following to the mixing process using twin screw extruder. A 49% enhancement in young's modulus recorded which shows a homogeneous dispersion of fillers into the polymer matrix. On the other hand as a result of incorporating the coupling agent the tensile strength increased by 11%.

(Shebani et al., 2016) investigate the influence of Libyan Kaolin clay on the impact strength properties of high density polyethylene (HDPE) clay nanocomposites. The authors first prepare test mixes with HDPE to clay weight ratio of 0, 2, 4, 6, and 8 wt. %. Results showed that specimen containing 2% by weight ratio of clay exhibit highest impact strength. To investigate the effect of compatibilizer, the authors were used 2, 4, 6, 8 and 10 wt. % of polyethylene grafted maleic anhydride (PE-g-MA) to mix with the best performed mix ratio and the best result was obtained for the mix with 2% of the compatibilizer. Finally the authors checked the effect of clay particle size on impact strength, where it showed significant influence. The addition of Libyan Kaolin filler has resulted in an improvement in the impact strength properties of HDPE.

(Tanniru et al., 2006) investigated the effect of adding clay to polyethylene on its mechanical response and micro mechanism deformation of plastics during impact loading using scanning electron microscope. For the purpose of testing specimens were manufactured using twin screw extruder apparatus which is rotating at 100 rpm followed by injection molding. A result shows that with the addition of clay to polyethylene retains adequately high-impact strength in the investigated temperature range of -40°C to70 °C.

(Yuan & Misra, 2006) on the other hand these authors compared the mechanical property of clay reinforced polypropylene to unreinforced PP under same processing condition. Twin screw and injection molding were used to mix the proper amount of clay to PP ratio and manufacture test specimens (tensile and Izod impact bars) respectively. For enhancement of bonding dimethyl dialkyl ammonium was incorporated as binding agent. A result shows the addition of clay to PP

increases the impact strength in the temperature range of 0 to 70°C, while the toughness remained unaffected between -40 to 0°C.

(Lei et al., 2007) properties like crystallization behavior, mechanical properties, water absorption, and thermal stability of clay, pine flour and HDPE hybrid composite were investigated. Melt compounding and injection molding were used to prepare testing specimens. Though the crystallization thickness not altered, the crystallization rate and temperature was decreased as result of clay addition. The paper presented that adding of 1% clay increases the flexural, tensile strengths, tensile modulus and tensile elongation by 19.6%, 24.2%, 11.8% and 13% respectively, but then decreased slightly as the clay content increased to 3%. But the unlike to the above mentioned mechanical properties impact strength lowered by 7% when 1% of clay was added, but did not decrease further as clay content was increased. Regarding the moisture content and swelling thickness properties show reduction as clay content added increases.

(Zheng et al., 2003) the authors used Haake mixer and twin screw extruder to manufacture graphite reinforced HDPE. The aim of the study was to investigate the Electrical and Mechanical Properties of the composite. Based on the experiments conducted increment in filler content (graphite) improves the mechanical properties, though the enhancement is significant. The Expanded Graphite composites demonstrated potentially useful attributes for antistatic, barrier, mechanical, electrical, and cost-effective applications.

2.10 Failure mechanism and damage mode of clay reinforced of HDPE composite

The failure mechanisms and damage modes of different materials vary due to differences in their composition, intermolecular bonding, and structural setup. Furthermore, the intended application, type of load, and mode of application can also influence the failure mechanisms of the same material even. Therefore, it is evident that the failure modes and mechanisms of a composite can differ from those of its constituent raw materials, as the composite's properties can be significantly different from those of the individual materials.

The literature on failure mechanisms and damage modes of clay-reinforced high-density polyethylene (HDPE) composites reveals a multifaceted understanding of the subject. For instance, the presence of clay platelets has been found to induce changes in the deformation mechanisms of polyamide-6 and polypropylene-based composite, leading to a dual-dilatational deformation mechanism by crazing and interfacial deboning (Mesbah et al., 2014). This indicates that adding of clay to HDPE plastic significantly affect the mechanical behavior and failure characteristics. Additionally, the microstructure and dielectric response of HDPE/clay composites have been reported to be closely related to the composite's microstructure and chemical composition, with the dielectric properties being influenced by moisture absorption (David et al., 2015).

Contradictions and interesting facts emerge when considering the effects of clay content and dispersion on the properties of HDPE composites. Full exfoliation of clay in HDPE was achieved using maleated HDPE, which enhanced the rheological, mechanical, and flame-retardant properties even with small amounts of clay (Lee et al., 2007). Moreover, the mechanical and tribological properties of HDPE nanocomposites reinforced with various inorganic Nano fillers, including clay, have been reconsidered, highlighting the importance of the treatment of Nano fillers and the need for a nuanced understanding of property correlations (Ahmed et al., 2020).

It is understood that, the literatures mentioned above indicated clay reinforcement in HDPE composites can lead to significant changes in failure mechanisms and damage modes, with factors such as clay content, dispersion, and the presence of compatibilizer playing crucial roles. The studies collectively suggest that while clay reinforcement can enhance certain properties of HDPE composites, it also introduces complexity in understanding and predicting failure behaviors. Future research should continue to explore these relationships to optimize the performance of clay-reinforced HDPE composites in various applications.

2.11 Effect of strain rate on Mechanical Properties of Particle reinforced polymer

In the subtopics discussed, past studies and investigations on the effect of reinforcing polymers with particulates have been reviewed. However, in addition to the type and amount of particulate,

as well as other manufacturing parameters (such as the mixing mechanism and mixing time), strain rate also has a vital impact on the properties of the composite, especially its mechanical properties.

Overall scholars agreed the strain rate plays a crucial role in determining the mechanical behavior of particle-reinforced composites, and understanding its effect is essential for tailoring material properties for specific applications (Cadoni et al., 2012; Hufenbach et al., 2011; Jung et al., 2016).

For characterizing particulate-reinforced polymer composites, past researchers recommended to use low strain rate, because it simulates real-world, long-term loading conditions, avoids dynamic effects, and provides a stable and accurate assessment of the material's mechanical properties. Experimental characterization of strain rate effects faces challenges, particularly at high rates, where inertial effects and mechanical resonance can obscure test results as it did not allow controlling the testing process (Jacob et al., 2004).It helps evaluate how the composite will behave under typical operational stresses, offering insights into its ductility, elasticity, and overall performance in various engineering applications.

Strain rate significantly influences the tensile, compressive, shear, and flexural properties of polymer composites. Generally, tensile strength and modulus increase with higher strain rates, although ultimate tensile strain tends to decrease. This behavior is attributed to changes in the material's failure mode as the strain rate rises. Similarly, shear properties, such as shear strength and modulus, exhibit a positive correlation with strain rate. Compressive strength also often increases, but in certain configurations, longitudinal properties may show strain rate insensitivity. Flexural properties, including strength and stiffness, typically improve at higher strain rates, enhancing the material's overall load-bearing capability (Jacob et al., 2004).

The study demonstrates that the tensile strength of HDPE/clay nanocomposite foams increases linearly with the logarithmic scale of strain rate. Similarly, as the strain rates increases the Young's modulus foams also raises, although increment rate reduces as the strain rate maximized. Crystallinity also plays a crucial role, in which modulus increases with crystallinity. But the effect of crystallinity is less promising at high strain rates, suggesting an interaction between crystallinity and strain rate effects. The study attributes these behaviors to the viscoelastic nature of the material

and the reinforcing effects of Nano-clays, which enhance stiffness but also interact with the polymer matrix (Jo & Naguib, 2008). This model, validated against experimental data, successfully describes the stress-strain response of the material under various conditions. Overall, the study presented to determine the mechanical properties of polymer, knowing and understanding of strain rate and crystallinity is crucial.

2.12 What are Armor materials?

Body armor is designed to protect against various threats, including bullets, knives, and other projectiles. The materials used in body armor vary depending on the level of protection required, weight considerations, and the specific threats they are designed to mitigate.

A book titled “Armour materials, Theory and Design” (AMTD Front matter.Pdf, 2016) explains how modern armor is designed, including its theory, uses, and materials, focusing on vehicles, ships, people, and buildings. It looks into the science and technology that help protect against explosions and bullets. The book discusses the materials used for protection and how changing the shape of blast waves can impact vehicles and people's bodies. It also describes ways to test armor against bullets.

Additionally, it covers different types of materials used for armor, such as ceramics, transparent armor, and various metals like aluminum, magnesium, titanium, and different kinds of steel. It also talks about composite armor systems and explosive reactive armor for vehicles. The book highlights advanced methods for processing these materials as well.

This paper (Hani et al., 2012) looks at the body armor industry and the recent progress in materials, design, and building methods. It also discusses efforts to improve how much force body armor can absorb. Researchers are actively exploring new body armor technologies because of existing constraints in weight and flexibility of recent body armors. Additionally, they are competing to create ballistic panels that are lighter, more flexible, more comfortable to wear, and cheaper to produce. On the other hand a paper published on 2019 discusses about body armor materials and gives a quick overview of what we know about how they work to absorb energy. It focuses on different types of materials like fibers, fabrics, plastic layers, and ceramics (Crouch, 2019).

Body armor can be classified based on the material composition of the protective layers (Cavallaro, 2011). Here are the primary categories:

1. Soft Armor

    Materials: Typically made from woven or laminated fibers.
    Aramid Fibers: Such as Kevlar and Twaron.
    Ultra-ballistic Fibers: Like Dyneema and Spectra.
    Usage: Designed to protect against handgun rounds and shrapnel. Commonly used in concealable vests, tactical vests, and police armor.

2. Hard Armor

    Materials: Composed of rigid materials to withstand rifle rounds.
    Ceramics: Such as alumina, silicon carbide, or boron carbide, typically used in plates.
    High-Density Polyethylene (HDPE): Provides a lightweight option that can be used in plates.
    Steel: Traditional hard armor made from high-carbon or other steel grades.
    Usage: Primarily used in military applications or for law enforcement in high-risk situations involving rifle threats.

2.13 Surface modification methods

Though it is important to mix thoroughly in order to disperse the reinforcements in to the matrix, sometimes due to the nature of both reinforcement and matrix it is difficult to obtain a homogenous mixture. For such cases it is important to add some compatibilizer, solvents or modify the surface of reinforcement in order to accelerate the mixing process.

(A. S. Alghamdi, 2018) in this study, the researcher explored how adding graphene could improve the mechanical and thermal properties of HDPE. Xylene was used as a solvent to help dissolve the HDPE pellets, and scanning electron microscopy (SEM) was used to examine how well the graphene was dispersed. Based on the image captured from SEM to some extent the graphene was

uniformly distributed in the solution, though small agglomeration developed. Unfortunately using 0.5% by weight of graphene resulted on large cavities and many agglomerations.

(Essabir, Boujmal, Bensalah, Rodrigue, Bouhfid, et al., 2016) On the study of hybrid composite of oil-palm fiber and clay reinforced HDPE composite to determine the mechanical and thermal properties, the authors were used a compatibilizer known as styrene triblock copolymer grafted with malic anhydride (SEBS-g-MA). The agent contains 1.4-2% of malic anhydride. The authors reported that the image obtained from SEM showed there is a good distribution of clay in the matrix and agglomeration was not created.

Incorporation of compatibilizer namely terpolymer which is a group of ethylene-acrylic ester-maleic anhydride enhances the water absorption resistance of agro-residue reinforced high-density polyethylene composites. The study also stated that the flexural strength of the composite decreased with increased amount of reinforcements (Panthapulakkal & Sain, 2007a).

2.14 Data Analysis and optimization Methods

The literature on data analysis methods for high-density polyethylene (HDPE) composites encompasses a variety of instrumental techniques and methodologies. Differential scanning calorimetry (DSC) is frequently used to investigate melting behavior and crystallinity, as seen in studies where DSC data indicated that the melting temperature and crystallinity of HDPE composites remained relatively constant with the addition of certain fillers (Pan et al., 2009a). Scanning electron microscopy (SEM) is another common technique for evaluating the morphological characteristics of composites, providing insights into the dispersion of fillers and the interfacial adhesion within the HDPE matrix (Pan et al., 2009b; Xuen et al., 2021; Zhang et al., 2017). Fourier transform infrared spectroscopy (FTIR) is utilized to assess the chemical interactions between HDPE and various fillers, revealing the presence or absence of new functional groups (Kiliç et al., 2021; Zhang et al., 2019).

Interestingly, while some studies report improved mechanical properties with the addition of fillers, such as enhanced creep resistance and stress relaxation properties (Zhang et al., 2017) others note a decrease in impact strength (Zhang et al., 2019). Additionally, thermal analysis

methods like thermo-gravimetric analysis (TGA) and measurements of thermal conductivity and coefficient of thermal expansion (CTE) are employed to understand the thermal stability and heat transfer characteristics of HDPE composites (Dey & Tripathi, 2010; Karmarkar & Shashidhara, 2018; Kiliç et al., 2021; Wu et al., 2006)

Optimization methods for polymer-clay composites, particularly high-density polyethylene (HDPE) reinforced with clay rely heavily on structured experimental designs and statistical tools. To identify the optimal process parameters techniques such as Response Surface Methodology (RSM) and Taguchi method are widely applied. These approaches minimize the number of experimental trials while providing accurate models of relationship between processing parameters and material properties. Parameters commonly optimized include amount of constituents, particle size, mixing temperature, mixing torque, mixing time, and filler loading during melt compounding, as well as injection molding variables like melting temperature, compression pressure, and curing time. The focus is on reducing defects such as shrinkage and warpage and enhancing mechanical performance metrics like tensile strength, flexural modulus, and impact resistance (Treesh et al., 2023).

In order to ensure uniform dispersion of clay particles in the polymer matrix, the optimization process typically begins with composite fabrication using melt mixing or twin-screw extrusion. Experimental designs, such as Box-Behnken and Taguchi orthogonal arrays, were employed to systematically vary process parameters and analyze their effects. Statistical models, including regression equations, contour plots, and signal-to-noise (S/N) ratios, are used to visualize the interactions between variables and identify the best conditions.

The author concluded that this approach is one of the most widely used and effective tools in design of experiments (DOE). Taguchi's method has been successfully applied worldwide in both manufacturing and research fields, including heat treatment, abrasive wear, damping characteristics, and many other applications. The method uses the "signal-to-noise (S/N) ratio" as a measure of quality, where the "signal" represents the desired mean value of the output and the "noise" reflects the unwanted variation around that value. In simple terms, the S/N ratio compares the average performance to its variability. Researchers can significantly reduce experimental time

while identifying optimal settings for controllable factors and minimizing the influence of uncontrollable variations by implementing Taguchi's method.

Validation of the optimized parameters is carried out through confirmatory tests, ensuring that experimental results align closely with predicted values. The findings consistently highlight the critical role of temperature as the most influential factor, while excessive filler loading or extreme processing conditions can lead to defects like agglomeration or material degradation. These methodologies demonstrate the effectiveness of statistical tools in optimizing processing conditions, enhancing composite performance, and minimizing manufacturing defects.

The optimization of processing conditions for PP/HDPE nanocomposites is achieved through a structured approach involving statistical methods, primarily Design of Experiments (DoE). The study utilizes Response Surface Methodology (RSM), specifically a Box-Behnken design, to systematically model and analyze the effects of four critical process variables: mixing temperature, mixing torque, mixing time, and Nano clay content (Treesh et al., 2023). This method enables the efficient exploration of parameter interactions and their influence on mechanical properties, minimizing experimental runs while ensuring accuracy.

The optimization methodology used in the studies involves employing statistical techniques like Design of Experiments (DOE) and Response Surface Methodology (RSM) to systematically explore and optimize the parameters influencing the performance of composites (Dan-asabe et al., 2019). The process includes defining key input variables, such as composition ratios, processing temperatures, and pressures, and measuring responses like flexural strength, density, shrinkage, or water absorption. Models are developed using polynomial equations (linear, quadratic, cubic, or quartic), with the goal of maximizing desired properties and minimizing defects or undesirable traits. Statistical tools, including regression analysis, ANOVA, and desirability functions, are used to validate the models, identify optimal conditions, and predict responses within and beyond experimental ranges. Confirmation tests ensure that the optimized parameters align with experimental results, providing robust and reliable processing conditions.

2.15 Research Gap

While a considerable amount of research has been conducted on clay-reinforced polymer composites, the majority of these studies have concentrated on nano-scale clays and their dispersion techniques within polymer matrices. These investigations predominantly target applications in packaging, automotive components, coatings, and biomedical devices, where improvements in barrier, thermal, or electrical properties are prioritized. In contrast, significantly less attention has been directed toward the utilization of naturally occurring, non-processed macro-scale clays, such as termite mound clay, particularly for applications involving high-strain or impact loading conditions such as body Armor. Consequently, the interaction behaviour of such natural clays with thermoplastic matrices like HDPE under low strain rate impact conditions remains insufficiently explored, creating a critical gap in understanding their structural response and performance in demanding, protective-use scenarios.

Furthermore, although HDPE has been extensively modified with various fillers including carbon nanotubes, rubber particles, and industrial waste materials, limited research has focused on integrating naturally sourced mineral reinforcements with the specific objective of developing personal protective equipment. The mechanical characterization of termite mound clay-reinforced HDPE composites especially, under low strain rate impact conditions relevant to body Armor applications has not been comprehensively investigated. In addition, standardized experimental evaluation and performance benchmarking against established body Armor criteria remain largely absent in existing studies.

Therefore, there exists a clear need for systematic investigation into the development and performance evaluation of termite mound clay-reinforced HDPE composites. This thesis addresses these identified gaps by developing such composites and conducting comprehensive mechanical and impact characterization, with particular emphasis on assessing their suitability for protective and impact-resistant applications.

CHAPTER-3

METHODOLOGY

3.1 Materials and Methods

3.1.1 Overview

This chapter detailed the methodology for characterizing the termite mound clay-reinforced HDPE (High-Density Polyethylene) composite, systematically outlining the experimental process. It began by describing the material selection, focusing on termite mound clay and HDPE, both chosen for their distinct properties, which enhanced the composite's potential strength, durability, and sustainability. The composite was prepared by mixing finely grinded termite mound clay with molten HDPE at different concentrations, following a designed experiment (DOE) to produce varied samples.

The processing techniques involved melt blending ensure even clay dispersion within the polymer matrix. The samples were then molded into test specimens using compression molding. Mechanical characterization included tensile, impact, and flexural tests, conducted according to standards to assess strength, toughness, and flexibility.

Additionally, physical properties such as water absorption and density were measured. Finally, statistical analyses, including ANOVA and regression, were applied to interpret the data and identify the optimal clay loading for peak performance. This through methodology provided a robust evaluation of the composite, establishing a foundation for its potential applications.

The overall procedure of this thesis work is summarized as shown in the figure below (

Figure 5).

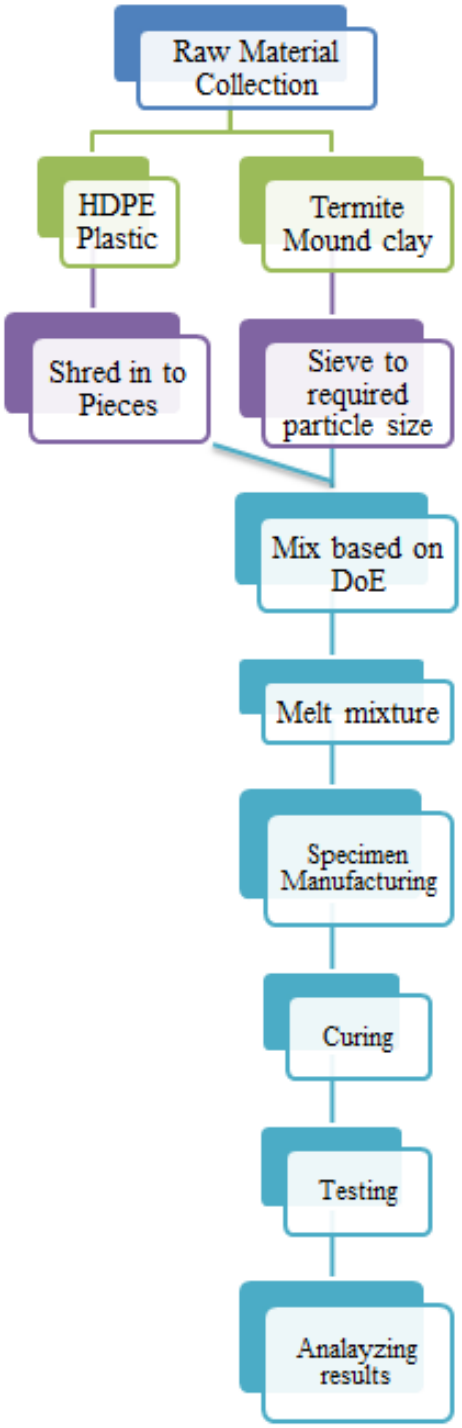

Figure 5 : Flow chart

3.2 Tools

The manufacturing of termite mound clay (TMC) a reinforced high-density polyethylene (HDPE) composite specimen via compression molding involves several key tools and equipment, each playing a specific role in preparing, processing, and shaping the materials. The induction furnace (Figure 6) was used to melt the HDPE granules uniformly without open flame, offering precise temperature control essential for preventing thermal degradation of the polymer. The crucible, made of a heat-resistant material, serves as a container for melting and mixing the HDPE prior to molding. Once the molten polymer was prepared, trowels (Figure 7) were utilized to manually spread or incorporate termite mound clay into the matrix and evenly distribute the mixture into the mold cavity. This ensures proper dispersion and uniformity in the final specimen structure.

Before molding, accurate weighing of HDPE and clay was performed using an electronic balance, which ensures the correct proportioning of materials, a critical factor in maintaining consistency in mechanical properties. The termite mound clay undergoes sieving through a sieving machine (Figure 9) to obtain uniform particles that can better bond with the polymer matrix. Once the mixture was ready, it was then subjected to high temperature and pressure to form the composite specimens. These tools collectively facilitate the effective processing of HDPE-TMC composites with enhanced structural and thermal characteristics.

Figure 6 : Induction furnace and crucible

Figure 7 : Trowels for mixing process and tools used for mixing

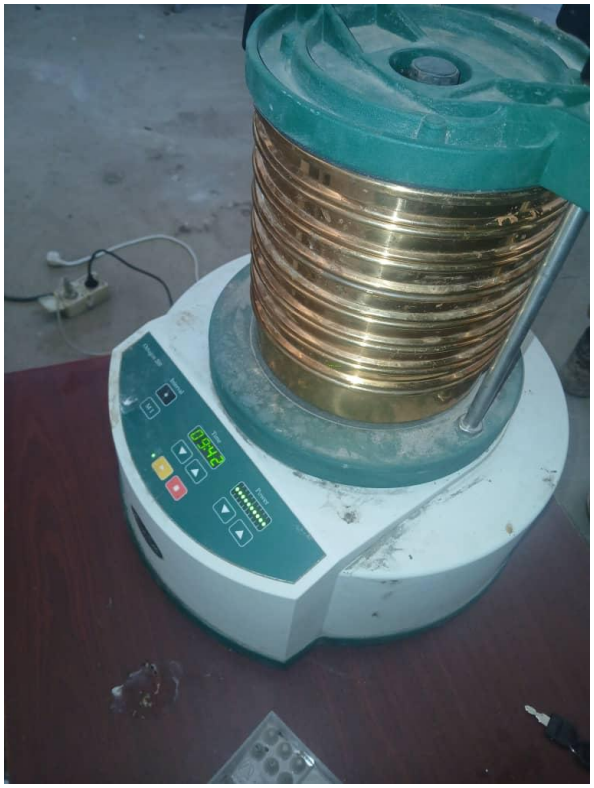

Figure 8 : Electronic Balance

Figure 9 : Sieve machine (Found in joining and Metallurgy lab, EiT-M)

Figure 10: Different molds for specimen manufacturing

3.3 Raw Materials and Tools

To achieve the objectives of this study, a detailed and systematic procedure has been followed, supported by comprehensive explanations for each step. The preparation of the composite specimens begins with the collection of essential raw materials, which include waste plastics, specifically High-Density Polyethylene (HDPE), and termite mound clay. The termite mound clay is first carefully heated to remove moisture and impurities, followed by sieving through standard sieving equipment to obtain a fine, uniform powder. For the HDPE plastic, the waste plastic is thoroughly washed to remove any contaminants, and then shredded into smaller pieces to facilitate easier processing. After these initial preparations, both the termite mound clay and HDPE plastic are ready for blending and incorporation into the composite material, ensuring that they are properly processed to meet the requirements for the intended application. This methodical approach ensures that both materials are effectively prepared for subsequent processing and composite formation.

3.3.1 Waste HDPE plastic

For this thesis work, waste oil containers (commonly known as "Hayat") and liquid detergent containers were collected from individual households of having density and melting temperature of 0.95 g/cm^3 and 120^{o}c respectively. A total of 5 kg of waste HDPE was gathered, consisting of approximately 15 pieces of oil containers and 20 pieces of liquid detergent containers. The paper labels, which indicated the brand of the company and listed ingredients, were removed from the containers before they were shredded into pieces. To facilitate the melting process and reduce the melting time, the collected waste HDPE plastics were shredded into small pieces, ranging in size from 3 to 7 mm as shown in Figure 11. The shredding process was carried out using a machine available at the Bruh Tesfa Plastic Factory in Mekelle.

High-Density Polyethylene (HDPE) is a versatile and widely used thermoplastic polymer known for its strong performance and various desirable properties. Some of the key properties of HDPE are Density, Strength and Durability, Chemical Resistance, Thermal Resistance, Electrical Insulation, Moisture Resistance, UV Resistance, Environmental Resistance, Ease of Processing, Cost-Effective.

Figure 11 : Shredded waste HDPE plastic

These properties make HDPE suitable for a wide variety of applications, including packaging, pipes, plastic bottles, geomembranes, automotive components, and medical supplies. Its strength, chemical resistance, and processing versatility are particularly beneficial in both consumer and industrial products.

3.3.2 Termite mound clay

The termite mound processed soil is collected from Tembien Abiy Adi. For the purpose of laboratory investigation the soil collected is crushed to a desired particle size as shown in Figure 12.

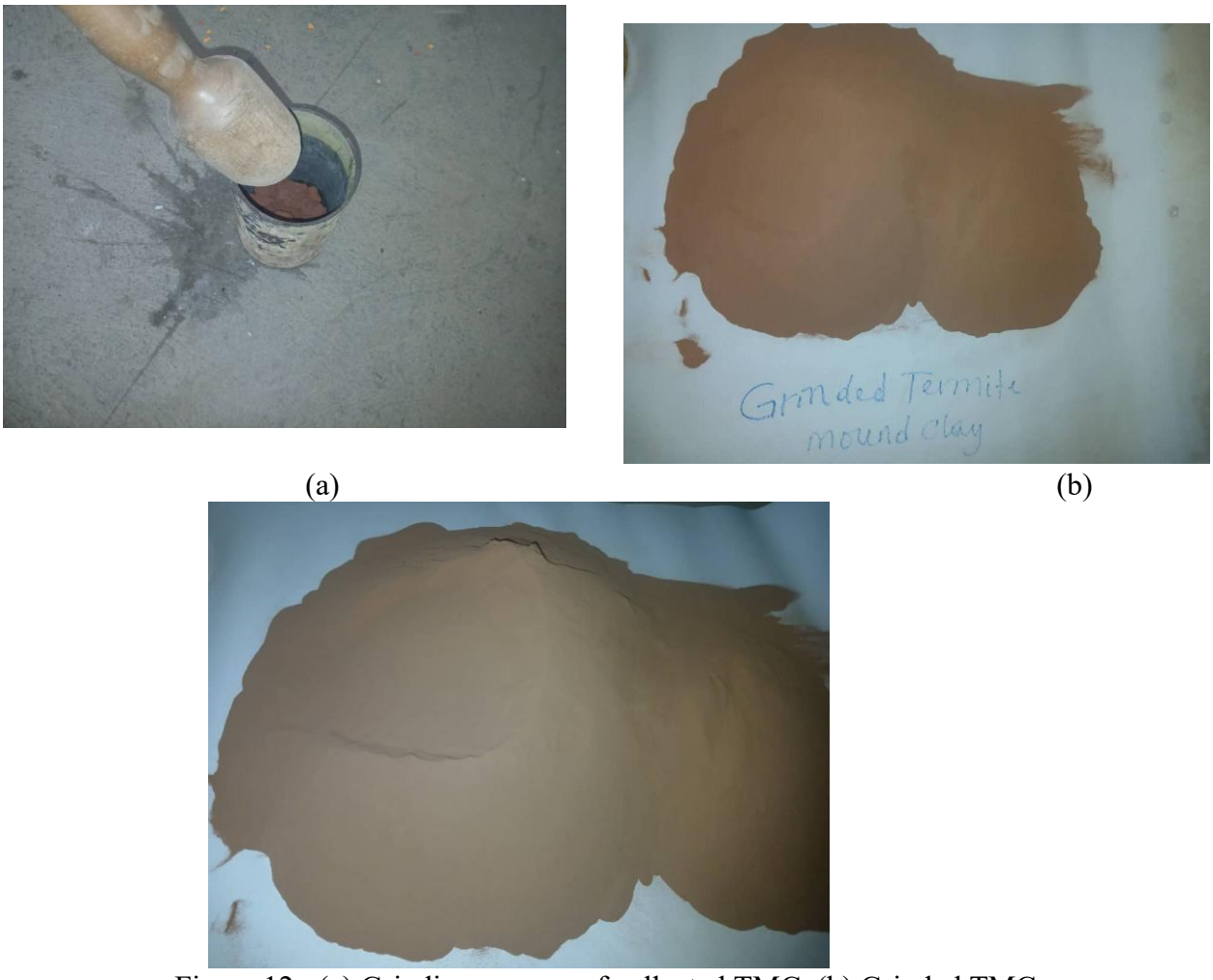

(a) (b)

Figure 12 : (a) Grinding process of collected TMC, (b) Grinded TMC

Although conducting tests to characterize the physical properties of termite mound clay is important, due to time and budget constraints and because the termite mound clay was mixed with molten waste HDPE plastic the determination of moisture content, liquid limit, and plastic limit was deemed irrelevant for this study. Therefore, pre-existing data on the physical properties of termite mound clay have been adopted and are presented in the table below.

Table 1: Physical parameters of termite mound clay used as reinforcement (Source: Akinjide, A., & Oke, S. (2012).

Parameters	**Value**
Maximum dry density (g/cm^3)	1.5-1.7
Optimal moisture content	15-22
Specific gravity	2.6-2.75
Liquid limit	30-50
Plastic limit	20-30
Plasticity index	10-25

Termite mound clay, often considered a natural material derived from termite mounds, has unique properties that make it an interesting candidate for use in composite materials. The exact properties of termite mound clay can vary depending on the geographical region and specific species of termites, but in general, it exhibits several distinct characteristics such as Composition, Particle Size Distribution, Plasticity, Moisture Absorption, Thermal Properties, chemical composition, cohesion and bonding ability, environmental resistance, eco-friendly and sustainable, low shrinkage and swelling, strength and hardness and eco-cultural significance.

Preheating Process of Termite Mound clay

For enhanced interfacial bonding between termite mound clay and molten recycled HDPE, the clay was preheated at 105 °C for 3 hours prior to compounding. This temperature and duration are consistent with standard moisture removal procedures for clay fillers and polymer composite processing, ensuring reduced hydrophilicity and improved dispersion within the HDPE matrix (Sinha Ray & Okamoto, 2003b). The procedures followed during preheating process are

(a) Termite mound clay was Crushed and sieved to the required particle size.
(b) Visible impurities were removed manually (grain stem, grass and so on).
(c) Spread the clay evenly in a stainless-steel tray.
(d) Place in oven at 105 °C.
(e) Maintain heating for 3 hours to remove absorbed moisture.
(f) Remove the tray and allow the clay to cool inside a closed container to prevent moisture reabsorption.
(g) Use the dried clay immediately for melt blending with recycled HDPE to avoid atmospheric moisture uptake.

In summary, termite mound clay possesses a range of properties, including fine particle size, plasticity, chemical stability, and eco-friendly characteristics, which make it a promising material for use in composite materials, especially when combined with polymers like HDPE. It can enhance the composite's mechanical, thermal, and environmental properties while contributing to the development of sustainable materials.

3.4 Design of experiment and specimen preparation

In the design of experiments (DOE), identifying and understanding the factors[2] and their respective levels[3] is crucial for obtaining valid and reliable results. A well-structured DOE takes into account the identified factors and their levels to systematically investigate their effects on the response variable. By carefully planning this stage, it is possible to maximize the quality of collection, leading to more robust conclusions and easier interpretation of results.

Since development of DOE involves a careful consideration of factors and their respective levels, it is mandatory to identify the factors and their levels effectively. Though there is no consensus on what should be the factors, it is possible to derive the factors from previous research works and

[2] Factors are the independent variables manipulated in an experiment to observe their effect on the response variable.

[3] Levels refer to the specific values or categories that a factor can take.

objective of the thesis work. Keep in mind of these guidelines; it was assumed that the factors should be the ratio of termite mounds clay to plastic, mixing time, and clay particle size. Here's a general overview of how these factors interact and their importance in the composite development.

(a) Ratio of Termite Mound Clay to Plastic (Factor A)

The ratio of termite mound clay to HDPE significantly influences the mechanical, thermal, and physical properties of the composite. Higher clay content can enhance stiffness and thermal stability but may also increase brittleness and reduce impact resistance. In addition to this the clay to plastic ratio have also influence on optimizing the properties of the composite. Such that it is essential to find an optimal ratio that balances strength, flexibility, and process ability. For instance, typical weight ratios might range from 10-30% clay for enhanced performance without compromising the plastic's inherent properties.

Therefore, it is essential to consider clay to plastic ratio factor as one prominent factor for preparing, characterizing and evaluating specimens manufactured from plastic and termite mound clay.

Taking previous studies and research as benchmark three levels (namely 70%, 80% and 90% by weight ratio of plastic) used to manufacture specimens. Which means that 70% plastic and 30% of clay, 80% of plastic and 20% clay, then finally 90% by weight of plastic and 10% clay was used.

(b) Mixing Time (Factor B)

The duration of mixing directly affects the dispersion of termite mound clay within the HDPE matrix. Insufficient mixing can lead to phase separation or non-uniform distribution, which negatively impacts mechanical performance. On the other hand, the mixing time affects the processing condition. Longer mixing times can increase the risk of thermal degradation of HDPE if not properly controlled. Therefore, optimal mixing time, often determined experimentally, ensures good distribution without thermal compromise. Furthermore, extended mixing can also influence the morphology of the composite, affecting both the crystalline structure of HDPE and the alignment of clay particles.

Generally, to consider the homogeneity of the mixture, processing temperature and Effect on Morphology, it is necessary to regulate the mixing time. Hence to understand the effect on properties (Physical and Mechanical) of the composite the mixing time is taken as one factor.

In general, mixing times can range from a few minutes to several hours, but achieving an optimal mix often requires experimentation to determine the best conditions for a specific formulation. A research conducted to see effect of processing and Nano dispersion used a mixing time at 1, 5, 10 and 15min. low mixing time gave minimum mechanical properties (Bourbigot et al., 2008). Effect of mixing conditions on the mechanical, thermal and physical properties of polyactide-montmorillonite clay was investigated at 7, 11 and 15 minutes (Jollands & Gupta, 2010). A research conducted to enhance the thermal resistance of Glass fiber reinforced unsaturated polyester composite by adding clay. The mixing time taken was 60, 90 and 120 minutes (Prabowo et al., 2024). Though the selection of mixing time seems exaggerated, may it was because of the incorporation of fiber, as fibers require more time to mix with clay and the unsaturated polyester.

Based on the literatures reviewed and existing constraints three levels, such that 5, 15 and 25 minutes were taken as mixing time to prepare the specimens required for testing.

(c) Particle Size of Termite Mound Clay

Particle size plays a pivotal role in determining the mechanical, thermal, and physical properties of polymer-based composites, particularly when using clay as a reinforcement material. In clay-reinforced composites, smaller particle sizes typically offer a higher specific surface area, which promotes stronger interfacial bonding with the polymer matrix, in this case, High-Density Polyethylene (HDPE). Enhanced bonding at the interface contributes to improved stress transfer, leading to better tensile, impact, and flexural performance of the composite material.

However, the relationship between particle size and composite performance is not linear. While finer particles improve surface interaction, excessively small particles tend to agglomerate due to high surface energy, which can hinder uniform dispersion and reduce process-ability. Agglomeration may lead to defects such as voids or weak spots in the matrix, compromising the mechanical integrity of the composite. Conversely, larger clay particles often result in weaker

interfacial adhesion due to their reduced surface area-to-volume ratio and poor matrix encapsulation, which may cause early failure under load.

To investigate the influence of particle size on composite behavior, a sieve analysis was performed using a standard sieve shaker with mesh sizes ranging from 63 µm to 250 µm. Based on the preliminary particle distribution and material handling characteristics, three representative size fractions were selected for further study:

- 63-90 µm – representing fine particles, with high surface area and potential for strong interfacial bonding;
- 90-125 µm – representing medium-sized particles, expected to provide a balance between dispersion and bonding;
- 125-150 µm – representing coarse particles, typically exhibiting lower interfacial interaction.

Figure 13 : Sieve analysis set up and process

Particles smaller than 63 µm were excluded due to their tendency to agglomerate, making them difficult to disperse uniformly and small amount obtained from the sieve analysis conducted. Particles larger than 125 µm were also eliminated from consideration, as their large size may compromise the mechanical performance of the composite due to inadequate matrix wetting and

reduced bond area. By selecting these three particle size groups (fine, medium, and coarse), the study aimed to systematically evaluate the effect of termite mound clay particle size on the performance of HDPE composites. This approach was consistent with findings in similar composite systems, where particle size optimization has been shown to significantly influence tensile strength, impact resistance, and thermal stability (M. N. Alghamdi, 2021; Alshammari et al., 2022; Gill et al., 2020).

3.4.2 DOE Matrix

To systematically investigate the effects of key processing parameters on the physical, mechanical, and other properties of termite mound clay-reinforced HDPE composites, a Design of Experiment (DOE) was formulated using Minitab software based on the Taguchi L9 orthogonal array[4]**.** The use of the L9 Taguchi DOE allowed for efficient evaluation of the main effects of HDPE plastic weight ratio, mixing time, and particle size on composite performance. This method minimized the number of experimental runs while enabling clear identification of the most influential factors and their optimal levels for specimen fabrication.

Factors and Levels

Three critical factors influencing the composite properties were selected for the DOE as discussed above, each varied at three discrete levels as indicated in Table 2:

Table 2 : Level of factors

Factor	Symbol	Levels
HDPE Plastic weight ratio (%)	A	90%, 80%, 70%
Mixing time (minutes)	B	5, 15, 25
Particle size of termite mound clay (µm)	C	63-90, 90-125, 125-150

[4] An orthogonal array is a type of experiment where the columns for the independent variables are “orthogonal” to one another, which makes analysis easy and saves effort of experiment.

These factors were chosen based on their expected influence on the composite's microstructure, dispersion of clay in the HDPE matrix, and ultimately the mechanical performance.

DOE Matrix

Using Minitab's L9 orthogonal array, a total of 9 experimental runs were generated, ensuring a balanced and efficient exploration of the factor space with minimal experimental effort. Each run corresponds to a unique combination of the three factors at specified levels, as shown below (

Table 3):

Table 3 : Design of Experiment matrix

Run	A (HDPE wt. %)	B (Mixing time)	C (Particle size)
1	90	5	63-90
2	90	15	90-125
3	90	25	125-150
4	80	5	90-125
5	80	15	125-150
6	80	25	63-90
7	70	5	125-150
8	70	15	63-90
9	70	25	90-125

3.5 Experimental Procedure

- Specimens for each experimental run were prepared according to the assigned factor levels(see Figure 14).
- Physical (density, water absorption), mechanical (tensile, flexural, impact) properties were measured.
- Each run was replicated three times to ensure statistical reliability and reproducibility.

Figure 14 : Mix ratio based on specified factor level and DOE

3.6 Experiments for Characterization of composite

3.7 Physical properties Characterization

3.7.1 Percentage of Water absorption

A composite material can absorb water in different modes. Most researchers and scholars agreed that moisture can penetrate into the composite materials as a result of the following three mechanisms namely, due to the diffusion of liquid molecules into micro voids between polymer chains, capillary transport in to the micro-gaps and flaws at the reinforcement (fiber) and matrix (polymer) interfaces and incomplete wettability and impregnation of reinforcement by the matrix. These creates micro cracks in the matrix that are formed during the composite fabrication process (Espert2004.Pdf, n.d.).

The water absorption test carried out in accordance with ASTM D570-98, and the test specimens for molded composites shall be prepared in the form of a disk 50.8mm in diameter and 3.2mm in thickness in three replications. A permissible variation of thickness ± 0.18 and ± 0.30mm for hot and cold molded specimens respectively is allowed (D20 Committee, n.d.). The temperature in the neighbourhood affects significantly the water-absorption value of specimen's material.

Hence the composite material shall be dried in an oven for 24 hrs. 50±3°C, then cooled and immediately weighed to the nearest 0.001 g.

The procedures followed to determine the percentage of water absorption capability of specimens given as shown below.

Procedures

1) First standard sized specimens were prepared and weight of each specimen was measured using the balance described on Tools and equipment's sub topic of this chapter.
2) After checked samples, free of any noticeable crack and voids, then they immersed in distilled water which was under normal condition (room temperature) for 24 hours.
3) After 24 hours immersion, the water on surface of specimens was cleaned and measured again the respective weights of each specimen.
4) Finally, the water absorption in percentage was calculated according the Equation 1, then average result obtained of the three specimens indicated percentage water absorption of the respective mix.

Having known the initial and final weight of each specimen, the percentage water absorption calculated using the formula given on Equation 1.

$$\%\mathbf{w} = \frac{\mathbf{final\ weight - initial\ weight}}{\mathbf{initial\ weight}}\mathbf{x100}\% \qquad \text{Equation 1}$$

3.7.2 Density

Density of composites can be determined using different methods. The most common and accepted by major researcher's ways of density determination are

1) Immersing of the specimen in to water stored in a jar of known volume, also the jar must be marked in order to show the change in volume
2) For regular shape specimens, density can be determined by calculating volume of specimen and measuring its weight.

3) Using theoretical method (mainly used for composite products) :- This method is working based on the rule of mixture.

To minimize potential measurement errors associated with dimensional calculations, the density of the composite specimens was determined using the water displacement method. The following procedures were followed:

1. Each specimen was cleaned and dried to remove any surface moisture or debris.
2. The mass of each specimen was measured using a calibrated digital weighing balance and recorded.
3. A jar was filled with a known initial volume of water (800 mL), and the volume was recorded.
4. The specimen was carefully immersed completely into the water, ensuring that it was fully submerged and that no air bubbles were trapped on its surface.
5. After immersion, the new water level was recorded.
6. The volume of the specimen was calculated by subtracting the initial water volume from the final water volume after immersion.
7. The density of each specimen was then calculated by dividing the measured mass by the displaced volume.

$$\rho = \frac{\mathrm{m}}{V_{final} - V_{initial}} \qquad \text{Equation 2}$$

where:

- ρ= density of the specimen
- m= mass of specimen
- $V_{initial}$= Initial volume of water in jar
- V_{final}= final volume (water and specimen)

8. The procedure was repeated for all specimens, and the average density value was reported.

Based on rule of mixture of composites the theoretical densities of specimens were also calculated to determine the percentage of voids according to ASTM 3203. Mathematically

$$\%\mathbf{void} = \frac{\boldsymbol{\rho_T - \rho_A}}{\boldsymbol{\rho_T}} \qquad \text{Equation 3}$$

Where $\rho_A = \text{Actual desntiy} = \frac{m}{V}$

$\rho_T = \text{Theoretical density}$

The theoretical density was calculated as following (refer Equation 4) based on the rule of mixture considering factors like volume fraction of crystalline and amorphous phases in High-Density Polyethylene (HDPE), density of reinforcement particle and matrix. The volume fraction of crystalline structure to amorphous structure depends on various factors such as processing conditions (e.g., cooling rate), molecular weight, and the crystallization behavior of the polymer (Mokarizadeh Haghighi Shirazi et al., 2020).

HDPE is known to have a relatively high degree of crystallinity compared to other polymers (Z. Wang et al., 2019). The crystalline fraction in HDPE typically ranges between 60% to 80% while the remainder of the HDPE structure, which is usually 20% to 40%, is amorphous (Ilinsky et al., n.d.). The amorphous fraction represents the disordered regions of the polymer where the chains are not arranged in a regular crystalline structure. Ignoring this arrangement difference (considering crystalline structure) here blow the equation implemented to obtain the values of each mix's theoretical density.

$$\rho = v_r\rho_r + (1 - v_r)\rho_m \qquad \text{Equation 4}$$

Where:

$\rho = \text{Theoretical density of composite}$
$v_r = \text{volume fraction of reinforcemnt particle}$
$\rho_r = \text{density of reinforcement particle}$
$\rho_m = \text{density of matrix}$

3.8 Mechanical properties Characterization

3.8.1 Tensile Strength

Tensile strength is materials ability to with stand (resist) failure under pulling (breaking) due to tensile stress. It is an important material property used for the design of construction and other structural members.

Tensile Testing Procedure

Tensile strength is a critical mechanical property for evaluating the performance of materials used in soft body armor applications. Materials in such applications must not only resist penetration but also maintain sufficient flexibility and strength to dissipate energy and prevent excessive deformation under tensile loading.

As termite mound clay-reinforced high-density polyethylene (HDPE) composites are being explored for their potential in body armor, understanding their tensile behavior is essential for assessing their suitability for real-world protective applications. Tensile testing provides key insights into a composite's strength, elasticity, ductility, and failure characteristics under uniaxial loading conditions. These parameters are especially relevant in the context of body armor, where materials may undergo stretching or pulling forces due to impact dispersion, body movement, or multi-axial stress during use.

Tensile tests were conducted in accordance with ASTM D638**,** the Standard Test Method for Tensile Properties of Plastics. This standard specifies specimen dimensions, test conditions, and procedures appropriate for HDPE and its composites.

Specimens were prepared based on the dimensions outlined in ASTM D638: a gauge length of 50 mm, overall length of 115 mm, a width of 13 mm at the narrow section, and a thickness of 3.2 mm. Three replications were prepared for each mix ratio, as shown in Figure 15. Specimens were manufactured via compression molding and were cooled under pressure of loading 770 N. All specimens were conditioned at room temperature ($23 \pm 2^{o}C$) prior to testing.

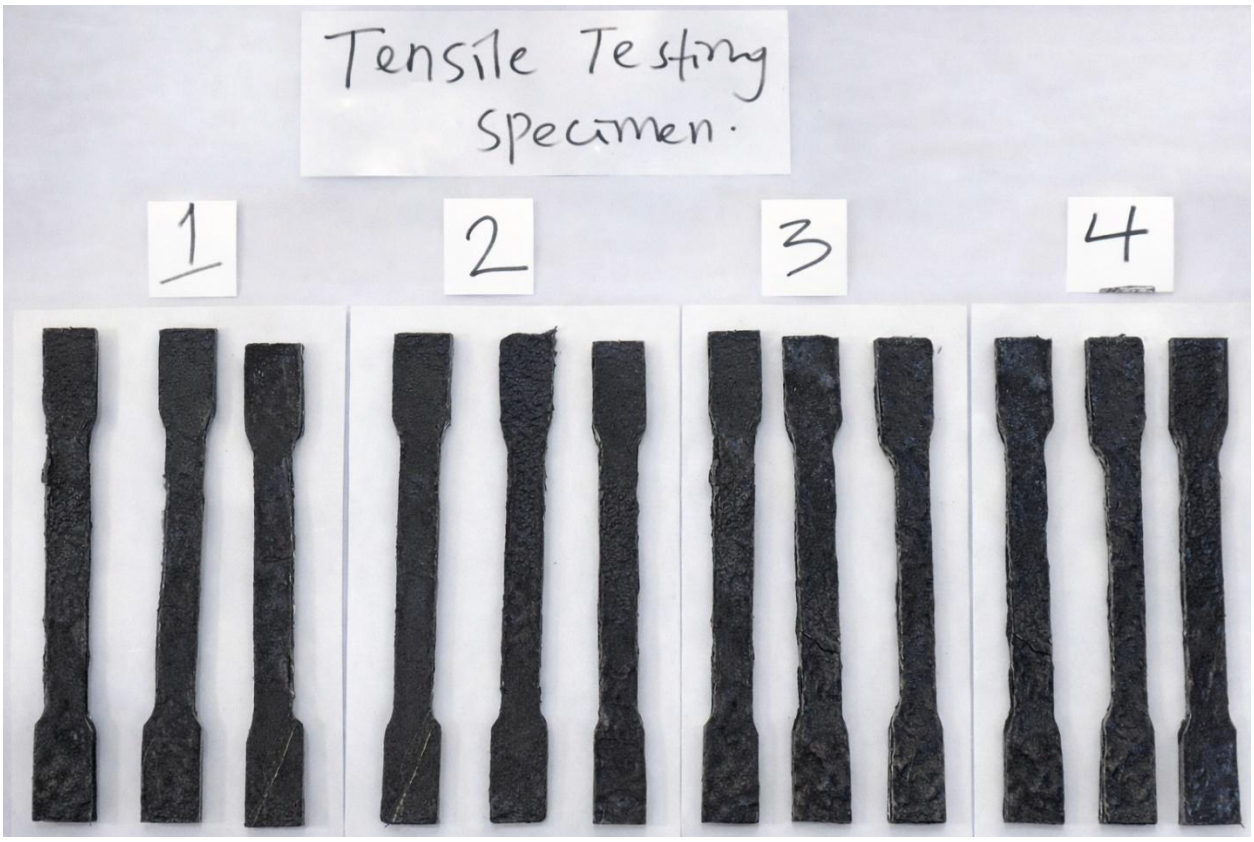

Figure 15 : Tensile Testing specimens

The following procedure was adopted to ensure that data from the tensile tests were recorded in a consistent and organized manner:

1. **Specimen Selection**: Specimens were selected and visually inspected to ensure they were free from notches, cracks, or surface defects that could negatively affect the test results. For each mix ratio, three replicate specimens were tested to ensure accuracy and reproducibility of results. Key physical dimensions (such as gauge length, specimen width and thickness) were recorded before testing.
2. **Machine Setup**: Before mounting the specimens, the testing machine's computer system was configured by inputting the necessary specimen information, including gauge length and width. The system was also set to record data and generates real-time load-deflection graphs.

3. **Testing and Data Collection**: The specimens were then mounted in the tensile testing machine, and the test was performed. During testing, data were recorded electronically in text files, and the load-deflection curve was displayed on the screen. Parameters such as maximum load, tensile strength, and elongation at break were derived from the test outputs. A visual representation of the test setup and apparatus is shown in the figure provided below.

Equations to Apply

The following equations were applied to calculate the key tensile properties of the composite specimens using the recorded values obtained from the universal tensile testing machine. These calculations were based on the ASTM D638 standard and were used to determine parameters such as tensile strength, strain, elongation at break, and modulus of elasticity. By applying these formulas to the measured dimensions and force data, the mechanical behavior of the HDPE–termite mound clay composites was quantitatively assessed and compared across different mix ratios.

Ultimate tensile strength

$$\boldsymbol{\sigma_{max} = \frac{F_{max}}{A}} \qquad \text{Equation 5}$$

Strain

$$\boldsymbol{\epsilon = \frac{\Delta L}{L_0}} \qquad \text{Equation 6}$$

Young's Modulus (Modulus of Elasticity)

This parameter, known as Young's modulus, can be determined from the initial, linear portion of the stress–strain curve, which represents the elastic behavior of the material. In this region, stress and strain are directly proportional, and the slope of the line reflects the stiffness of the specimen. A steeper slope indicates a stiffer material. Young's modulus is calculated as the ratio of stress to strain within this linear range and can also be evaluated using the equation provided below.

$$\mathbf{E} = \frac{\Delta\sigma}{\Delta\epsilon} \qquad \text{Equation 7}$$

Percentage Elongation

$$\textbf{Elongation}\ (\%) = \frac{\Delta L}{L_o}\mathbf{x100} \qquad \text{Equation 8}$$

In addition to the parameters calculated above, the data recorded from the universal tensile testing machine were also analyzed to determine the mode of failure of each specimen. This analysis helped to conclude whether the specimens exhibited brittle or ductile failure behavior, providing further insight into the mechanical performance of the HDPE–termite mound clay composites.

3.8.2 Flexural Strength

Flexural testing is employed to assess both tensile and compressive strengths of materials by subjecting them to beam-type loading. Commonly referred to in literature as the transverse beam test, it helps determine how materials behave under bending forces. In addition to tensile and compressive failure modes, materials such as armor components may also fail due to bending stresses, making flexural evaluation essential. These stresses can cause the material to deform and ultimately fail under bending loads.

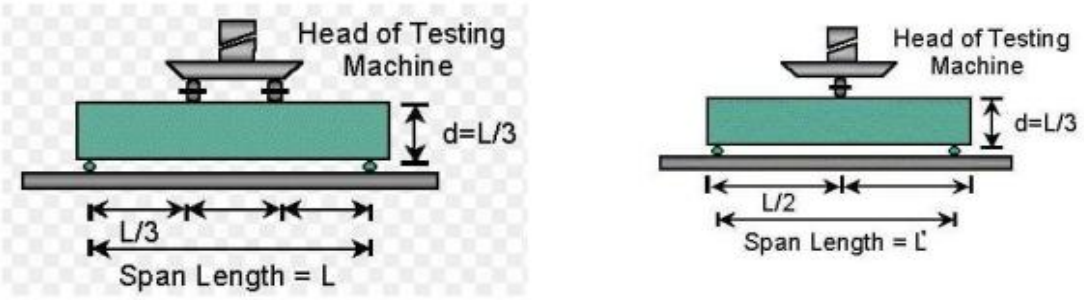

Figure 16 : Two-Point (ASTM C78) and one- Point Load test (ASTM C293)

The test setup configurations are shown in Figure 16, providing a visual representation of the apparatus arrangement. Studies suggest that the three-point bending test typically yields flexural strength values that are significantly higher than those obtained using four-point (center-point)

loading, due to the concentrated stress at a single loading point. For example, it has been observed that four-point loading often produces significantly lower flexural strength values compared to three-point testing and empirical results for instance, in dental polymers consistently demonstrate higher strength under three-point loading (Hein & Brancheriau, 2018). Per ASTM D790, the horizontal distance from the load application point to the nearest support should be 1.5 times the depth of the specimen, within a tolerance of ±2%. Figure 17 illustrates the proper test configuration.

Figure 17 : Diagrammatic View of a Suitable Apparatus for Flexure Test

According to the standard, specimen faces must be perpendicular to the loading surfaces, and free from defects such as scars or identification marks. While ASTM D790 outlines detailed testing procedures, practical application may vary depending on machine specifications. The steps followed in this study are summarized below:

1. **Specimen Preparation:** A total of 27 specimens were prepared and marked at the center to indicate the load application point.
2. **Dimensional Measurement:** Length, width, and height of each specimen were measured using a ruler or caliper.

3. **Surface Cleaning:** Contact surfaces on the specimen and rollers were cleaned to remove debris.
4. **Placement:** Specimens were placed on supports ensuring a minimum 10 mm overhang on each side; a 20 mm gap was maintained in this study. Placement considered mold direction as specified in ASTM, assuming the load was applied perpendicular to the mold filling direction.
5. **Loading:** Load was applied steadily, adhering to the machine's preset speed, and peak load and fracture type were recorded.

Load was applied ensuring that the strain rate remained within the limits of the low strain rate range (10^{-6}–10^{-3} s^{-1}). Several studies and research works have shown that the crosshead speed of the testing machine required to achieve a specified strain rate depends on the size and configuration of the test specimen. Accordingly, to determine the appropriate crosshead speed for the testing machine, the following equation was used:

$$\mathbf{V = \frac{\dot{\varepsilon} * L^2}{6 * t}} \qquad \text{Equation 9}$$

Where:

- v = crosshead speed (m/s)
- $\dot{\varepsilon}$= strain rate (s^{-1})
- L = support span (mm)
- t = specimen thickness (mm)

This equation allows for adjusting the machine's speed to ensure testing conditions fall within the desired low strain rate range.

6. **Data Recording:** The modulus of rupture was calculated to determine the flexural strength of each specimen.

In this study, flexural performance was assessed using 27 specimens, each measuring 140×20×10 mm, with three repetitions per mix. The specimens were simply supported at both ends and loaded

at a constant rate of 25 mm/min. This property is commonly determined using standardized methods such as the three-point bending test (ASTM D790) or the four-point loading test (ASTM D6272). Since the available equipment at the School of Civil Engineering, Mekelle University, supports center-point loading, ASTM D790 was adopted for this research (Figure 17).

The recorded values were then compared with values calculated which is given by,

$$\sigma_b = \frac{3PL}{2wt^2} \qquad \text{Equation 10}$$

Where σ_b = flexural strength (Modulus of rapture)

P = maximum applied load indicated by the testing machine (N)

L = span length (mm)

w = average width of specimen, at the fracture (mm)

t = average depth (thickness) of specimen, at the fracture (mm)

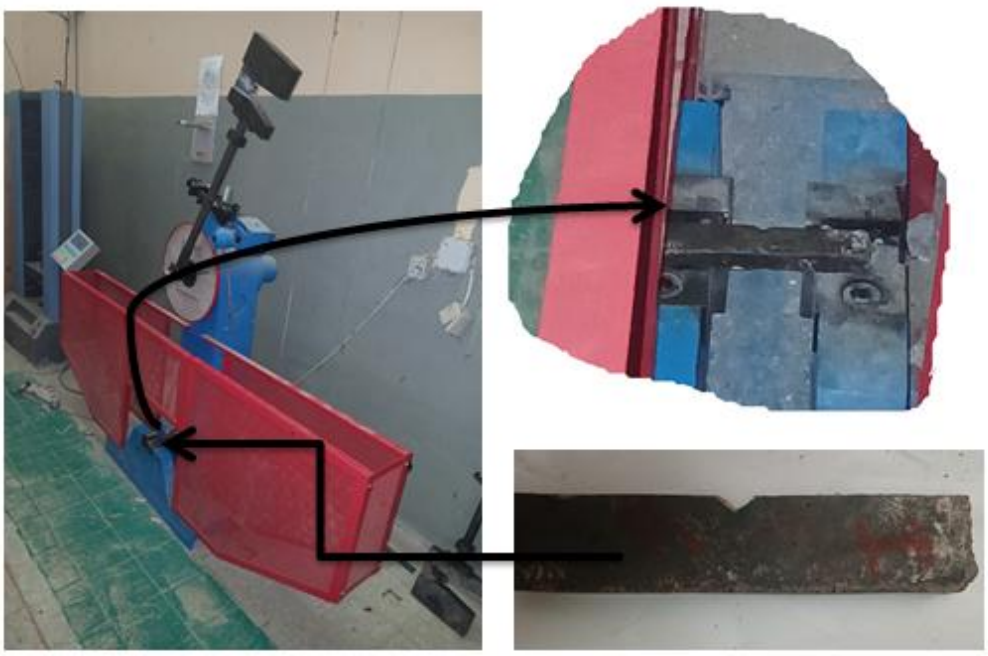

Figure 18 : Charpy Impact Testing Machine and set up (Material Testing lab, EiT-M)

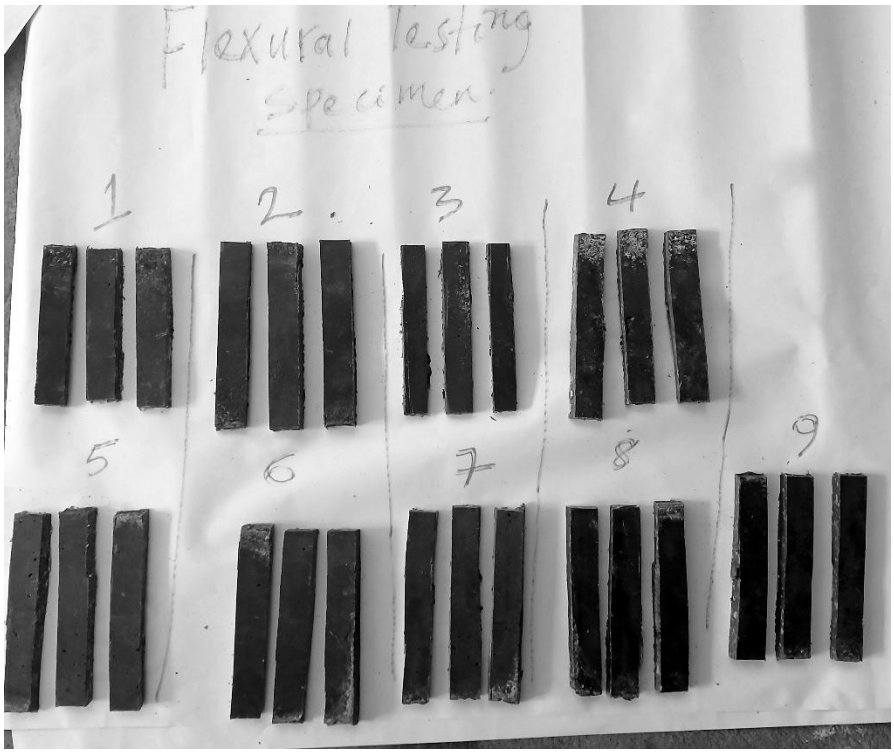

Figure 19 : Specimens for Flexural Testing

3.8.3 Impact Strength

In the development of materials for soft body armor applications, impact resistance is a critical performance metric. The ability of a material to withstand sudden, high-energy forces without catastrophic failure directly correlates with its protective capabilities. Termite mound clay-reinforced high-density polyethylene (HDPE) composites are being explored as potential alternatives or supplements to conventional armor materials due to their enhanced stiffness, toughness, and energy dissipation characteristics.

Impact testing is employed to evaluate the dynamic response of these composites under conditions that simulate blunt force or ballistic threats. This test helps to determine how effectively the material can absorb and dissipate energy, resist crack initiation and propagation, and maintains structural integrity upon sudden loading. For soft armor applications, such behavior is essential to minimize trauma and maximize wearer safety during impact events.

The following section details the methodology used to conduct impact testing on termite mound clay-reinforced HDPE specimens. Specimens were prepared and tested in accordance with ASTM D6110, which involves striking a notched specimen with a swinging pendulum and recording the energy absorbed during fracture.

For each mix ratio, developed based on the Design of Experiments (DOE), rectangular specimens with dimensions of 135 × 20 × 10 mm were manufactured. Three replications were made for each mix. A V-notch (2 mm deep at a 45° angle) was machined into each specimen to serve as a stress concentrator.

Each test specimen was then mounted horizontally on the supports of a Charpy impact testing machine, as illustrated in

Figure 18. According to the standard, the notch should be on the side opposite the pendulum (facing away from the striker), to create a stress concentration point where fracture initiates and be centered at the point of impact to ensure accurate results.

During testing, the pendulum is released from a known height and allowed to swing downward, striking the specimen at the notched section. There are two possible outcomes: either the specimen fractures as the pendulum continue its swing upward on the opposite side, or the specimen remains unbroken. If the specimen does not fracture, it indicates that the material is capable of absorbing the entire energy stored in the pendulum. In such cases, either the pendulum's mass or its release height must be increased to provide higher impact energy, as both parameters are directly related to potential energy.

If the specimen fractures upon impact, the height reached by the pendulum after the break is recorded. The energy absorbed by the specimen is then calculated based on the difference in potential energy before and after impact, as determined by the swing height as provided in Equation 11. Mathematically,

$$\mathbf{E = P.E_1 - P.E_2} \qquad \text{Equation 11}$$

Where

$$E = \text{Energy absorbed}$$

$$P.E_1 = \text{pendulum potential energy before impacting the specimen (J)}$$

$$= mgh_1$$

$$h_1 = pre - \text{release postion height (m)}$$

$$P.E_2 = \text{pendulum potential energy impacting the specimen (J)}$$

$$= mgh_2$$

Having obtained the energy absorbed, the impact strength is calculated based on the Equation 12 specified below.

$$\textbf{Impact Strength} = \frac{\mathbf{E}}{\mathbf{b} * \mathbf{d}} \qquad \text{Equation 12}$$

For, Impact Strength in $\frac{kJ}{m^2}$

$$b = \text{specimen width (m)}$$

$$d = \text{specimen thickness (m)}$$

In addition to the values obtained, it is also necessary to record whether the specimen breaks completely or partially, as both outcomes have different interpretations. A complete break indicates lower toughness, meaning the material absorbs less energy before fracturing. This type of failure is typically associated with rigid fillers such as clay and is reported as brittle fracture.

In the case of a partial break, the specimen does not fully separate but may remain attached at one end or show significant deformation. Such failure indicates higher toughness and ductility,

meaning the material absorbs more energy during fracture. These results are reported as ductile fracture. Therefore, these fracture characteristics were recorded for each specimen during testing.

Impact Velocity

During the impact testing process using a Charpy impact testing machine, the impact velocity the speed at which the pendulum strikes the specimen was also determined. This value is not directly measured, but rather derived from fundamental physical principles, specifically the law of conservation of energy. This law states that energy cannot be created or destroyed, only transformed from one form to another. In the context of the Charpy test, the potential energy stored in the pendulum at its raised initial position is converted entirely into kinetic energy as it swings downward toward the specimen.

At the lowest point of the pendulum's arc just before impact this kinetic energy reaches its maximum, and from this, the velocity of impact can be calculated. The relationship between potential and kinetic energy provides a straightforward way to estimate this velocity using known parameters such as the mass of the pendulum and the height from which it is released. Based on this energy-based approach, and consistent with values reported in previous studies, the impact velocity for standard Charpy testing conditions is typically around 5.2 meters per second.

$$\textbf{Mechanical Energy}_1 = \textbf{Mechanical Energy}_2 \qquad \text{Equation 13}$$

$$\mathbf{mgh_1} + \frac{\mathbf{1}}{\mathbf{2}}\mathbf{mv_1^2} = \mathbf{mgh_2} + \frac{\mathbf{1}}{\mathbf{2}}\mathbf{mv_2^2}$$

But the pendulum was initially at rest hence $v_1 = 0$ m/s and final position of the pendulum was at origin based on the relative reference taken, which mean $h_2 = 0$ m. Substituting and rearranging

$$\mathbf{v_2} = \sqrt{\mathbf{2gh_1}} \qquad \text{Equation 14}$$

Where $g =$ accleration due to gravity $\left(\frac{m}{s^2}\right)$

$h_1 =$ initial pendulum vertical position (m)

3.9 Analytical Software and Data Analysis Approaches

As described in the earlier sections, the raw materials (waste HDPE plastic and termite mound clay) were collected, processed (crushed and sieved), and used to manufacture composite specimens intended for body armor applications. The specimen formulations were developed based on a pre-specified Design of Experiment (DoE) to assess the effect of various composition levels on the physical and mechanical performance of the composites.

The results obtained from characterization tests (e.g., density, tensile strength, flexural strength, and impact resistance) were statistically analyzed using Minitab software version 19. The primary goal of the analysis was to evaluate the influence of multiple factors on each property of the composite specimens and identify significant patterns or interactions among variables.

Taguchi Design and Orthogonal Array

To reduce the number of experimental runs while maintaining analytical effectiveness, a Taguchi design was created using Minitab's DOE module (Figure 20). An orthogonal array format was selected to systematically vary key input factors (e.g., percentage of termite mound clay, time of mixing and particle size). This design allowed the experiment to evaluate multiple factor combinations efficiently, ensuring that factor interactions could be observed and statistically validated.

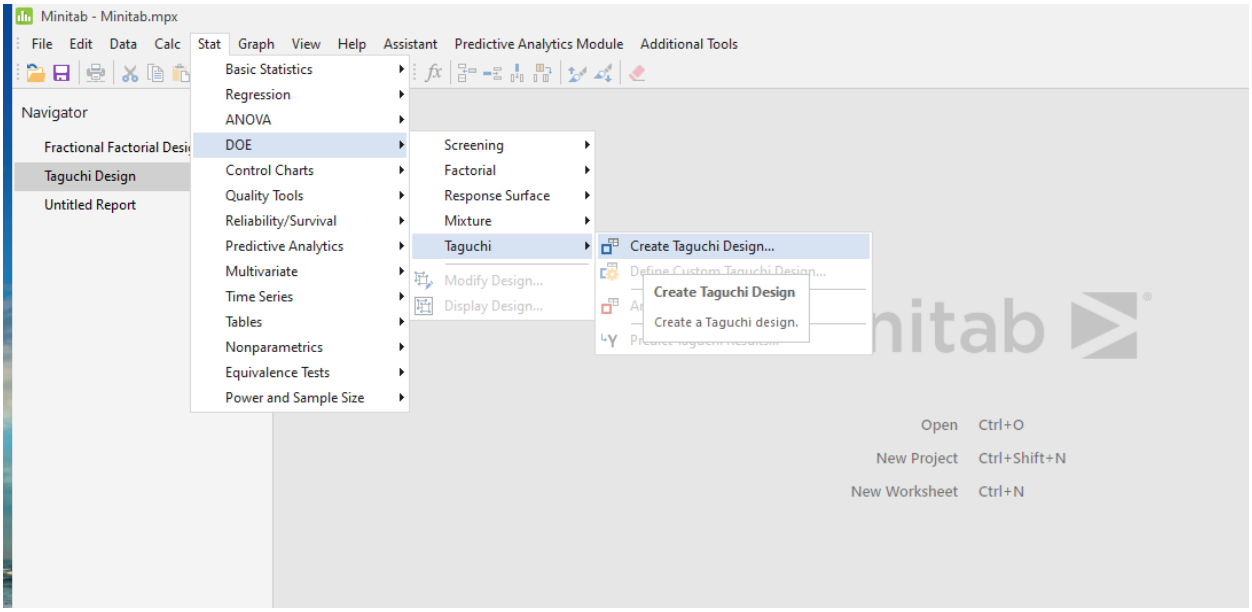

Figure 20 : Minitab's DoE module

Descriptive and Graphical Analysis

It is known that to analyze the influence of processing parameters on the physical and mechanical performance of termite mound clay-reinforced HDPE composites for body armor, a Taguchi design of experiment was implemented in Minitab 19. The analysis was based on three critical process variables, each varied at three levels:

- ✓ Factor A: HDPE weight ratio (70%, 80%, 90%)
- ✓ Factor B: Mixing time (5 min, 15 min, 25 min)
- ✓ Factor C: Clay particle size (63-90 µm, 90-125 µm, 125-150 µm)

The objective was to determine how each factor and their interactions influence mechanical (e.g., tensile strength, flexural strength) and physical (e.g., density, moisture absorption) properties of the composite. After inputting the test data into Minitab, several statistical tools and plots were generated, as here below discussed.

Main Effects Plots

Main Effects Plots were generated using Minitab to show the average response value (e.g., tensile strength or density) at each level of a given factor. These plots help determine whether changing a factor has a significant effect on a particular property.

Each factor's influence was isolated, holding others constant, to assess its individual effect on composite performance.

Interaction Plots

While main effects plots evaluate factors individually, interaction plots assess how two factors behave together and whether the effect of one factor depends on the level of another.

These insights are critical in optimizing the formulation of body armor composites, as material properties often depend on synergistic effects.

Analysis of Variance (ANOVA)

A one-way and multi-factor ANOVA was performed under the General Linear Model (GLM) module to determine whether variations in input factors led to statistically significant changes in composite properties. The output table generated from Minitab included:

- ✓ Degrees of freedom (DF),
- ✓ Sum of squares,
- ✓ F-values,
- ✓ P-values.

The p-value was particularly important in determining the statistical significance of each factor. At a confidence level of 95% ($\alpha = 0.05$), a p-value below 0.05 indicated that the factor had a significant effect on the response. This allowed for acceptance or rejection of hypotheses.

Hypotheses Used in the Analysis

- ✓ Null Hypothesis (H_0): Changing the levels of termite mound clay particle size, mixing time or HDPE weight ratio has no significant effect on the mechanical or physical properties of the body armor composite.
- ✓ Alternative Hypothesis (H_1): Varying the levels of termite mound clay particle size, mixing time or HDPE weight ratio significantly affects the mechanical or physical properties of the body armor composite.

The ANOVA results were used to draw conclusions about which factors most significantly affected composite performance and which combinations yielded optimal results.

Signal-to-Noise Ratio Analysis

To evaluate the influence of each factor on the composite's performance, the Signal-to-Noise (S/N) ratio was calculated for each property based on its desired outcome.

- ✓ For physical properties (density and water absorption), the "smaller-the-better" criterion was applied, as lower values are preferable to minimize weight and moisture uptake.
- ✓ For mechanical properties (tensile strength, flexural strength, and impact strength), the "larger-the-better" criterion was implemented to maximize the material's strength and toughness.

The S/N ratio values were then used to identify the most prominent factors influencing each property and to determine the optimal level of each factor.

CHAPTER-4

RESULT AND DISCUSSION

This section thoroughly analyzes the experimental results from testing composite specimens made of recycled high-density polyethylene (HDPE) reinforced with termite mound clay. As tried to mention in the above sections the study aimed to assess the material's physical and mechanical properties to determine its suitability for real-world applications (body armor purpose).

Key findings include measurements of physical properties such as density and water absorption, along with mechanical performance indicators like tensile, impact, and flexural strength. For clarity, all results were systematically presented in tables, facilitating easy comparison. In addition to data reporting, the discussion interprets the observed trends, explaining the material’s behavior and the mechanisms influencing each outcome.

As outlined in the methodology, Minitab statistical software was used to analyze the experimental data. This chapter integrates Minitab’s analytical outputs to validate trends, assess variability, and determine the significance of the results. Each finding is explained in terms of its physical implications, with any anomalies critically evaluated. The analysis connects the composite’s performance to its composition, microstructure, and processing conditions, offering a comprehensive understanding of its behavior under different mechanical and environmental stresses.

4.1 Physical Property Characterization

4.1.1 Percentage of Water Absorption

To determine the amount of water absorbed, specimens of each mix with three replications immersed in to water for 24 hours. The data required to determine the percentage of water absorbed were the initial weight of each specimen and weight after 24 hours immersed in water. The initial and final weights termed in some literatures as dry and wet weight respectively. Then based on Equation 1 of previous section the percentage of water absorption determined. Here below is given

table show summarized initial, final and change in weight of each of the nine specimens and percentage water absorption of each mix calculated according to Equation 1.

Table 4 : Percentage of water absorbed by each specimen

Mix No.	Initial Weight (g)			Final weight (g)			Percentage of water absorbed (%)			
	S-1	S-2	S-3	S-1	S-2	S-3	S-1	S-2	S-3	Avg.
1	13.25	8.72	12.588	13.27	8.75	12.6	0.15	0.34	0.10	0.20
2	12.85	13.32	13.52	12.854	13.34	13.53	0.03	0.15	0.07	0.09
3	8.44	11.25	10.01	8.46	11.26	10.02	0.24	0.09	0.10	0.14
4	10.58	13.47	12.54	10.595	13.47	12.56	0.14	0.00	0.16	0.10
5	12.385	12.57	12.961	12.4	12.58	12.973	0.12	0.08	0.09	0.10
6	16.25	14.02	14.16	16.26	14.036	14.17	0.06	0.11	0.07	0.08
7	13.27	17.17	14.3	13.31	17.2	14.353	0.30	0.17	0.37	0.28
8	13.55	14.49	13.93	13.57	14.52	13.94	0.15	0.21	0.07	0.14
9	12.84	11.92	12.58	12.85	11.93	12.583	0.08	0.08	0.02	0.06

In general, as noted from the table presented above (Table 4), the water absorption values for every specimen are very close to the values typically obtained for plastic materials. In addition, the variation between the three replicate samples (S-1, S-2, and S-3) for every mix is very small, demonstrating a very good level of repeatability and consistency in specimen preparation and testing. The water absorption percentages for all the specimens are less than 0.5%, a value that is considered to be negligible. The results demonstrate that the composite material developed has excellent resistance to moisture, making it suitable for use in applications involving exposure to water.

The experimental design involves three variables plastic weight ratio, mixing time, and termite mound clay particle size, each investigated at three levels. There is a need to consider the individual effects of each variable and its respective levels on water absorption. Hence here below is discussed the factor level effects on water absorption by grouping the appropriate mixes. In this

method of analysis only one factor is considered as active ignoring the other two factors, such that if plastic ratio is considered both mixing time and particle sizes are ignored.

To further confirm and visualize the experimental results, Main effects plot for all the factors involved were constructed with the aid of Minitab 19 statistical software. These graphical plots make it easier to visualize which particular levels of each factor have the most significant effect on the water absorption behavior of the termite mound clay-reinforced HDPE composite. The interpretation is based on the trends and slopes of the lines shown in the plots, for example, a steep downward slope indicates a large effect, while a horizontal line means little or no effect, and a curved line could imply a nonlinear relationship. This visual evaluation aids in the understanding of each individual factor's contribution to the composite material's overall performance.

Table 5: Factor A (Plastic Weight Ratio)

Plastic Ratio	Mixes	Avg. Absorption
90%	1, 2, 3	(0.20 + 0.09 + 0.14)/3 = **0.14**
80%	4, 5, 6	(0.10 + 0.10 + 0.08)/3 = **0.093**
70%	7, 8, 9	(0.28 + 0.14 + 0.06)/3 = **0.16**

By examining the results provided in Table 4, which outlines data pertaining to various levels of the three factors, the average water absorption for the respective levels of weight ratio was calculated and summarized in Table 5. Based on these results, samples with an 80% plastic weight ratio demonstrated the lowest average water absorption compared to those with 70% and 90% plastic content. By contrast, samples with a plastic ratio of 70% displayed the highest water absorption, indicating lower resistance to water penetration. This trend indicates that both too high a proportion of plastic (90%) and too low a proportion (70%) weaken the water absorption resistance of the composite as shown also in Figure 21 that indicates the percentage water absorption due to plastic weight.

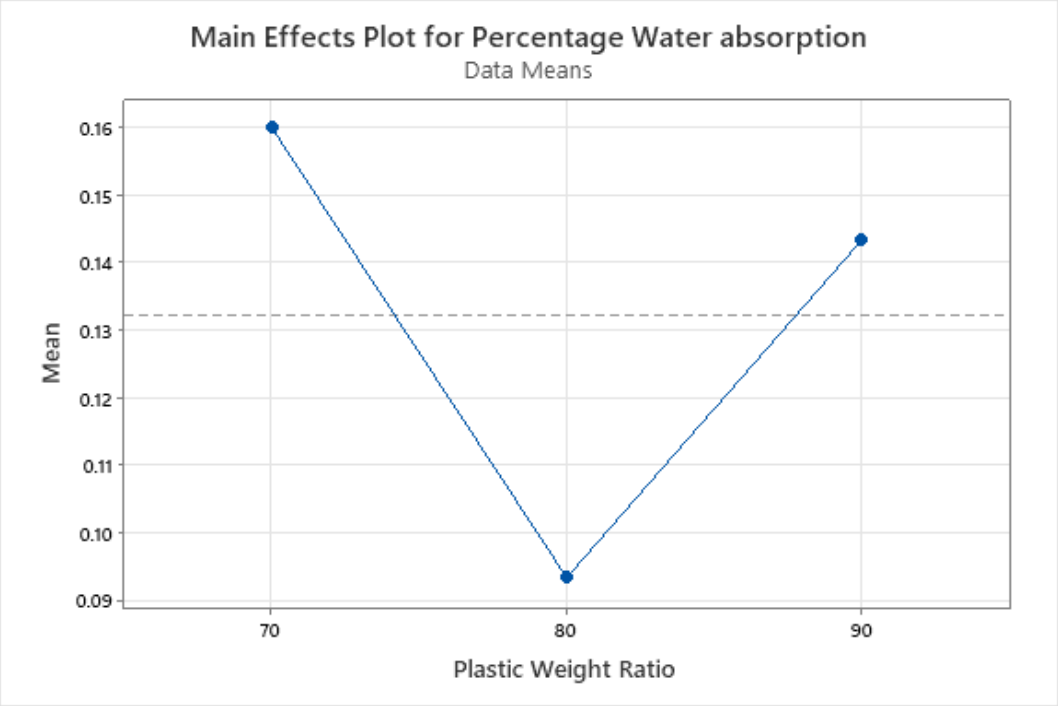

Figure 21 : Main Effects plot of water absorption due to plastic weight ratio variation

The probable reason for this is that too high proportion of plastic can prevent efficient incorporation and homogeneous dispersion in the clay matrix, creating poor structural bond and micro-voids. Too low a proportion of plastic, on the other hand, may not ensure adequate binding or cohesion among particles, causing a more open structure with increased water penetration. Thus, the 80% plastic proportion seems to present an optimum trade-off for improved matrix development and reducing voids responsible for water absorption.

Mixing time

It is clear that the water absorption is favorably affected by increasing the mixing time. That is, as the mixing time is increased, the water absorption of the composite is lowered. This is because longer mixing times enhance the distribution of the termite mound clay particles (reinforcements) in the molten high-density polyethylene (HDPE) plastic matrix. Better distribution increases the homogeneity of the composite material and minimizes the creation of micro-voids or weak points that will absorb water.

Table 6: Factor B (Mixing Time)

Mixing Time	Mixes	Avg. Absorption
5 min	1, 4, 7	(0.20 + 0.10 + 0.28)/3 = **0.193**
15 min	2, 5, 8	(0.09 + 0.10 + 0.14)/3 = **0.11**
25 min	3, 6, 9	(0.14 + 0.08 + 0.06)/3 = **0.093**

The results shown in Table 6 confirm this observation. That is, the mixing time of 25 minutes had the lowest water absorption average, reflecting better matrix-reinforcement particle integration. The enhanced bonding and dispersion are probably responsible for a less porous and denser composite structure.

Conversely, a shorter mixing time of 5 minutes resulted in a significantly higher percentage of water absorption. More precisely, the water absorption after 5 minutes of mixing was approximately 107.53% higher than that at 25 minutes and 75.5% higher than at 15 minutes. The results strongly underscore the critical role of adequate mixing time in allowing the uniform dispersal of clay particles and the achievement of a water-resistant and cohesive composite structure.

The main effects plot (Figure 22), generated using Minitab 19 statistical software, confirms these findings. As can be seen in the plot, the rate of reduction in water absorption gets increasingly pronounced as the mixing time is increased from 5 minutes to 15 minutes compared to the change achieved from 15 minutes to 25 minutes. This is confirmed by the steeper slope of the line between 5 and 15 minutes, representing a greater effect within this timeframe. However, beyond 15 minutes, the slope of the line becomes less steep, meaning that there is little added benefit of increasing mixing time beyond 25 minutes.

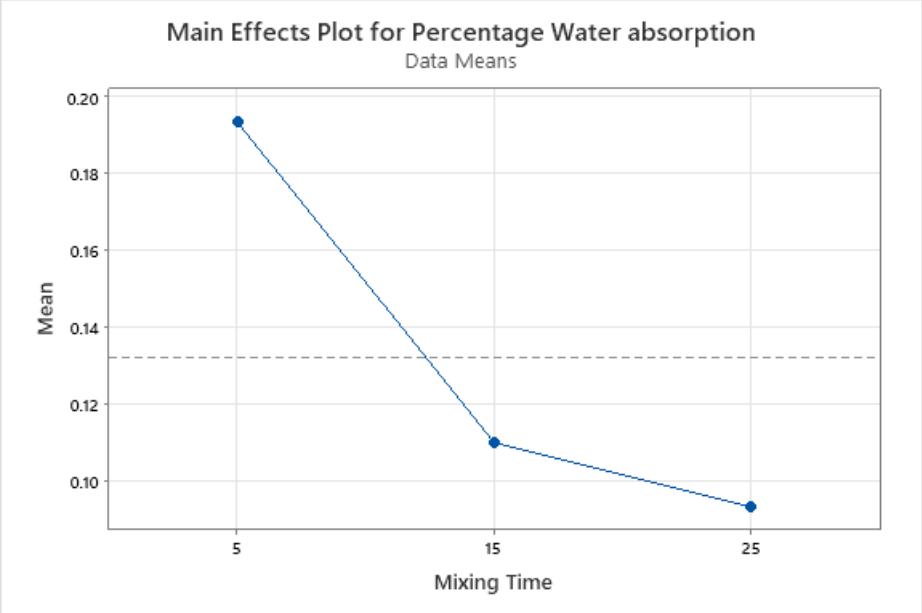

Figure 22 : Main Effects plot of water absorption due to mixing time variation

Though extended mixing time improves water resistance; there could be some practical limitations. Extended mixing is likely to cause a loss in the workability of molten HDPE as it continuously cools and solidifies with time. If not controlled properly, this could have a negative effect on the uniformity and quality of the end product. Therefore, while a longer mixing time is recommended for water resistance improvement, it needs to be balanced with the thermal and rheological properties of HDPE for ensuring efficient processing.

Particle Size

The particle size of the particles in termite mound clay has a profound effect on the water retention capacity of the composite material, and this effect can be either positive or negative depending on the range of particle size. When the particle size is very fine there is a significant increase in surface area. This increased surface area can lead to the agglomeration or clustering of particles upon incorporation into the molten HDPE plastic matrix. The agglomerates are responsible for the creation of voids and porosity in the composite material, thus increasing its capacity for water absorption.

Conversely, the addition of coarse clay particles from termite mound could result in increased porosity, though for different reasons. The addition of bigger particles tends to create more void spaces in the matrix, which is due to less effective packing and a lower surface contact area with the plastic matrix. These voids also create channels for water penetration, thus increasing absorption.

Table 7: Factor C (Particle Size)

Particle Size	Mixes	Avg. Absorption
63 µm	1, 6, 8	(0.20 + 0.08 + 0.14)/3 = **0.14**
90 µm	2, 4, 9	(0.09 + 0.10 + 0.06)/3 = **0.083**
125 µm	3, 5, 7	(0.14 + 0.10 + 0.28)/3 = **0.173**

These findings were also validated by the results in Table 7. The maximum water absorption percentage was noted in samples that had termite mound clay particles of 125-150 µm (coarse), followed by 63-90 µm (fine) and then 90-125 µm (medium). Notably, the fine and coarse particle sizes had water absorption deviations of about 68.7% and 108.4%, respectively, from the medium particle size range (90-125 µm).

These results imply that water uptake increases more noticeably with increasing particle size outside an optimal range, as compared to decreasing particle size. Hence, an intermediate particle size like the range 90-125 µm seems to offer the optimal trade-off, reducing porosity and improving the composite's resistance to water absorption.

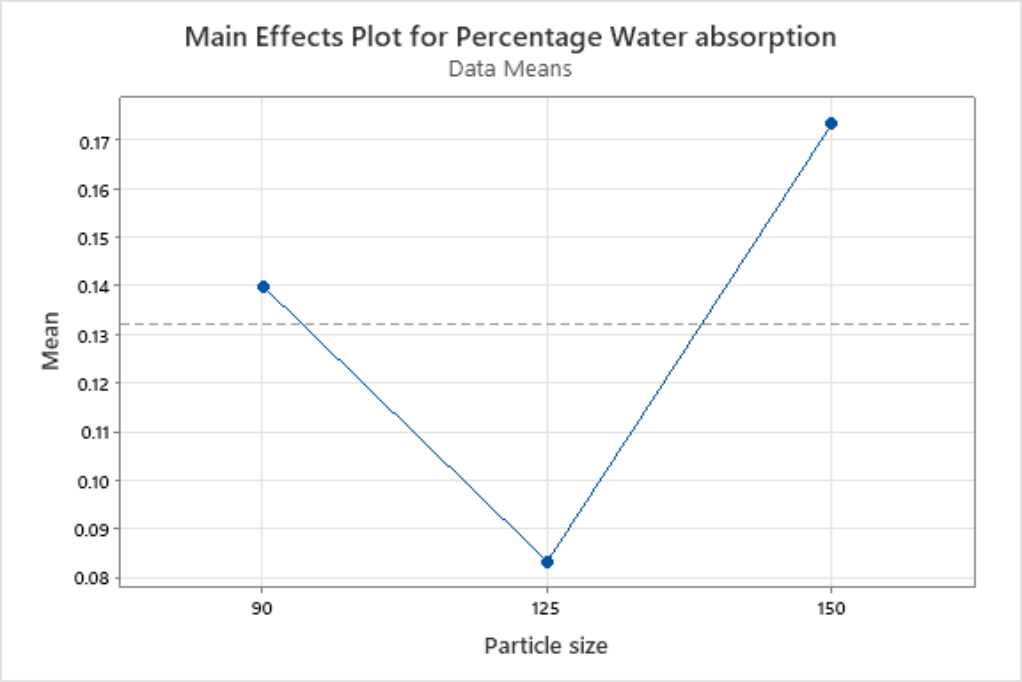

Figure 23 : Main Effects plot of water absorption due to Particle size variation

Interaction Plot

An interaction plot was also created via Minitab 19, founded on the data obtained from separate specimens produced as per the Design of Experiments (DOE). The main reason for creating this plot is to graphically analyze how the interaction of two factors affects the response variable, in this scenario being the water absorption percentage.

Main effects plots show the separate effect of each variable on water absorption; in contrast, interaction plots provide a more nuanced view of the relationship between two variables namely, whether one variable's effect depends on the level of the other. This effect is assessed by examining the pattern of the lines in the interaction plot:

When the lines are parallel, it means that the factors have independent action with no interaction.

The crossing or spreading apart of the lines signifies a statistically significant interaction, which means that the combined effect of the two variables is not the same as the sum of their individual effects.

In the context of this study, interaction plots are used to determine whether the combinations of plastic weight ratio, mixing time, and clay particle size have nonlinear or synergistic impacts on water absorption. Understanding these interactions is important for optimizing the composite formulation to improve water resistance.

From this background, the next section gives an analysis of the interaction effects of the factors examined on the percentage water absorption, based on the interaction plots from Minitab statistical software.

Interaction effect of plastic weight ratio and mixing time on water absorption

Figure 24 shows how the combination of plastic weight ratio (70%, 80%, 90%) and mixing time (5, 15, and 25 minutes) affects water absorption in the termite mound clay-reinforced HDPE composite. The y-axis displays the average water absorption percentage, and each line on the plot represents a different mixing time.

Looking at the plot, it's clear that the effect of plastic weight ratio on water absorption depends a lot on the mixing time, which means these two factors interact in an important way. It can be seen this from the lines crossing and not being parallel which indicates that understanding one factor requires considering the other. Here below is discussed in detail how the levels of each factor interact with the other factor and their combined impact on water absorption of the composite.

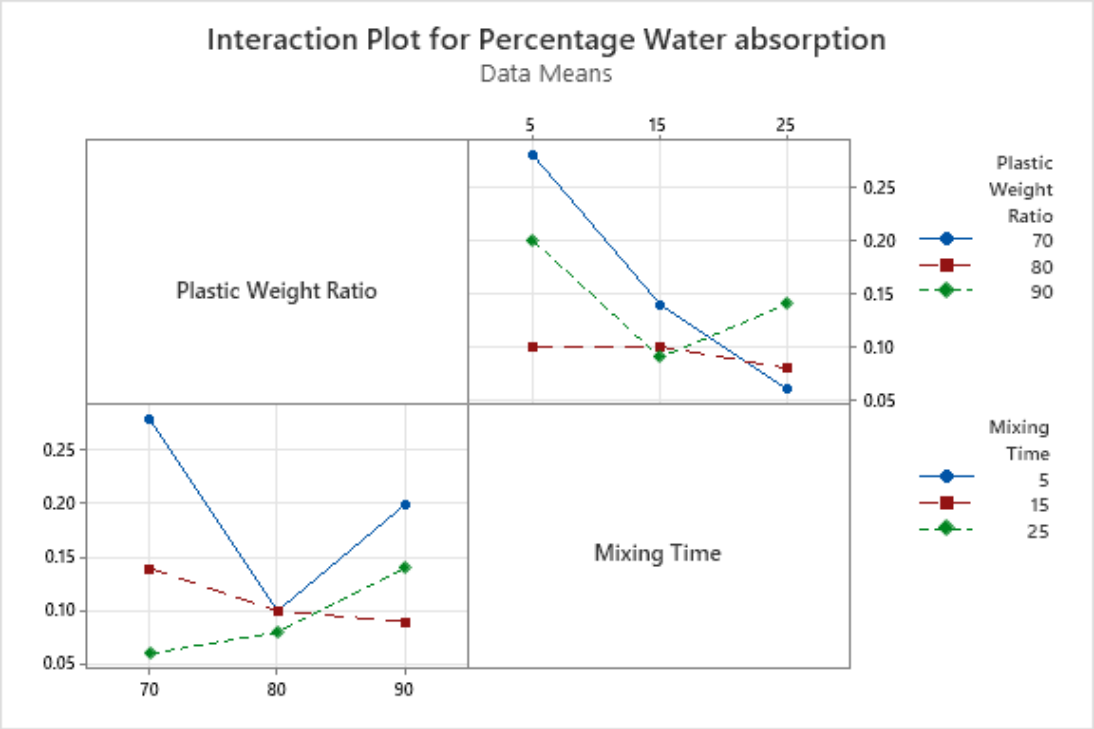

Figure 24 : Interaction plot of plastic weight ratio and mixing time on water absorption

At 5 minutes of mixing time (Blue solid Line) water absorption drops sharply when increasing plastic content from 70% to 80%, but then rises again at 90%. This suggests that around 80% plastic is the best at shorter mixing times, probably because it mixes and bonds more evenly. But the increase in water absorption at 90% could be due to weaker bonding or more voids forming because the mix wasn't good enough at higher plastic levels and shorter mixing time.

At 15 minutes of mixing time (Red Dashed Line) water absorption stays fairly consistent across different plastic amounts, with just a slight decrease as plastic increases. This shows that 15 minutes might be enough time for the material to mix evenly, no matter how much plastic is used to manufacture the composite.

At 25 minutes of mixing time (Green Dotted Line) water absorption is at its lowest overall, suggesting that longer mixing makes the layers bond better and creates fewer voids. However, at 90% plastic, there's a small increment in water absorption again, probably because too much mixing causes particles to accumulate together or spread unevenly.

In general, the plot makes it clear that plastic amount and mixing time work together and for the lowest water absorption, the best conditions seems 80–90% plastic with 25 minutes of mixing, or 80% plastic with 15 minutes of mixing.

This emphasizes that how important it is to find the right balance of both factors. Just adding more plastic won't necessarily make the composite more water-resistant unless it’s mixed properly to get good dispersion and bonding between the plastic and filler.

Interaction effect of Plastic weight ratio and Particle size

The interaction plot (Figure 25) shows how both the plastic weight ratio at 70%, 80%, and 90% and the clay particle size at 90 µm, 125 µm, and 150 µm together affect the percentage water absorption of termite mound clay-reinforced HDPE composite. As tried to mention above the y-axis shows the average water absorption values, and each line represents different particle sizes.

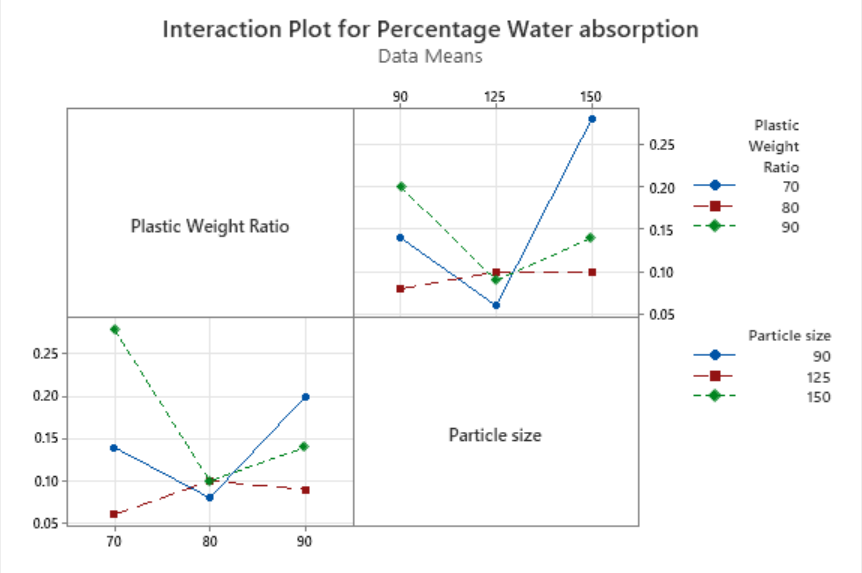

Figure 25 : Interaction plot of plastic weight ratio and particle size on water absorption

Based on the plot generated the way plastic weight ratio affects water absorption really depends on the particle size. For example, with the smallest particles at 63-90 µm (the blue line), water absorption drops a bit when increasing plastic content from 70% to 80%, but then jumps back up

at 90%. On the other hand, the 90-125 µm particles (the red dashed line) show pretty consistent water absorption no matter how much plastic is added. The largest particles at 125-150 µm (the green dotted line) have a bumpier pattern with highest absorption at 70% plastic, dropping at 80%, and then rising again at 90%.

The way the lines cross and don't run parallel confirms that the effect of plastic content on water absorption really depends on the particle size, and vice versa. Basically, picking the right combo of plastic percentage and clay size is super important to keep water absorption low. For instance, 80% plastic seems to give the lowest water absorption overall, making it a pretty good target. Also, smaller particles might help improve bonding and lower absorption at moderate plastic levels, but that advantage might fade or even backfire at higher plastic ratios due to agglomeration. Overall, this plot just goes to show how essential it is to consider both plastic weight and particle size together to develop a composite with better water resistance.

Interaction effect of Mixing time and particle size

Interaction plot (refer Figure 26) illustrates the combined effect of mixing time (5, 15, and 25 minutes) and clay particle size (90 µm, 125 µm, and 150 µm) on the percentage water absorption of the termite mound clay-reinforced HDPE composite. The plot indicates that mixing time interacts significantly with particle size, as evidenced by the lines not being parallel and the different trends for those factor levels. Here below is discussed in detail.

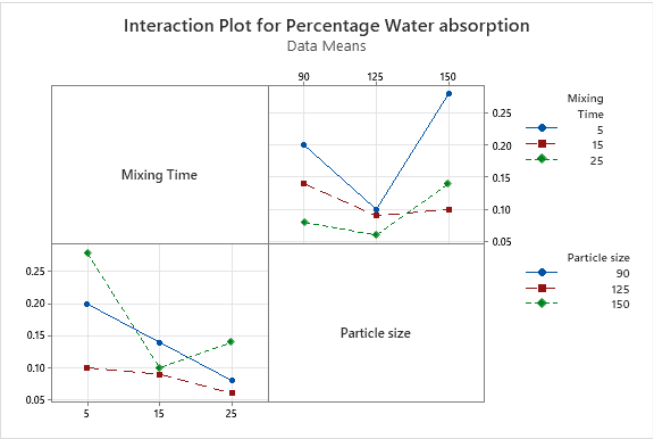

Figure 26 : Interaction plot of mixing time and particle size on water absorption

The figure presented above illustrated that for the smallest particle size, of 63-90 μm (blue line), water absorption decreased markedly as mixing time increased from 5 to 25 minutes, implying that longer mixing times lead to better dispersion and bonding of finer clay particles into the HDPE matrix, hence less water uptake. Compared to this, for particle size of 90-125 μm, medium level of particle (red dashed line), and water absorption pretty much remains unaltered significantly over a range of mixing times except for a slight downward trend at longer mixing durations. This suggests that even medium-sized particles are dispersed uniformly within the matrix even at shorter mixing times; hence mixing time has less significant effect on water absorption.

The 125-150 μm size (green dotted line), however, has the trend of distinct initial decrease upon increasing the time from 5 to 15 minutes but soon after tends to a slight increase at the 25 minutes mark. It apparently suggests that particle dispersion and low water absorption follow from moderate mixing times but that extreme mixing can result in agglomeration of particles or adverse changes in composite structure due loose of workability of the molten plastic, which will eventually lead to high water uptake.

Overall, mixing time has a different effect on water absorption for different particle sizes. Fine particles benefited significantly from longer mixing times, while coarser particles had less than optimal water resistance when mixed for longer periods. These results showed that water absorption in the composite material can be improved by optimizing both mixing time and particle size together.

In general, the interaction plots from experiment with the termite mound clay-reinforced HDPE composite clearly give evidence of significant interaction effects of the factors under test which were plastic weight ratio, mixing time, and clay particle size-on percentage water absorption.

Each plot reveals the dependence of these factors and their complex interaction in affecting water absorption. The interaction of plastic weight ratio and mixing time shows an example in which the optimal plastic content for minimizing water absorption depends on mixing duration and suggests that adequate mixing would help to achieve better bonding. Likewise, the plastic weight ratio and particle size interaction shows that the effectiveness of plastic content in reducing water absorption

depends on clay particle size and that some combinations yield lower absorption due to better dispersion and bonding.

In all the interactions, the combination between mixing time and particle size: the finer the particle size, the more it would benefit under longer mix times. Coarse particles would not benefit similarly; rather, there would probably be decline or negative effects of longer mixing times, possibly due to agglomeration and loose of workability.

Generally it can be concluded that the interaction plots showed it is mandatory to optimize all specified processing parameters (amount of plastic, mixing time and particle size) at the same time in order to improve water resistance in the composite as performance improvements cannot arise by considering a single factor in isolation.

Signal-to-Noise Ratio Analysis

The Signal-to-Noise (S/N) ratio analysis was performed based on the "smaller-is-better" criterion in order to capture the variability and robustness of the results since the average-based analysis performed and obtained above does not completely indicate the performance consistency across replications. The following sections display and discuss these results in detail which mainly focused on response table analysis of variance for signal to ratios.

The response table for Signal-to-Noise (SN) ratios illustrated below in Table 8 gives useful clues about how different factors like Plastic Weight Ratio, Mixing Time, and Particle Size impact how reliably the system absorbs water. The SN ratios tells how steady the signal is compared to noise, so higher numbers mean better consistency with less fluctuation.

Table 8 : Response Table for Signal to Noise Ratios

Level	Plastic Weight Ratio	Mixing Time	Particle Size
1	16.83	13.99	16.98
2	20.00	18.88	20.68
3	16.43	20.39	15.61
Delta	3.57	6.40	5.07
Rank	3	1	2

Out of all the factors, Mixing Time stands out with a big delta value of 6.40, which means it causes the most variation in SN ratios across its different levels. Basically, thinking how long mixed really can make a big difference in how consistent the water absorption behaves. Looking at the averages, SN ratios go from about 13.99 at level 1 to approximately 20.39 at level 3, suggesting that longer mixing times could help make the process more stable.

Particle Size comes next with a delta of 5.07. Its SN ratios jump from roughly 17 at the smallest size (level 1) to nearly 21 at the middle size (level 2), then drop down again to around 16 at the biggest size (level 3). This shows that choosing a medium particle size (level 2) seems to give the most stable water absorption, but going bigger after that might make things worse.

In case of plastic weight ratio, it's a bit less influential as it attained smallest delta value (3.57) compared to mixing time and particle size. Its SN ratios stay fairly steady, peaking modestly at about 20 at level 2. So, changing the plastic weight ratio doesn't seem to have as much of an effect on stability compared to mixing time and particle size.

In general the response table clearly points out that Mixing Time is the biggest factor influencing stability, followed by Particle Size, with Plastic Weight Ratio being the least impactful. Knowing this helps to focus on the right parameters when trying to make water absorption more consistent. It also give clue where to look next for improvements, emphasizing that small adjustments in mixing time and particle size are most likely to make a difference.

ANOVA results for the Signal-to-Noise ratio were also generated in order to analyze how the three main factors (Plastic Weight Ratio, Mixing Time, and Particle Size) influence the overall variation in the response considering 95% level of confidence.

Table 9 : Analysis of Variance for SN ratios

Source	DF	Seq SS	Adj SS	Adj MS	F	P
Plastic Weight Ratio	2	23.003	23.003	11.501	3.29	0.233
Mixing Time	2	67.146	67.146	33.573	9.61	0.094
Particle Size	2	41.265	41.265	20.633	5.90	0.145
Residual Error	2	6.989	6.989	3.495		
Total	8	138.403				

Based on result presented in Table 9 with sum of squares of 67.146 and an F-value of 9.61 mixing time seems to have the biggest impact mean that contributed the most to the variance. Even though its p-value is 0.094, which is just above the typical cutoff of 0.05 (95% level of confidence), it still hints that mixing time might play a meaningful role in how water absorption behaves. Particle Size also has a moderate effect, with a sum of squares of 41.265 and an F-value of 5.90, but its p-value of 0.145 suggests it's statistically insignificant at the 5% level though it might be worth if it explored more with other additional levels. Plastic weight ratio seems to have the smallest influence, with a sum of squares of 23.003, an F-value of 3.29, and a p-value of 0.233, which indicates it's probably not having much of an effect in this setup. The residual error is very low, meaning the model does a good job of explaining most of the variability in the SN ratio.

Overall, it looks like mixing time is the most important factor for affecting the signal-to-noise ratio and the stability of water absorption, while particle size and plastic weight ratio seem less influential under the current experimental conditions.

Based on the ANOVA results, the null hypothesis is accepted (i.e., not rejected) for all three factors, meaning no statistically significant effect was detected at the 5% level. However, mixing time shows the strongest practical influence, suggesting it might be important in real-world applications even if not statistically confirmed in this small dataset.

4.1.2 Density

Density of each specimen determined based on Equation 2 as illustrated in the previous chapter. The value of the unknown variables (volume and mass of each specimen) measured based on the procedures mentioned on materials and methods chapter of this thesis work. Each specimen immersed in a jar containing of known volume of water (800ml), then volume of water increased as soon the specimens were immersed. The volume of the specimen was determined using the water displacement method, which relies on the principle that the volume of water displaced equals the volume of a fully immersed object. This was calculated by subtracting the initial water volume from the final water volume after immersion. Table 10 shows summarized initial volume and variation in volume of each specimen.

Table 10 : Volume of Specimen

Mix No.	Initial water volume	Final volume (water & specimen)			Volume of Specimens		
		S-1	S-2	S-3	S-1	S-2	S-3
1	800	819	820	823	19	20	23
2	800	843	840	845	43	40	45
3	800	828	822	825	28	22	25
4	800	837	840	845	37	40	45
5	800	837	842	838	37	42	38
6	800	842	840	844	42	40	44
7	800	843	845	843	43	45	43
8	800	845	842	840	45	42	40
9	800	837	840	835	37	40	35

Having obtained volume of each specimen and mass of each specimen recorded the density presented in Table 11 was obtained using Equation 2. As standard unit of density is kg/m^3 or g/cm^3, it was necessary to convert the unit of specimen's volume. Such that based on the metric system's definition both milliliter (ml) and cm^3 are equivalent.

Table 11 : Density of specimens

Mix No.	Volume of Specimens			Mass of Specimens			Density of Specimens			
	S-1	S-2	S-3	S-1	S-2	S-3	S-1	S-2	S-3	Avg.
1	19	20	23	25.9	26	26.1	1.363	1.300	1.135	1.266
2	43	40	45	45.83	45.8	46	1.066	1.145	1.022	1.078
3	28	22	25	25	25.1	26	0.893	1.141	1.040	1.025
4	37	40	45	39.3	39.6	40	1.062	0.990	0.889	0.980
5	37	42	38	39.8	41.2	40.5	1.076	0.981	1.066	1.041
6	42	40	44	41.3	40.7	42.3	0.983	1.018	0.961	0.987
7	43	45	43	46.1	46.4	45.9	1.072	1.031	1.067	1.057
8	45	42	40	49.6	48.9	48.3	1.102	1.164	1.208	1.158
9	37	40	35	41.6	42.5	41.1	1.124	1.063	1.174	1.120

Table 12 : Plastic weight ratio effect on density

Level	Mixes	Avg. Densities	Mean Density
1	1, 2, 3	1.266, 1.078, 1.025	1.123
2	4, 5, 6	0.980, 1.041, 0.987	1.003
3	7, 8, 9	1.057, 1.158, 1.120	1.112

The specimen density is found to be highest at two levels of plastic weight ratio: Level 1, that is, 90%, with a density of 1.123 g/cm^3, and Level 3, that is, 70%, with a marginally lower but nevertheless high density value of 1.112 g/cm^3. The specimen at an 80% plastic weight ratio gave the lowest value of density among the three levels. This decrease in density at 80% constitutes about an 11.9% decrease compared to the density at 90%, and around 10.9% compared to the density at 70%. These findings point toward a non-linear variation of plastic weight ratio and specimen density.

This trend indicates that samples produced with either relatively low or high plastic weight ratios have a greater density compared to those produced at in-between ratios. The increased density measured at the lower plastic weight ratio of 70% can be attributed to the larger amount of

reinforcement materials included in the mix. This larger content of reinforcement is expected to allow a denser and more interlocked structure, leading to an increased overall density.

On the other hand, the higher plastic weight ratio (90%) may lead to denser specimens through a different mechanism. In this case, the manufacturing process is likely more effective as higher amount of plastic was used; specimen manufactured is assumed to be more compacted, minimizing the presence of voids or air pockets within the specimen. This compactness directly contributes to an increase in density, as fewer voids mean more mass per unit volume. Conversely, the medium plastic weight ratio (80%) seems to yield specimens that are less dense. This may be the result of less than optimum reinforcement content together with production conditions that do not compact the material enough to leave fewer void spaces and hence lower density.

The main effects plot shown in Figure 27 serves to visually confirm these results with a clear illustration of the fluctuation in mean values of the densities through the varying plastic weight ratios, highlighting the increased densities at the lower and upper levels and lower value in density at the middle level.

Table 13 : Mixing time effect on density

Level	Mixes	Avg. Densities	Mean Density
1	1, 4, 7	1.266, 0.980, 1.057	1.101
2	2, 5, 8	1.078, 1.041, 1.158	1.092
3	3, 6, 9	1.025, 0.987, 1.120	1.044

As indicated by the Table 13 above, the specimen density slightly decreases as the mixing time is increased. The highest average density is at Level 1, which corresponds to the lowest mixing time of 5 minutes, and the lowest density is at Level 3, which corresponds to the highest mixing time of 25 minutes. This trend may indicate that extended mixing can be detrimental to the compaction or bonding efficiency in the composite material. Though it seems odd to say that the density is lower with longer mixing time, this result can be attributed to a loss in workability of the molten waste HDPE plastic. Overmixing might make the material less cohesive and thus more void which in turn decreases the density.

The main effects plot in Figure 26 also demonstrates this behavior. It reveals a drastic change in density when mixing time is changed from 15 minutes to 25 minutes, as seen from the steep slope of the graph. Quantitatively, this is represented through an increase in density by 0.8% from 5 to 15 minutes, followed by a much bigger 4.4% decrease from 15 to 25 minutes. These findings suggest that there is a range of optimum mixing time to get maximum density, after which over-mixing can be harmful to the structural integrity of the composite.

Table 14 : Particle size effect on density

Level	Mixes	Avg. Densities	Mean Density
1	1, 6, 8	1.266, 0.987, 1.158	1.137
2	2, 4, 9	1.078, 0.980, 1.120	1.059
3	3, 5, 7	1.025, 1.041, 1.057	1.041

Similar to the effects observed for plastic weight ratio and mixing time, the influence of particle size on density is examined here by considering different factor levels. Based on the results presented in Table 14, the highest density is recorded at Level 1, which corresponds to the smallest particle size. As particle size increases, the density progressively decreases. This trend indicates that smaller particles are able to pack more tightly together, effectively reducing the likelihood and number of voids within the composite. The reduction of voids directly contributes to a higher final density.

The main effects plot shown in Figure 27, generated using Minitab, clearly illustrates this behavior. The density decreases sharply between the smallest particle size and the next level, with a notable reduction of approximately 7.4%. Beyond this point, the rate of decrease slows down significantly, as indicated by the much shallower slope in the graph, with only a 1.7% reduction in density from the second to the third particle size level. This pattern suggests that the effect of increasing particle size on density is most pronounced at the smaller scale, where tight packing is more critical.

It can be concluded that as particle size increases, the surface contact area between particles also increases, which paradoxically leads to a greater likelihood of void formation. Larger particles do not pack as efficiently as smaller ones, creating more spaces or gaps within the material matrix.

These voids reduce the overall density of the composite. This observation aligns with well-established principles in materials science, where particle packing efficiency strongly influences the mechanical properties and density of composites.

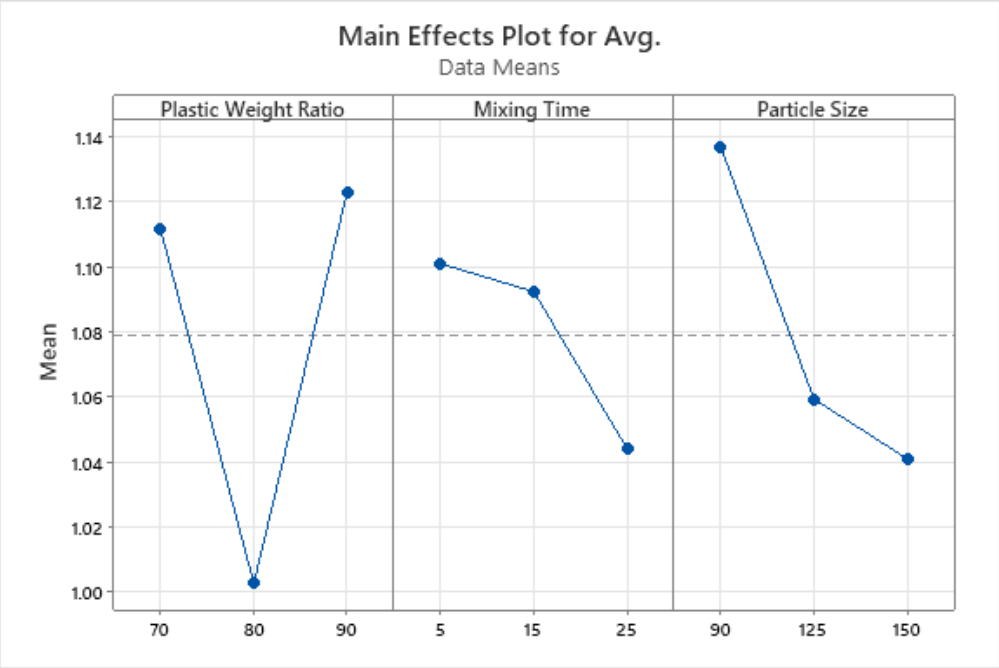

Figure 27 : Main effects plot of Density for all factors

Interaction plot

The interaction plot from Minitab, shown in Figure 28, shows how plastic weight ratio and mixing time together affect the density of a composite made from termite mound clay and waste HDPE. The plot clearly shows a strong interaction between these two factors, with lines that cross rather than run parallel.

At lower plastic weight ratios (70% and 80%), changing the mixing time doesn't cause much difference in density. The values stay fairly steady across 5, 15, and 25 minutes, with percentage changes between about 5% and 9.5%. This means that for these mixes, mixing time has little effect on the final density.

But at a higher plastic weight ratio of 90%, mixing time has a much bigger impact. The density stays relatively low at longer mixing times (around 1.08 g/cm³ at 15 minutes and 1.03 g/cm³ at 25 minutes), but it jumps sharply to about 1.26 g/cm³ with just 5 minutes of mixing. This suggests that with more plastic, shorter mixing times might improve how well the materials pack together or reduce empty spaces, leading to a denser composite. On the other hand, mixing for too long at this ratio might cause poor mixing or damage the plastic, lowering the density. This shows why it's important to find the right balance between plastic content and mixing time to get the best material properties.

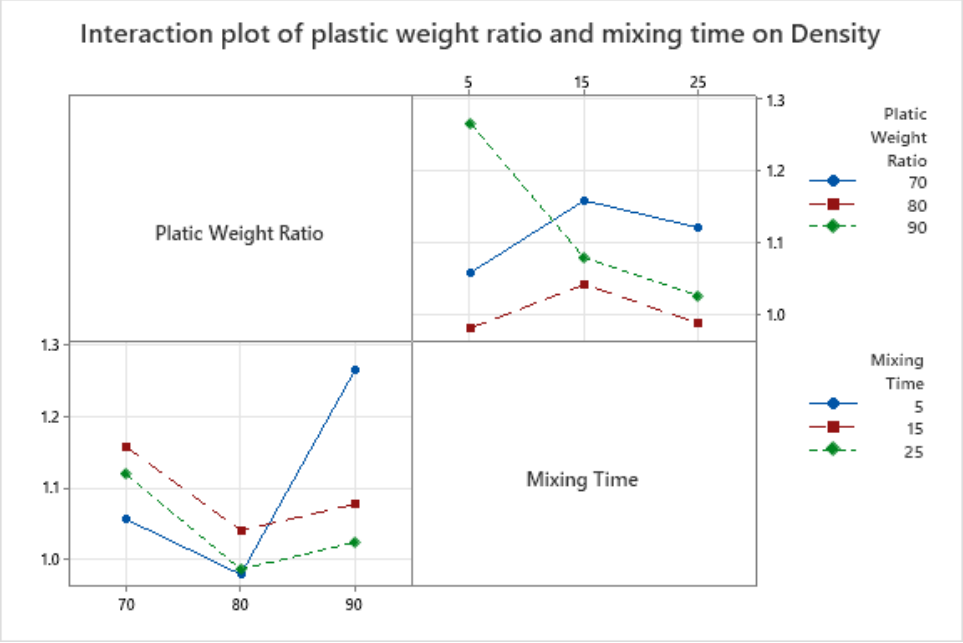

Figure 28 : Interaction plot of plastic weight ratio and mixing time on density

The plot also points out that the condition for highest density is at 90% plastic with a 5-minute mixing time, where density becomes about 1.26 g/cm³. This means that at higher plastic levels, a shorter mixing time is enough to properly mix and bond the HDPE with the clay, improving packing and cutting down voids in the composite.

For lower plastic ratios (70% and 80%), increasing mixing time only slightly improves density. The density stays pretty stable across different mixing times, suggesting that good mixing is already achieved with shorter times. Mixing longer doesn't add much benefit here.

Overall, these results highlight how important it is to consider plastic content and mixing time together, rather than separately. Adjusting both at the same time is mandatory for making less dense, well-formed composites from termite mound clay and recycled HDPE.

Effect of Plastic weight ratio and Particle size

In order to illustrate the combined effects of plastic weight ratio and termite mound clay particle size on the density of the composite specimens an interaction effect plot. Notably, the non-parallel lines in the plots (refer Figure 29) indicate a significant interaction between these two variables. At a plastic weight ratio of 90%, density varies significantly with particle size, showing a sharp decrease from approximately 1.26 g/cm³ at 90 µm to around 1.03 g/cm³ at 150 µm. This suggests that finer clay particles (90 µm) contribute to denser composites at high plastic content, likely due to better packing and improved interfacial contact between the clay and HDPE. Conversely, at lower plastic contents (70% and 80%), density remains relatively stable across different particle sizes, implying that particle size has less influence when plastic content is low.

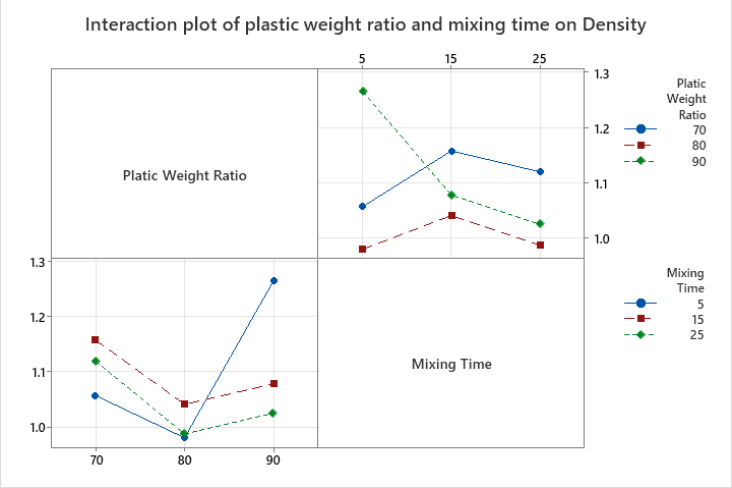

Figure 29 : Interaction plot of plastic weight and mixing time on density

The plot also shows that the highest density overall occurs at 90% plastic weight and 90 µm particle size, supporting the idea that both high plastic content and fine clay particles promote denser composites. Interestingly, as particle size increases to 150 µm, density tends to decrease across all plastic weight ratios, though the effect is most pronounced at 90%. This trend may be attributed to

the reduced surface area and poorer dispersion of larger particles, which may hinder effective bonding and packing within the matrix. These results highlight the importance of optimizing both particle size and plastic content together to maximize or minimize density, rather than considering either parameter in isolation.

Table 15: Analysis of variance for Signal-to-Noise ratio

Level	Platic Weight Ratio	Mixing Time	Particle Size
1	-0.91814	-0.80129	-1.08189
2	-0.03273	-0.76531	-0.50120
3	-0.99578	-0.38004	-0.36356
Delta	0.96305	0.42125	0.71833
Rank	1	3	2

The response table for the signal-to-noise (SN) ratios, under the “smaller is better” criterion, clearly demonstrates the relative influence of each factor on response variability. Notably, the Plastic Weight Ratio emerges as the most influential parameter, exhibiting the largest delta value of 0.96305. This substantial effect underscores its critical role in minimizing system noise and enhancing process stability.

Particle Size follows, with a delta of 0.71833, indicating a moderate yet noteworthy impact on the SN ratio. In contrast, Mixing Time displays the least influence, evidenced by a delta of just 0.42125, and is consequently ranked third among the studied variables.

A closer examination of mean SN ratios across factor levels reveals that the second level of Plastic Weight Ratio (-0.03273) achieves the lowest noise, thus optimizing system robustness.

In summary, this analysis identifies Plastic Weight Ratio as the primary factor to target for minimizing variability in the composite's response, followed by Particle Size. Mixing Time exerts a relatively insignificant effect.

4.2 Mechanical Property Characterization

4.2.1 Tensile Strength

Tensile testing was conducted using a universal testing machine under quasi-static loading conditions at a constant crosshead speed of 20 mm/min. Given the gauge length of 50 mm, the corresponding strain rate was calculated as 6.67×10^{-3} s^{-1}, which falls within the low strain rate regime.

The specimens were manufactured using a composite blend of termite mound clay and recycled high-density polyethylene (HDPE) plastic. A total of 27 specimens were prepared, consisting of three replications for each of the nine different mix ratios. The specimen preparation and testing were carried out in accordance with the ASTM D638 standard. The procedures and steps followed during specimen fabrication and testing are detailed in the Methodology chapter.

Table 16 : Tensile strength test results

Mix No.	Specimen Size (mm)		Failure load (N)			Tensile Strength (MPa)			Avg.
	S-1		S-1	S-2	S-3	S-1	S-2	S-3	
	w	t							
1	18.5	6.5	2.4	1.8	2	19.96	14.97	16.63	17.19
2	18.5	6.5	2.8	3	2.4	23.28	24.95	19.96	22.73
3	18.5	6.5	1.8	2	1.8	14.97	16.63	14.97	15.52
4	18.5	6.5	2	2.2	2.2	16.63	18.30	18.30	17.74
5	18.5	6.5	2.2	2	2	18.30	16.63	16.63	17.19
6	18.5	6.5	1.6	2	2	13.31	16.63	16.63	15.52
7	18.5	6.5	0.9	1.2	1.1	7.48	9.98	9.15	8.87
8	18.5	6.5	2.5	2.4	2.8	20.79	19.96	23.28	21.34
9	18.5	6.5	2.1	2.3	2.2	17.46	19.13	18.30	18.30

Table 16, presents the tensile testing results obtained from specimens subjected to tensile force using a Universal Testing Machine. Each row corresponds to a different mix number, and for each

mix, three specimens (S-1, S-2, and S-3) were tested. The specimen dimensions remained constant across all tests, with a width (w) of 18.5 mm and a thickness (t) of 6.5 mm. The failure load (in kN) were recorded and corresponding tensile strength (in MPa) were calculated for each specimen based on Equation 5.

Based on the Main Effects Plot (refer Figure 30) and the tabulated experimental data, here below is discussed the independent effects of each of the three factors amount of plastic (HDPE content), mixing time, and particle size on the tensile strength of the HDPE–termite clay composite.

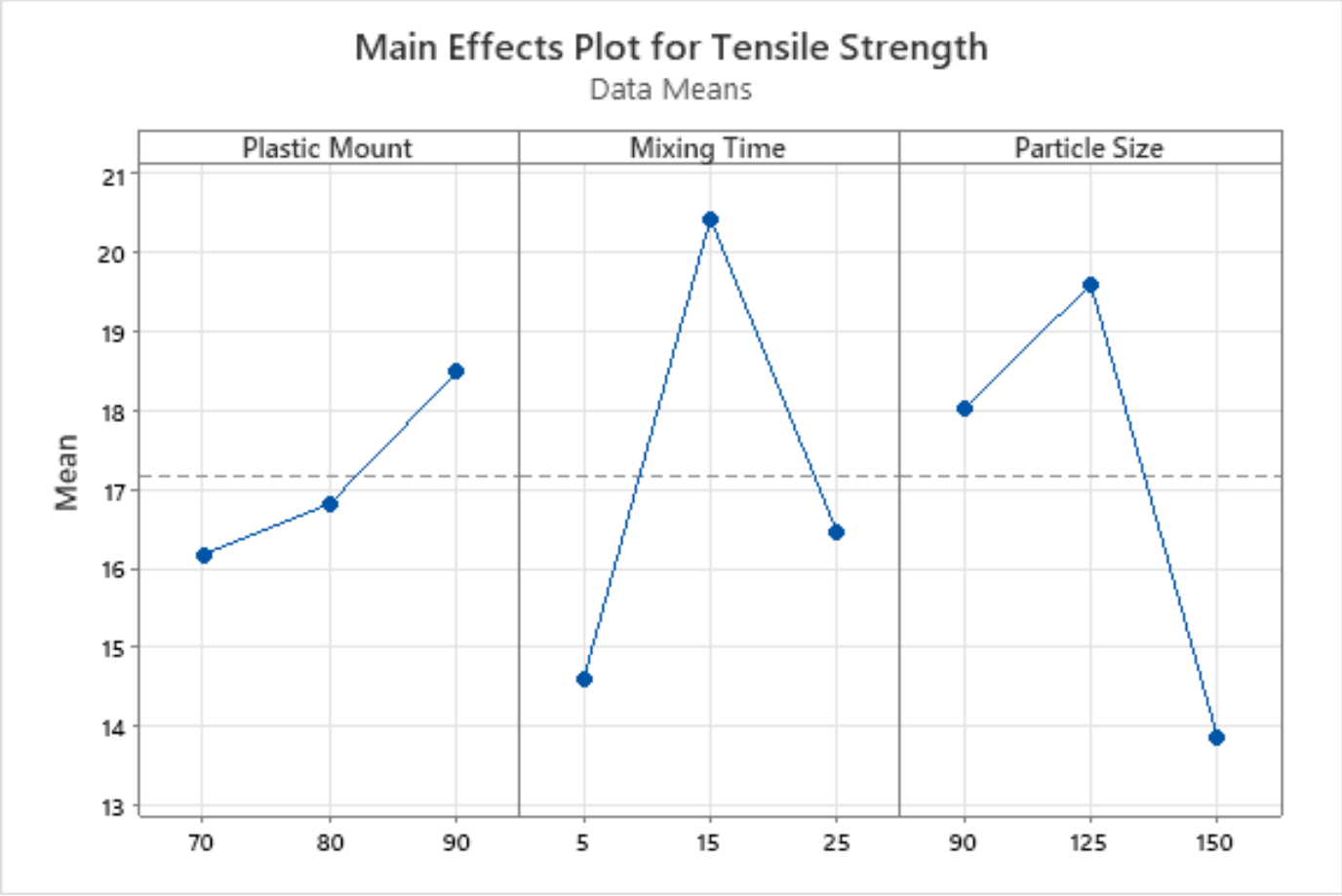

Figure 30 : Main effect plot for Tensile Strength

Effect of Plastic Amount (HDPE Content)

The main effects plot demonstrates a clear positive linear trend in tensile strength with increasing HDPE content. As the HDPE percentage rises from 70% to 90%, the average tensile strength steadily increases. Specifically, at 70% HDPE, the average tensile strength is the lowest approximately 14.79 MPa, with the poorest individual result recorded in Mix 7 (8.87 MPa). In contrast, at 90% HDPE, the tensile strength reaches its peak, averaging around 19.86 MPa, with Mix 2 achieving the maximum recorded value of 22.73 MPa.

The rate of increase is more significant between 80% and 90% than between 70% and 80%, indicating a stronger reinforcing effect as HDPE content approaches the upper limit. This linear trend highlights HDPE's critical role as the load-bearing matrix in the composite. Higher HDPE content improves ductility, interfacial cohesion, and stress distribution, whereas excessive clay (being brittle and less ductile) reduces these properties by disrupting load transfer. Therefore, increasing HDPE improves the overall mechanical performance of the composite.

Effect of Mixing Time

Mixing time has a non-linear but pronounced impact on tensile strength. As shown in the plot, the tensile strength is lowest at a 5-minute mixing time (average 15.24 MPa). This may be due to inadequate dispersion of clay particles in the molten HDPE, possibly resulting in void formation and weak interfacial bonding.

At 15 minutes, the tensile strength increases sharply to an average of 19.22 MPa, representing the optimal mixing condition. At this duration, the clay particles appear to be evenly dispersed, leading to better interfacial bonding and a more cohesive composite structure.

However, extending the mixing time to 25 minutes resulted in a drop to 17.00 MPa. This decrease could rise from over-mixing, which may degrade the HDPE, reduce its workability, or cause clay particle agglomeration. These conditions hinder proper bonding and uniformity, compromising tensile performance. Thus, 15 minutes emerges as the optimal mixing duration, balancing homogeneity, dispersion, and material stability.

Effect of Particle Size

Particle size also significantly affects the tensile strength of the composite, exhibiting a non-linear trend similar to that of mixing time. Among the three size ranges:

- 90–125 µm particles yield the highest tensile strength (19.6 MPa), suggesting this is the optimal range for achieving good interfacial bonding and even distribution.
- At 63–90 µm, the tensile strength is slightly lower (18.0 MPa), showing an 8.2% reduction from the peak. This decline may result from the agglomeration of very fine particles, which can hinder dispersion and create weak zones within the matrix.
- At the coarsest range, 125–150 µm, tensile strength drops sharply to approximately 14.00 MPa, likely due to the reduced surface area of larger particles. These coarse particles may act as stress concentrators, reducing load transfer efficiency and leading to early failure.

In conclusion, intermediate particle sizes (90–125 µm) provide the best balance between surface area and dispersion stability, enhancing interfacial bonding and tensile strength. Finer particles cause clumping, while coarser ones reduce bonding efficiency.

Interaction Plot

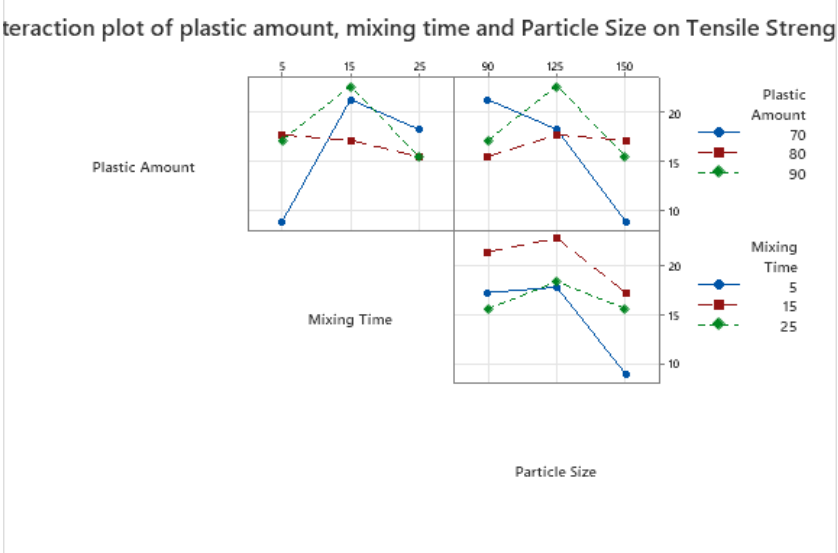

Figure 31 : Interaction plot of factors on Tensile Strength

In addition to analyzing the main effects of individual factors on tensile strength, it is essential to examine the interaction plot to understand how combinations of plastic amount, mixing time, and particle size influence composite performance. The interaction plot reveals that the relationship between these factors is not simply additive but rather interdependent, indicating that the effect of one factor may change depending on the level of another. This complexity highlights the importance of considering factor interactions when optimizing composite manufacturing parameters.

From the plot of the left-hand corner (refer Figure 31), it is evident that plastic amount interacts strongly with mixing time. At a plastic content of 90%, tensile strength peaks at 15 minutes of mixing time and then decreases at 25 minutes, consistent with the main effects plot. However, for 70% plastic content, the tensile strength is much lower overall, but the relative improvement at 15 minutes is even more pronounced, suggesting that optimal mixing time can partially compensate for lower plastic content. Conversely, at 80% plastic, tensile strength remains relatively stable across mixing times, indicating a less sensitive response. Unlike the 70% and 90% plastic amounts, the 80% plastic content shows a decreasing trend as mixing time increases.

The plot also shows a significant interaction between plastic amount and particle size. For 90% plastic, the tensile strength remains consistently high at moderate and larger particle sizes (90–125 μm and 125–150 μm), but drops sharply at the smallest particle size (63–90 μm). This suggests that finer particles may cause agglomeration or poor bonding when the plastic content is high. In contrast, at 70% plastic, tensile strength peaks at the finer particle size range (63–90 μm) and drops notably at larger particle sizes, indicating the creation of voids and reduced surface adhesion due to lower plastic content and the larger surface area of the fillers. The relatively higher tensile strength observed for lower plastic content combined with fine particle size suggests reduced clumping, which is attributed to the small particle size.

Finally, the interaction between mixing time and particle size further supports the optimal conditions identified. Tensile strength is highest at 15 minutes of mixing time regardless of particle size, but this effect is more pronounced at the 90–125 μm particle size range. At the extreme particle sizes (63–90 μm and 125–150 μm), prolonged mixing times (25 minutes) lead to

significant drops in strength, indicating that over-mixing exacerbates the negative effects of suboptimal particle sizes. Overall, the interaction plot emphasizes the need to optimize all three factors simultaneously to maximize tensile strength, with particular attention to the synergy between mixing time and particle size at different plastic contents.

Generally, tensile strength is highest at 80% plastic amount**,** 90–125 μm particle size, and 15 minutes mixing time.

Analysis of Variance for Signal-to-Noise Ratio

An Analysis of Variance (ANOVA) was performed on the Signal-to-Noise (S/N) ratios, adopting the "larger-is-better" approach to optimize the tensile strength of the composite for robustness. This analysis aims to identify factors that significantly affect performance and to determine parameter settings that minimize the effect of noise, rather than simply maximizing the mean response.

The ANOVA results, presented in Table 17, show the p-values for plastic amount, mixing time, and particle size all exceed the standard significance threshold of 0.05. This indicates that, within the scope of this experimental design, none of the factors demonstrated a statistically significant effect on the S/N ratio for tensile strength at a 95% confidence level. Consequently, the null hypothesis for each factor is accepted.

It is important to interpret this outcome with caution, such that the relatively high p-values may be influenced by the limited number of experimental runs, which can reduce the statistical power of the test and increase the probability of a Type II error (failing to detect a true effect). Constraints of time and budget precluded a larger experimental array in this phase. Therefore, while the results suggest that factor level changes did not cause significant variation, this conclusion should be considered preliminary and warrants verification through further, more extensive study.

Table 17 : Analysis of Variance for SN ratios

Source	DF	Seq SS	Adj SS	Adj MS	F	P
Plastic Amount	2	3.960	3.960	1.980	0.67	0.598
Mixing Time	2	16.029	16.029	8.015	2.72	0.269
Particle Size	2	17.867	17.867	8.933	3.03	0.248
Residual Error	2	5.894	5.894	2.947		
Total	8	43.750				

The Response Table for S/N Ratios (refer Table 18) provides critical insight into the practical influence of each factor on tensile strength. The relative impact, determined by the Delta values (the range between the highest and lowest average S/N ratio for each factor), express a clear hierarchy:

- ✓ Particle Size (Delta: 3.29) exerts the strongest influence.
- ✓ Mixing Time (Delta: 3.26) has a very similar, strong influence.
- ✓ Plastic Amount (Delta: 1.62) has a comparatively minor effect.

This ranking demonstrates that simply increasing the plastic content is a less effective strategy for enhancing tensile strength than optimizing particle size and mixing duration.

The remarkable impact of mixing time and particle size is directly linked to the microstructural properties of the composite. Mixing time is crucial for achieving a homogeneous dispersion of clay particles within the HDPE matrix; optimal mixing ensures thorough wetting and strong interfacial adhesion, thereby improving cohesion. Conversely, particle size governs the available surface area for bonding. While finer particles offer greater surface area for adhesion, they also increase the tendency for agglomeration, which can create weak points. Therefore, the synergy between these two factors is vital in determining the quality of the interfacial bonding and the resulting mechanical integrity of the composite.

Table 18 : Response Table for Signal to Noise Ratios (Larger is better)

Level	Plastic Amount	Mixing Time	Particle Size
1	23.60	22.88	25.04
2	24.50	26.14	25.79
3	25.22	24.29	22.49
Delta	1.62	3.26	3.29
Rank	3	2	1

4.2.2 Flexural Strength

As tried to mention in the previous section in order to conduct flexural test according to ASTM D790 specimens of 27 amount were manufactured based on the DOE as shown in Figure 19. To conduct test based on the standard speed of the cross head should be determined as the test must be with in the low strain rate range (10^{-6}-10^{-3} s^{-1}) based on Equation 11. Given that strain rate of 10^{-3} s^{-1}, span length mm and specimen thickness of 10 mm. Substituting the values, the cross head speed of the testing machine will be,

$$V = \frac{0.001 * 140^2}{6 * 100} = 0.327 \ \frac{mm}{s}$$

So the crosshead speed is approximately 20 mm/min, and this speed was feed to the machine via its computer interface to conduct test in order to ensure the testing is under quasi-static condition (low strain rate).

As already described in the previous chapter the flexural strength of termite mound clay-reinforced HDPE composites was evaluated using specimens measuring 140 mm in length, 20 mm in width, and 10 mm in thickness. The flexural strength was calculated based on the recorded maximum load at failure and the known geometry of the specimens. This calculation was performed using Equation (10), which was detailed in the preceding chapter.

As shown in Table 19 across nine different mix formulations, the maximum load at failure varied from 0.30 kN to 0.90 kN. Correspondingly, the calculated flexural strength ranged from 31.5 MPa to 94.5 MPa. Mix No. 2 exhibited the highest average flexural strength, at 90.65 MPa, indicating optimal reinforcement and dispersion of clay particles within the HDPE matrix. In contrast, Mix No. 8 recorded the lowest average flexural strength, at 34.3 MPa, reflecting suboptimal composite performance. These results highlight the significant influence of mix composition on the mechanical behavior of the composites, demonstrating a clear trend that clay content, plastic content and processing parameters substantially affect flexural properties. The data suggest that proper optimization of the mix design can enhance the structural integrity and load-bearing capacity of these composites.

Table 19 : Flexural strength test result

Mix No.	Specimen Size (mm)			Maximum load (kN)			Flexural Strength (MPa)			Avg.
	L	w	T	S-1	S-2	S-3	S-1	S-2	S-3	
1	140	20	10	0.66	0.63	0.66	69.3	66.15	69.3	68.25
2	140	20	10	0.9	0.82	0.87	94.5	86.1	91.35	90.65
3	140	20	10	0.66	0.66	0.8	69.3	69.3	84	74.2
4	140	20	10	0.61	0.58	0.6	64.05	60.9	63	62.65
5	140	20	10	0.52	0.52	0.48	54.6	54.6	50.4	53.2
6	140	20	10	0.52	0.48	0.5	54.6	50.4	52.5	52.5
7	140	20	10	0.47	0.4	0.44	49.35	42	46.2	45.85
8	140	20	10	0.32	0.36	0.3	33.6	37.8	31.5	34.3
9	140	20	10	0.5	0.61	0.52	52.5	64.05	54.6	57.05

Discussion on the Effect of Factors on Flexural Strength

The data from the nine mix formulations reveal significant variations in flexural strength, ranging from an average of 34.3 MPa (Mix 8) to 90.65 MPa (Mix 2). This indicates that the manipulated factors (amount of plastic, mixing time and particle size) have a vital impact on the composite's

flexural strength. The analysis of main effects and interaction plots generated with the aid of Minitab 19 could lead to the following conclusions:

Main Effects (Individual Factor Influence)

This plot as shown in Figure 32 illustrates the individual effect of the three key factors, Plastic Amount, Mixing Time, and Particle Size on the average flexural strength of the termite mound clay-reinforced HDPE composites. The plot show how the mean strength changes as the level of each factor is varied, allowing in identifying the optimal settings for maximizing performance. Here is the analysis of each factor's individual effect:

Effect of Plastic (HDPE) Amount

The plot confirms a strong positive correlation between the HDPE content and the average flexural strength. The strength increases from a lower value at 70% plastic to a significantly higher value at 90%. Here the critical observation on the rate of increase is crucial; such that the incremental gain in strength is more pronounced between 80% and 90% than between 70% and 80%. This non-linear response suggests that the benefit of a richer polymer matrix becomes especially critical at higher concentrations, likely because it provides a more continuous phase to effectively wet, enclose, and transfer stress to the reinforcing clay particles, thereby minimizing agglomeration and stress concentration points.

Effect of Mixing Time

The average flexural strength shows a considerable improvement as mixing time increases from 5 to 25 units. This trend underscores the profound importance of sufficient energy input for achieving optimal composite properties. As it can be noted from the plot Figure 32 extended mixing ensures superior dispersion and distribution of clay particles, breaking up agglomerates and maximizing the interfacial area for stress transfer between the clay and the HDPE matrix. This leads to a more homogeneous and stronger composite, though sometimes and some other properties, excessive mixing can lead to thermal or mechanical degradation of plastic. However,

within the tested range (5 to 25), the benefits of dispersion significantly balance any potential for degradation, as evidenced by the consistent positive trend.

Effect of Clay Particle Size

The average flexural strength of the composite increases significantly as the clay particle size increases from 63-90 µm to 90-125 µm, but then radically falls as the particle size increased to 125- 150 µm. it is known that Smaller sized particles have a higher surface area-to-volume ratio, which enhances the interfacial bonding with the polymer matrix and contributes to improved mechanical performance. This stronger interfacial adhesion allows for more efficient load transfer between the matrix and the filler. However, when the particles become excessively fine, the flexural strength may begin to diminish due to agglomeration. Extremely fine particles tend to cluster together, reducing the effective surface area available for bonding and creating weak points within the composite. In contrast, larger particles often behave like defects or voids, acting as stress concentrators that can initiate cracks and cause premature failure under lower loads.

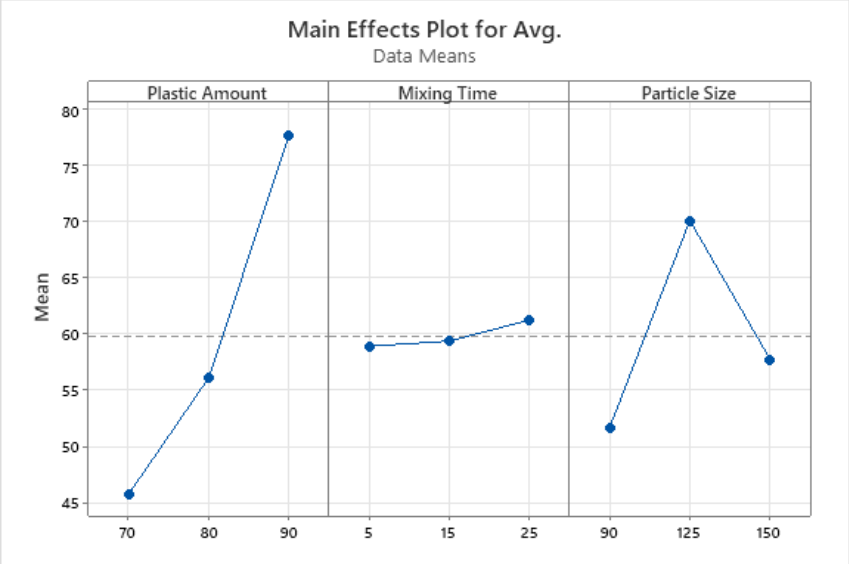

Figure 32 :Main effect plot for flexural strength

Interaction effect of factors

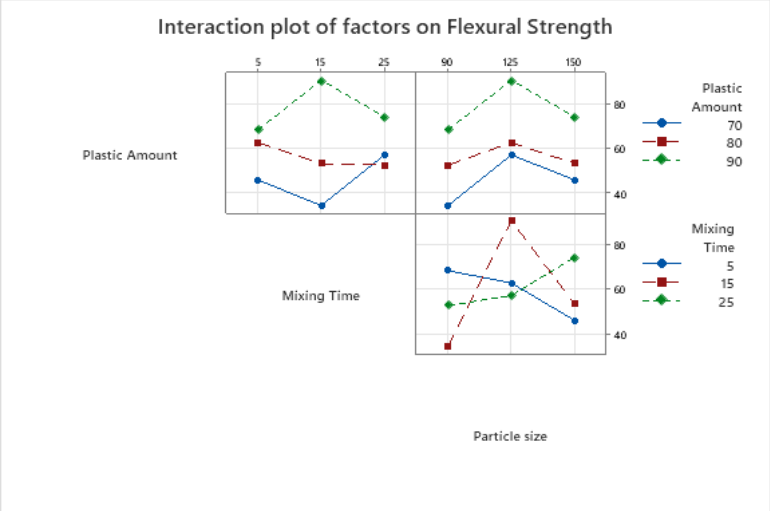

Figure 33 : Interaction plot of factors on Flexural strength

As shown in the interaction plot of Figure 33, nearly all factor combinations exhibit a significant influence on the flexural strength of the composite except for the interaction between plastic amount and particle size. In the top-right plot, the lines representing different plastic amounts do not intersect, indicating that there is no significant interaction between these two factors. This suggests that the effect of one factor (plastic amount) on flexural strength does not depend on the level of the other factor (particle size) or its dependency is negligible.

However, even though their interaction is not statistically significant, it is clear from the plot that higher plastic content (90%) consistently leads to higher flexural strength across all particle sizes. Conversely, the lowest flexural strength was recorded at the 70% plastic content, demonstrating that increased plastic content enhances the composite's ability to resist flexural stress. Regarding particle size, flexural strength initially increases with particle size but decreases as the particles become coarser. This trend suggests that the optimal particle size for flexural strength is in the range of 90–125 µm, likely due to an ideal balance between surface area for bonding and resistance to agglomeration. In contrast, the bottom-right plot shows a clear interaction between mixing time and particle size, as the lines intersect. This indicates that the effect of particle size on flexural strength depends on the level of mixing time, and vice versa.

For all mixing times, the highest flexural strength is generally observed at a particle size of 90–125 μm, except for the 25-minute mixing time, where the trend continues upward. Specifically:

- ✓ At 5 minutes, flexural strength decreases as particle size increases. This may be due to inadequate mixing, which fails to uniformly distribute larger particles, leading to voids and poor interfacial bonding.
- ✓ At 25 minutes, flexural strength increases with particle size, suggesting that extended mixing time improves particle dispersion and bonding, particularly for coarser particles.
- ✓ At 15 minutes, flexural strength initially increases with particle size but then declines. This could be attributed to a combined effect of particle agglomeration and limitations in HDPE plastic workability, where the matrix may begin to lose its ability to effectively wet and bond with excessively large or poorly distributed particles.

Analysis of Variance for SN ratios

The Analysis of Variance (ANOVA) results for the signal-to-noise (S/N) ratios as tabulated in Table 20 provide insight into the significance of each input factor, plastic amount, mixing time, and particle size, on the flexural strength of the composite. The goal in this analysis is to determine which factors have a statistically significant influence on the response variable and to guide optimization based on the "larger-is-better" quality criterion.

Table 20 : Analysis of variance for Signal-to-Noise Ratios of Flexural strength

Source	DF	Seq SS	Adj SS	Adj MS	F	P
Plastic Amount	2	33.879	33.879	16.9396	23.83	0.040
Mixing Time	2	1.105	1.105	0.5524	0.78	0.563
Particle Size	2	11.975	11.975	5.9876	8.42	0.106
Residual Error	2	1.422	1.422	0.7109		
Total	8	48.381				

Unlike to the previous test results, the ANOVA results reveal that among the three factors, plastic amount has a statistically significant effect on the flexural strength of the composite. This is evident from its p-value of 0.040, which is less than the commonly used significance level of 0.05 (5%). This implies that the null hypothesis is rejected for plastic amount, and the alternative hypothesis is accepted, confirming that changes in the plastic content meaningfully affect the composite's flexural strength.

On the other hand, both mixing time ($p = 0.563$) and particle size ($p = 0.106$) have p-values greater than 0.05, indicating that their effects are not statistically significant at the 95% confidence level. Therefore, for these two factors, the null hypothesis is accepted, and their influence on flexural strength cannot be confidently distinguished from random variation within the limited number of experimental runs. However, it's worth noting that particle size has a relatively lower p-value compared to mixing time, suggesting that it may still have a moderate effect worth exploring in more detailed studies with increased sample sizes or additional levels.

Response Table for Signal to Noise Ratios

The response table for the signal-to-noise ratios follows the "larger-is-better" criterion, which is suitable for flexural strength as the objective is to maximize performance. The delta value (difference between the highest and lowest S/N ratio at different levels) indicates the relative influence of each factor.

- ✓ Plastic amount has the highest delta (4.73) and is ranked first, confirming it as the most influential factor.
- ✓ Particle size, with a delta of 2.81, is the second most influential factor.
- ✓ Mixing time has the lowest delta (0.85), suggesting it has the least impact on flexural strength among the three.

Table 21 : Response table for S/N of flexural strength (Larger is better)

Level	Plastic Amount	Mixing Time	Particle Size
1	33.02	35.28	33.93
2	34.95	34.79	36.74
3	37.75	35.65	35.05
Delta	4.73	0.85	2.81
Rank	1	3	2

These findings align well with the ANOVA results and reinforce the conclusion that increasing the plastic content, especially to 90%, significantly enhances the flexural strength of the composite. This can be attributed to better matrix continuity and improved stress transfer within the material.

In contrast, while mixing time appears less impactful, particle size still plays a notable role. Previous tests supports that an optimal particle size range (such as 90–125 μm) helps balance surface area for bonding and minimizes agglomeration or void formation, both of which are crucial for flexural performance.

4.2.3 Impact test

As mentioned in previous chapter to enhance the mechanical performance of polymer composites particularly their impact resistance the incorporation of natural fillers such as termite mound clay into high-density polyethylene (HDPE) has gained growing interest. To evaluate the influence of termite mound clay on the impact strength of HDPE, a total of 27 specimens (comprising 9 mix ratios with three replications each) were prepared for Charpy impact testing. As stated in the previous section, the specimens were fabricated in accordance with ASTM standards, and the tests were conducted using the Charpy impact testing machine located at the School of Mechanical and Industrial Engineering, Mekelle University.

This testing machine is equipped with two pendulum systems**:**

- A large pendulum capable of delivering impact energy in the range of 150–300 J, and
- A small pendulum designed for impact energies ranging from 0–150 J.

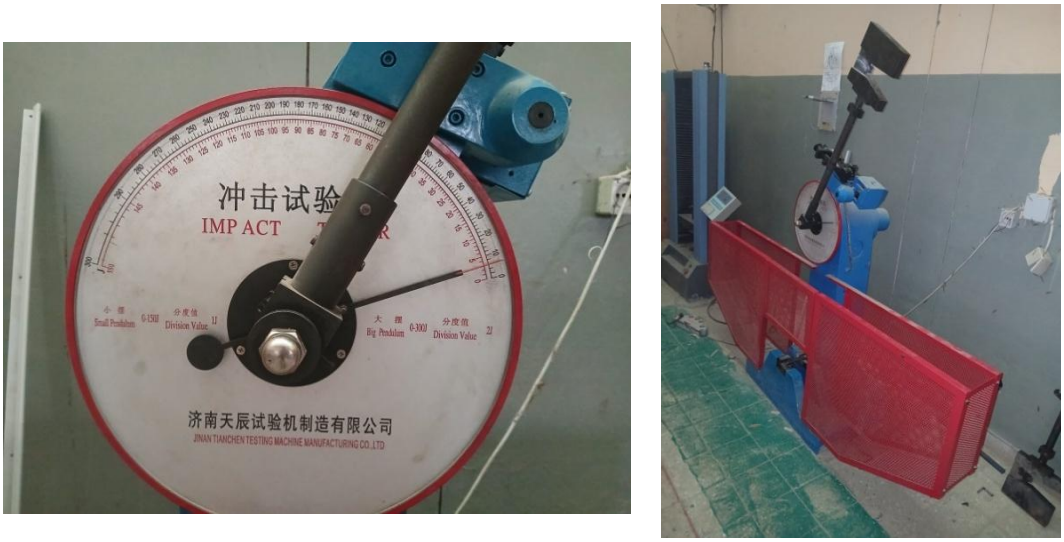

Figure 34 : Impact testing machine (Solid mechanics and Design chair, Material Testing Lab.)

For this study, the appropriate pendulum was the smaller which is selected based on the expected energy absorption of the specimens. Prior to performing the tests and analyzing the results, the impact speed of the pendulum was calculated to ensure accurate interpretation of the energy imparted during fracture which is given based on equation (). The impact speed is a critical parameter in Charpy testing, as it directly influences the strain rate experienced by the specimen during failure.

$$v = \sqrt{2 * g * h_1}$$

Where

$$g = 9.81 \frac{m}{s^2}$$

$$h_1 = 1.5 \text{ m (manually measured)}$$

Substituting the values and solving for impact velocity, this is given by

$$v = \sqrt{2 * 9.81 * 1.5}$$

$$= 5.43 \frac{m}{s}$$

As shown above, the impact speed obtained is 5.43 m/s. Given this value and knowing that the thickness of the specimen is 10 mm, the resulting strain rate is 543 s^{-1}, which falls within the category of high strain rates. Therefore, it can be concluded that impact testing using the Charpy machine is a high strain rate test method. As discussed in Chapter 2, low strain rates are defined as being below 100 s^{-1}.

Table 22 : Impact test results

Mix No.	Cross section of specimen (mm^2)			Impact Energy absorbed (J)			Impact Strength (kJ/m^2)			
	S-1	S-2	S-3	S-1	S-2	S-3	S-1	S-2	S-3	Avg.
1	210	220	200	2.4	2.5	2.6	11.43	11.36	13.00	11.93
2	200	210	200	2.5	2.6	3	12.50	12.38	15.00	13.29
3	200	200	220	2.3	2.5	2.4	11.50	12.50	10.91	11.64
4	200	210	220	2.8	2.5	2.4	14.00	11.90	10.91	12.27
5	200	200	200	3.2	3	3.2	16.00	15.00	16.00	15.67
6	200	220	200	2.5	2.6	2.6	12.50	11.82	13.00	12.44
7	210	210	200	2	1.8	1.9	9.52	8.57	9.50	9.20
8	200	220	200	1.9	1.8	2.2	9.50	8.18	11.00	9.56
9	210	200	220	2.6	2.8	2.4	12.38	14.00	10.91	12.43

To study the independent effects of each variable (factors) on impact strength, a main effects plot was constructed using the data given in Table 22. The plot, obtained using the Minitab software, clearly illustrates the effect of plastic amount, mixing time, and particle size on the average impact strength of the composite material produced from termite mound clay and HDPE. The strength of this analysis was confirmed and validated using ANOVA, as will be discussed in the next pages.

The plot (refer Figure 35) reveals that the plastic amount has the most significant impact. The increase in plastic content from 70% to 80% improves impact strength considerably, reaching a maximum average of about 13.5 kJ/m^2 at 80%. However, further increase in the plastic content to 90% results in a slight drop. This trend suggests that although HDPE is responsible for energy absorption up to a certain extent, an excess of plastic might deteriorate the bonding with the clay

matrix or cause hardening of the material, as recycled waste plastic has been known to exhibit brittle properties resulting in a slight decline in impact strength.

The average impact strength increases tremendously from 5 minutes to 15 minutes, with the optimum performance at 15 minutes (~12.8 kJ/m²). In contrast, an increment of mixing time to 25 minutes results in a slight reduction in performance. It is thus likely that 15 minutes is the optimum mixing time, which may be due to better dispersion and greater interfacial bonding between HDPE and clay particles. Extending the mixing time to 25 minutes can cause polymer degradation or poor particle cohesion, which may undermine the structural integrity of the composite.

In terms of particle size, medium-sized particles (90–125 µm) performed better than the finest range (63–90 µm), with the highest average (approximately 12.7 kJ/m²). Finer particles might have led to excessive compactness or air entrapment during molding, both of which are detrimental to strength. Conversely, coarser particles (125–150 µm) produced the lowest average strength, likely because of low packing density and poor particle bonding. This trend indicates that an intermediate particle size must be chosen that optimally achieved packing efficiency and interfacial bonding in the composite material.

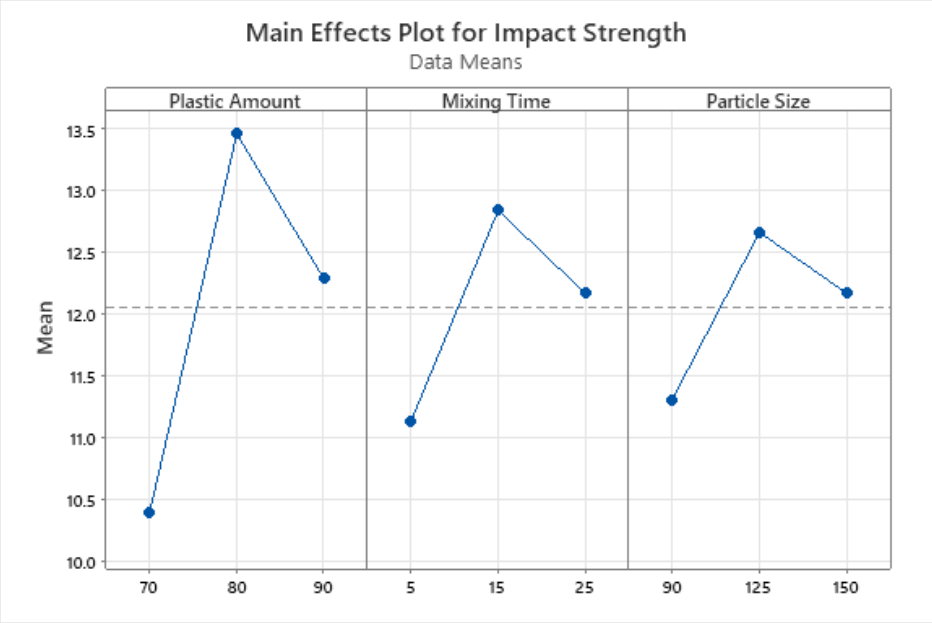

Figure 35 : Main effects plot on impact Strength

Interaction plot

In addition to the main effects plot, an interaction plot was generated to examine the combined effects of the factors on impact strength, similar to what was done for the water absorption and density properties.

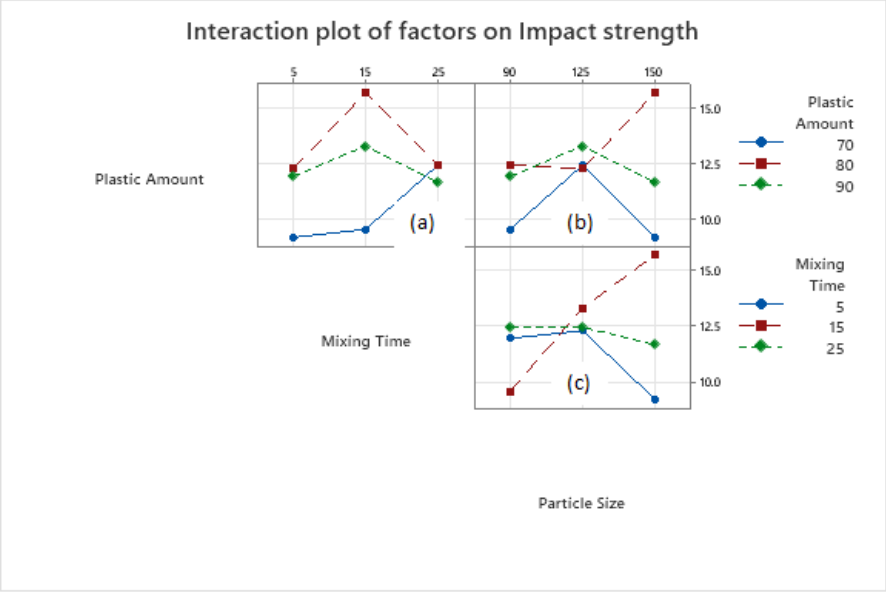

Figure 36 : Interaction plot of factors on impact strength

The interaction plot shows how impact strength is affected by the combined effects of three factors: plastic content, mixing time, and particle size. Each subplot displays the interaction between two of these factors while keeping the third one constant.

The top-left subplot (Fig. 31-a) shows the interaction between plastic content and mixing time. It shows that at 80% plastic content, the impact strength reaches its highest point, especially at 15 minutes of mixing. For both 80% and 90% plastic content, impact strength increases as mixing time goes from 5 to 15 minutes, then drops when mixing time extends to 25 minutes. This drop might be due to reduced workability or thermal damage to the polymer from too much heat during mixing, which matches findings from earlier studies on polymer processing.

For 70% plastic content, the trend starts similarly but continues to increase even after 15 minutes. Although the increase is slower than at 80% and 90%, it doesn't drop at 25 minutes. This might be because the higher clay content in the 70% mix helps keep the molten plastic workable longer by absorbing heat and adding structure. Earlier research suggests that fillers like clay can improve thermal stability and make processing easier, especially with lower plastic content.

Overall, impact strength is lower at 70% and 90% plastic content, indicating that 80% is the best amount for maximizing impact strength.

The top-right subplot (Fig. 31-b) looks at the interaction between plastic content and particle size. Like before, 70% plastic content results in lower impact strength across all particle sizes. The highest impact strength appears at 80% plastic content with a particle size of 150 μm, suggesting that bigger particles improve impact strength when plastic content is optimal.

Both the 70% and 80% mixes show a similar pattern—impact strength first rises, then falls as particle size reaches 150 μm. However, for the 80% mix, there's a slight initial drop (about 1.4%), followed by a big increase, peaking at 15.67 kJ/m². This suggests a combined effect of particle size and plastic content, where the right balance boosts energy absorption and resistance to breaking.

The bottom-right subplot (Fig. 31-c) shows the interaction between mixing time and particle size. For mixing times of 5 and 25 minutes, increasing particle size from 63–90 μm to 90–125 μm has little effect on strength. But increasing it further to 125–150 μm (coarse particles) lowers impact strength. In contrast, at 15 minutes mixing time, impact strength grows almost steadily with particle size, indicating that at this mixing time, larger particles help improve impact resistance.

At smaller particle sizes (63–90 μm and 90–125 μm), impact strength stays fairly steady across different mixing times. This means mixing time has more effect with larger particles, likely because bigger particles need more thorough mixing to spread evenly.

Since the lines in the plots cross, it shows these factors interact significantly. This means it's important to look at them together, not separately, because ignoring their interaction could lead to

wrong conclusions. This matches well-known ideas in materials science and experimental design, where interactions between factors often play a key role in the final properties of composites.

Analysis of Variance

Table 23 : Analysis of Variance for SN ratios

Source	DF	Seq SS	Adj SS	Adj MS	F	P
Plastic Amount	2	8.000	8.000	4.0001	2.01	0.332
Mixing Time	2	2.072	2.072	1.0358	0.52	0.657
Particle Size	2	1.602	1.602	0.8010	0.40	0.713
Residual Error	2	3.973	3.973	1.9866		
Total	8	15.647				

As presented in Table 23, the ANOVA for average impact strength signal-to-noise ratio shows that all three factors (plastic amount, mixing time, and particle size) have p-values higher than 0.05. More specifically, the p-values for plastic amount ($p = 0.332$), mixing time ($p = 0.657$), and particle size ($p = 0.713$) reveal that none of the factors have a statistically significant influence at the 5% significance level. Therefore, the null hypothesis that there is no significant impact on impact strength of variations in these factors is not rejected.

This lack of statistical significance is due to the limited test specimens (degrees of freedom = 2 for each factor and residuals) and the use of an orthogonal array in the design, which by definition limits replication and statistical power.

However, consistent with empirical trends, discernible trends in experimental results suggest that variations in plastic content, mixing time, and particle size indeed impact termite mound clay-reinforced HDPE composites' impact strength. This gives some support to increasing sample size and, perhaps, to the implementation of a more robust experimental design in further studies for better efficacy in catching these effects.

To identify the most influential factor affecting the impact strength, a response table for the signal-to-noise (S/N) ratio was generated based on the "larger-is-better" principle using Minitab, as presented in Table 24. The table summarizes the average S/N ratios for each level of the factors: plastic amount, mixing time, and particle size.

Table 24 : Response Table for Signal to Noise Ratios (Larger is better)

Level	Plastic Amount	Mixing Time	Particle Size
1	20.26	20.86	21.01
2	22.52	21.99	22.05
3	21.77	21.70	21.50
Delta	2.27	1.13	1.03
Rank	1	2	3

The Delta value, representing the difference between the highest and lowest S/N ratio for each factor, indicates the magnitude of influence on the impact strength. Based on these results:

- ✓ Plastic amount has the highest Delta value (2.27), making it the most influential factor.
- ✓ Mixing time ranks second (Delta = 1.13).
- ✓ Particle size has the least influence (Delta = 1.03).

Thus, the order of influence on impact strength is: Plastic Amount > Mixing Time > Particle Size.

This analysis provides further insight into factor importance, even though the ANOVA did not show statistical significance again likely due to the limited sample size and design constraints.

4.3 Optimized Mix Ratio

4.3.1 Grey Relation Analysis (GRA)

In engineering applications involving composite materials, we often find that different performance criteria need to be optimized at the same time. Here in this research work, impact strength, flexural strength, tensile strength, water absorption, and density were considered as five main responses to evaluate the performance of termite mound clay-strengthened HDPE composites.

As an increase in any attribute can potentially damage another attribute, a multi-response optimization technique is required. For achieving this aim, Grey Relational Analysis has been utilized. GRA is a strong methodology derived from Grey System Theory that can transform multi-response issues into a unified Grey Relational Grade (GRG) which further serves to rank experimental runs along with determining optimal process parameters. Detailed information regarding the calculation and derivation of the Grey Relational Grade (GRG) values is provided in the appendix section of this document, including supporting tables and step-by-step explanations. However, for clarity and ease of reference, the final tabulated GRG results are presented below.

Table 25 : GRG values

Run	Plastic Amount (%)	Mixing Time (min)	Particle Size (μm)	GRG	Rank
1	90	5	63-90	0.469992	8
2	90	15	90-125	0.791042	1
3	90	25	125-150	0.581269	6
4	80	5	90-125	0.660767	3
5	80	15	125-150	0.683876	2
6	80	25	63-90	0.642955	4
7	70	5	125-150	0.407218	9
8	70	15	63-90	0.507374	7
9	70	25	90-125	0.614208	5

From the GRA results, it is evident that Run 2 achieved the highest GRG value of 0.791, making it the optimal mix. This corresponds to a plastic content of 90%, mixing time of 15 minutes, and particle size of 125 μm. This combination delivers the most balanced performance across all five critical properties.

The trend observed suggests that:

- Higher plastic content (90%) improves mechanical properties due to increased polymer matrix presence.
- A moderate mixing time (15 min) provides sufficient dispersion without degrading the materials.
- A medium particle size (90-125 μm) offers a good balance between interfacial bonding and surface area.

This analysis demonstrates the effectiveness of Grey Relational Analysis in solving multi-response optimization problems in composite material development. The use of Minitab 19 streamlined the calculations and provided a clear ranking of experimental runs based on overall performance.

Optimized mix

In order to obtain the optimized mix using Grey Relational Analysis (GRA), a systematic procedure consisting of seven key steps was followed, utilizing Minitab software for data handling and computation. As outlined in the methodology section and further elaborated in the results and discussion chapter, a Design of Experiments (DOE) was developed using an orthogonal array with three factors, each at three levels. This experimental design allowed for the efficient exploration of factor effects while minimizing the number of experimental trials.

Specimens were then prepared and tested in accordance with the relevant ASTM standards for each of the selected critical properties, namely: density, percentage water absorption, tensile strength, flexural strength, and impact strength. These properties were chosen to comprehensively evaluate the performance characteristics of each mix.

The application of Grey Relational Analysis required the raw experimental data to be normalized, as the method relies on dimensionless and comparable values. Therefore, the following seven-step procedures were adopted to carry out GRA in Minitab. The corresponding values obtained are presented in appendix 1.

Step-1: Data Acquisition

The experimental results obtained from the DOE were compiled, including all measured response values of the selected properties.

Step-2: Data Normalization

Normalization was performed to bring all data into a comparable range (0 to 1). Since the objective was to maximize mechanical properties such as tensile strength, flexural strength, and impact strength, the 'larger-the-better' normalization criterion was applied to these responses. For properties like percentage water absorption and density, the appropriate normalization technique (e.g., 'smaller-the-better' or 'nominal-the-best') was applied, based on performance expectations.

Step-3: Deviation Sequence Calculation

The deviation between the ideal (best normalized) values and each normalized response was computed. This step helps in assessing how far each experimental result is from the ideal solution.

Step-4: Grey Relational Coefficient (GRC) Calculation

Using the deviation sequences and a distinguishing coefficient (typically set to 0.5), the Grey Relational Coefficients were calculated for each response, reflecting the closeness of each experiment to the ideal solution.

Step-5: Grey Relational Grade (GRG) Calculation

The GRG for each experiment was calculated by averaging the GRCs across all response variables. This GRG represents the overall performance of each trial considering all responses simultaneously.

Step-6: Ranking of Experimental Trials

Based on the calculated GRG values, all trials were ranked in descending order. The trial with the highest GRG was identified as the optimal mix combination, indicating the best compromise among the multiple performance criteria.

Step-7: Analysis and Confirmation:

The factor levels corresponding to the optimal GRG were analyzed to determine the best mix design. These optimal factor settings were then validated through confirmatory testing or further analysis, as needed. All values and results obtained during Grey Relational analysis for identifying the optimum mix are given in appendex-1.

Based on the analysis conducted using Minitab 19 statistical software the optimized mix ratio obtained is summarized in the table below.

Solution	Plastic Amount	Mixing Time	Particle Size	Impact Fit	Flexural Fit	Tensile Fit	percentage water Absorption Fit	Density Fit
1	90	7.02020	90-125	13.0295	78.5415	15.8187	0.175572	1.06106

4.4 Key Findings and Validation

The experimental results showed that all tested composites exhibited improved mechanical properties within tolerable limits for applications requiring low strain rates, consistent with findings reported for clay-reinforced HDPE systems where tensile strength improvements of 10–30% and flexural enhancements up to 40–60% have been documented (Alexandre & Dubois, 2000b; Sinha Ray & Okamoto, 2003a). These observations represent one of the key findings of the present work, demonstrating that the incorporation of reinforcement within the HDPE matrix contributes to measurable improvements in load-bearing capacity and structural stiffness under quasi-static loading conditions. The obtained tensile strength (22.73 MPa) falls within the typical range reported for reinforced HDPE composites (20–30 MPa depending on filler loading), while the flexural strength (90.65 MPa) compares favourably with values reported for natural fiber and nano-clay reinforced HDPE systems used in semi-structural applications (Han et al., 2008c, 2008c; Hao et al., 2020). This agreement with previously reported ranges provides validation that the developed composite system behaves consistently with established reinforced HDPE materials documented in literature. Similarly, the measured impact strength (15.67 kJ/m²) is comparable to values documented for modified HDPE composites intended for energy-absorbing applications, indicating that the developed material achieves competitive mechanical performance relative to previously reported systems. These results collectively confirm that the mechanical behaviour obtained from the experimental investigation is within the performance envelope of similar composite materials and therefore validates the reliability of the developed formulation for applications involving low strain rate loading conditions.

Physically, the composites exhibited desirable traits such as negligible water absorption (maximum 0.28%) and low density consistent with pure HDPE (maximum 1.266 g/cm³), aligning with reported density ranges of HDPE composites (0.94–1.30 g/cm³ depending on filler loading) and moisture resistance characteristics of polyolefin-based systems (Callister & Rethwisch, 2020). These physical characteristics represent another important outcome of the present investigation because low density and minimal moisture uptake are critical parameters for materials intended for lightweight structural and protective applications. Compared to many natural fiber–reinforced systems where water absorption may exceed 1–3%, the significantly lower water uptake observed

in this study indicates improved dimensional stability and environmental resistance. The consistency of these physical properties with previously reported ranges further validates that the synthesized composites maintain the intrinsic advantages of HDPE-based materials while simultaneously benefiting from reinforcement effects. These characteristics make the developed composites suitable for applications involving weight minimization and moisture barrier requirements. Collectively, the mechanical and physical performance achieved in this work demonstrates comparable or improved behaviour relative to several clay-modified HDPE systems reported in literature, thereby highlighting a promising application area of the synthesized composites in applications such as soft body Armor and structural elements subject to low-speed collisions, where quasi-static and low strain rate performance is critical (Grujicic et al., 2006).

For optimizing multi-response performance simultaneously in several physical and mechanical behaviours, Grey Relational Analysis (GRA) was employed, a method widely validated for multi-objective optimization in polymer composite processing (Deng, 1989; Taguchi & Konishi, 1987; Datta et al., 2009). The adoption of this approach represents an important analytical step in identifying the most effective processing conditions capable of producing balanced improvements across multiple performance indicators. It enabled converting multi-response data into one Grey Relational Grade (GRG) across every experimental iteration, thereby facilitating systematic comparison among the different experimental combinations. The maximum GRG value of 0.791 obtained in this study lies within the range (0.70–0.85) commonly reported in composite optimization investigations, indicating effective parameter convergence and balanced property enhancement (Chakraborty et al., 2023). This agreement with the commonly reported GRG ranges further validates the effectiveness of the optimization approach used in the present study. Through this analysis, it was established that optimum mix ratio should be formed from a composition of 90% plastic material, a mixing time of 7 minutes, and particle size of 125 μm. Optimum overall performance across all tested properties was realized in this particular setup that rendered maximum GRG (0.791) value, demonstrating that the developed composite system achieves competitive multi-response optimization performance comparable to established reinforced HDPE systems reported in literature.

CHAPTER-5

CONCLUSION AND RECOMMENDATION

5.1 Conclusion

This research was successful in developing and characterizing termite mound clay-reinforced high-density polyethylene (HDPE) composites tailored to enhance their physical and mechanical behavior against low strain rate impacts. High-density polyethylene was utilized as matrix material while termite mound clay with varying particle sizes was utilized to serve as a reinforcement agent. An orthogonal array-driven Design of Experiments (DOE) approach was employed in order to regulate systemically three most critical factors, plastic weight ratio, mixing duration, and particle size, with every parameter having three levels. ASTM compliance was witnessed in order to eliminate specimen preparation and corresponding testing method variations in mechanical characterization. Statistical analysis was carried out via Minitab 19 software.

The experimental results showed that all tested composites exhibited improved mechanical properties within tolerable limits for applications requiring low strain rates. Optimal tensile strength (22.73 MPa), flexural strength (90.65 MPa), and impact strength (15.67 kJ/m^2) were attained corresponding to their optimal factor combinations. Physically, the composites exhibited desirable traits such as negligible water absorption (maximum 0.28%) and low density consistent with pure HDPE (maximum 1.266 g/cm^3) that make them suitable for applications involving weight minimization and moisture barrier requirements. These properties highlight a promising application area of the synthesized composites in applications such as soft body armor and structural elements subject to low-speed collisions. For optimizing multi-response performance simultaneously in several physical and mechanical behaviors, Grey Relational Analysis was employed. It enabled converting multi-response data into one Grey Relational Grade (GRG) across every experimental iteration. Through this analysis, it was established that optimum mix ratio should be formed from a composition of 90% plastic material, a mixing time of 15 minutes, and particle size of 125 μm. Optimum overall performance across all tested properties was realized in this particular setup that rendered maximum GRG (0.791) value.

Statistical analyses performed via ANOVA and signal-to-noise (S/N) ratio analysis determined that plastic amount made the largest impact upon flexural strength, supported by a p-value of 0.040, which corroborates a statistically significant influence. Though mixing time and particle size failed to reach statistical significance within experimental parameters, interaction plots and response tables made apparent that these two still influenced mechanical performance. Notably, a particle size between 90–125 μm was found to be most optimal in strength augmentation due to higher surface area-to-volume ratios and better interfacial bond properties.

Overall, this research confirms that termite mound clay is a sustainable and operational reinforcement material for polymer composites provided that it is processed and fabricated optimally. Although some parameters would benefit extension to higher numbers of samples and broader experimental design, this research shows that composites fabricated from recycled HDPE and reinforced with termite mound clay can meet structural and environmental specifications. Optimization of mixing procedure, validation of large production scales' viability, and identification of novel functional applications for this composite system fabricated from biomass should be dealt within subsequent studies

5.2 Recommendations and future work

5.2.1 Recommendations

Based on the experimental results and analysis of this study, the following recommendations are made for the manufacturing and application of termite mound clay-reinforced HDPE composites.

i. To moderate the agglomeration of fine clay particles, it is essential to implement a rigorous drying process for the termite mound clay before mixing. Furthermore, sieving the clay to ensure strict adherence to the desired particle size ranges will improve consistency and composite performance. Pre heating of the clay to appropriate range of temperature is also essential to increase ease of mixing.
ii. Consistency in the mixing process is critical. Manufacturers should invest in high-shear mixers and ensure process parameters (time, temperature, and speed) are tightly controlled to guarantee uniform dispersion of clay particles within the HDPE matrix, thereby minimizing defects and maximizing mechanical strength.

5.2.2 Future Work

This study has established a strong foundation for the development of termite mound clay-reinforced HDPE composites. To build upon these findings and advance the technology towards commercial applications, the following areas are proposed for future research:

a) A more extensive DoE should be conducted, incorporating additional factors such as compatibilizer type/concentration, mixing temperature, and cooling rate utilizing a Central Composite Design or a full factorial design would provide a more robust model for understanding complex interactions and precisely optimizing the formulation.
b) Future work should explore advanced dispersion methods such as twin-screw extrusion, or the use of surfactants/coupling agents to achieve a more homogeneous distribution of clay particles, particularly at the finer size ranges, and to further enhance the interfacial adhesion between the clay and the HDPE matrix.

c) Investigate the effects of environmental aging, including exposure to UV radiation, moisture, and cyclic thermal loading, on the mechanical properties and dimensional stability of the composite.
d) Study the long-term creep resistance and fatigue life of the composite to determine its suitability for structural applications bearing sustained or cyclic loads.
e) A detailed microstructural analysis using Scanning Electron Microscopy (SEM) of fracture surfaces is crucial to visually confirm filler dispersion, identify failure mechanisms (e.g., particle pull-out, matrix cracking), and understand the quality of the matrix-filler interface.
f) Move beyond standardized test specimens to fabricate and test functional prototypes for specific applications, such as protective panels, automotive components, or construction materials. Collaboration with industry partners would be helpful for this stage to ensure the product meets real-world requirements and standards.

REFERENCE

1. Adekayode, F. O., & Ogunkoya, M. O. (n.d.). *Comparative study of clay and organic matter content of termite mounds and the surrounding soils*.
2. Ahmed, A., Chouhan, H., Kartikeya, K., & Bhatnagar, N. (2020). Study on low and high strain rate behaviour of the adhesive bonds for armour application. *The Journal of Adhesion*, *96*(1–4), 345–358. https://doi.org/10.1080/00218464.2019.1696195
3. Aiza Jaafar, C. N., Zainol, I., Izyan Khairani, M. I., & Dele-Afolabi, T. T. (2022). Physical and Mechanical Properties of Tilapia Scale Hydroxyapatite-Filled High-Density Polyethylene Composites. *Polymers*, *14*(2), 251. https://doi.org/10.3390/polym14020251
4. Akinyemi, B. A., Omoniyi, Temidayo. E., & Adeyemo, M. O. (2016). Prospects of Coir Fibre as Reinforcement in Termite Mound Clay Bricks. *Acta Technologica Agriculturae*, *19*(3), 57–62. https://doi.org/10.1515/ata-2016-0013
5. Akter, T., Nur, H. P., Sultana, S., Islam, Md. R., Abedin, Md. J., & Islam, Z. (2018). Evaluation of mechanical properties of both benzoyl peroxide treated and untreated teak sawdust reinforced high density polyethylene composites. *Cellulose*, *25*(2), 1171–1184. https://doi.org/10.1007/s10570-017-1620-3
6. Alexandre, M., & Dubois, P. (2000a). Polymer-layered silicate nanocomposites: Preparation, properties and uses of a new class of materials. *Materials Science and Engineering: R: Reports*, *28*(1–2), 1–63. https://doi.org/10.1016/S0927-796X(00)00012-7
7. Alexandre, M., & Dubois, P. (2000b). Polymer-layered silicate nanocomposites: Preparation, properties and uses of a new class of materials. *Materials Science and Engineering: R: Reports*, *28*(1–2), 1–63. https://doi.org/10.1016/S0927-796X(00)00012-7
8. Alghamdi, A. S. (2018). Synthesis and Mechanical Characterization of High Density Polyethylene/Graphene Nanocomposites. *Engineering, Technology & Applied Science Research*, *8*(2), 2814–2817. https://doi.org/10.48084/etasr.1961
9. Alghamdi, M. N. (2021). Effect of Filler Particle Size on the Recyclability of Fly Ash Filled HDPE Composites. *Polymers*, *13*(16), 2836. https://doi.org/10.3390/polym13162836

10. Alshammari, B. A., Alenad, A. M., Al-Mubaddel, F. S., Alharbi, A. G., Al-shehri, A. S., Albalwi, H. A., Alsuabie, F. M., Fouad, H., & Mourad, A.-H. I. (2022). Impact of Hybrid Fillers on the Properties of High Density Polyethylene Based Composites. *Polymers*, *14*(16), 3427. https://doi.org/10.3390/polym14163427
11. *AMTD_Frontmatter.pdf*. (n.d.).
12. *Astm.d2216.1998*. (n.d.).
13. Bandaru, A. K., Ahmad, S., & Bhatnagar, N. (2017). Ballistic performance of hybrid thermoplastic composite armors reinforced with Kevlar and basalt fabrics. *Composites Part A: Applied Science and Manufacturing*, *97*, 151–165. https://doi.org/10.1016/j.compositesa.2016.12.007
14. Boran, S. (2016). Mechanical, Morphological, and Thermal Properties of Nutshell and Microcrystalline Cellulose Filled High-Density Polyethylene Composites. *BioResources*, *11*(1), 1741–1752. https://doi.org/10.15376/biores.11.1.1741-1752
15. Bourbigot, S., Fontaine, G., Bellayer, S., & Delobel, R. (2008). Processing and nanodispersion: A quantitative approach for polylactide nanocomposite. *Polymer Testing*, *27*(1), 2–10. https://doi.org/10.1016/j.polymertesting.2007.07.008
16. Cadoni, E., Dotta, M., Forni, D., Bianchi, S., & Kaufmann, H. (2012). Strain rate effects on mechanical properties in tension of aluminium alloys used in armour applications. *EPJ Web of Conferences*, *26*, 05004. https://doi.org/10.1051/epjconf/20122605004
17. Callister, W. D., & Rethwisch, D. G. (2020). *Materials Science and Engineering: An Introduction*. Wiley. https://books.google.co.in/books?id=dmoTEQAAQBAJ
18. Cavallaro, P. V. (2011). *Soft Body Armor: An Overview of Materials, Manufacturing, Testing, and Ballistic Impact Dynamics:* Defense Technical Information Center. https://doi.org/10.21236/ADA549097
19. Chakraborty, S., Datta, H. N., & Chakraborty, S. (2023). Grey Relational Analysis-Based Optimization of Machining Processes: A Comprehensive Review. *Process Integration and Optimization for Sustainability*, *7*(4), 609–639. https://doi.org/10.1007/s41660-023-00311-4
20. Claggett, N., Surovek, A., Capehart, W., & Shahbazi, K. (2018). Termite Mounds: Bioinspired Examination of the Role of Material and Environment in Multifunctional

Structural Forms. *Journal of Structural Engineering*, *144*(7), 02518001. https://doi.org/10.1061/(ASCE)ST.1943-541X.0002043

21. Crouch, I. G. (2019). Body armour – New materials, new systems. *Defence Technology*, *15*(3), 241–253. https://doi.org/10.1016/j.dt.2019.02.002
22. D20 Committee. (n.d.). *Test Method for Water Absorption of Plastics*. ASTM International. https://doi.org/10.1520/D0570-22
23. Dan-asabe, B., Yaro, S. A., Yawas, D. S., & Aku, S. Y. (2019). Statistical modeling and optimization of the flexural strength, water absorption and density of a doum palm-Kankara clay filler hybrid composite. *Journal of King Saud University - Engineering Sciences*, *31*(4), 385–394. https://doi.org/10.1016/j.jksues.2017.11.003
24. David, E., Zazoum, B., Frechette, M. F., & Rogti, F. (2015). Dielectric response of HDPE/clay nanocomposites containing 10%wt of organo-modified clay. *2015 IEEE Conference on Electrical Insulation and Dielectric Phenomena (CEIDP)*, 531–534. https://doi.org/10.1109/CEIDP.2015.7352149
25. Dey, T. K., & Tripathi, M. (2010). Thermal properties of silicon powder filled high-density polyethylene composites. *Thermochimica Acta*, *502*(1–2), 35–42. https://doi.org/10.1016/j.tca.2010.02.002
26. Elinwa, A. U. (2018). Strength development of termite mound cement paste and concrete. *Construction and Building Materials*, *184*, 143–150. https://doi.org/10.1016/j.conbuildmat.2018.06.220
27. Erni-Cassola, G., Zadjelovic, V., Gibson, M. I., & Christie-Oleza, J. A. (2019). Distribution of plastic polymer types in the marine environment; A meta-analysis. *Journal of Hazardous Materials*, *369*, 691–698. https://doi.org/10.1016/j.jhazmat.2019.02.067
28. *Espert2004.pdf*. (n.d.).
29. Essabir, H., Boujmal, R., Bensalah, M. O., Rodrigue, D., & Bouhfid, R. (2016). Mechanical and thermal properties of hybrid composites: Oil-palm fiber/clay reinforced high density polyethylene. *Mechanics of Materials*. https://doi.org/10.1016/j.mechmat.2016.04.008
30. Essabir, H., Boujmal, R., Bensalah, M. O., Rodrigue, D., Bouhfid, R., & Qaiss, A. E. K. (2016). Mechanical and thermal properties of hybrid composites: Oil-palm fiber/clay

reinforced high density polyethylene. *Mechanics of Materials*, *98*, 36–43. https://doi.org/10.1016/j.mechmat.2016.04.008

31. Gabr, M. H., Okumura, W., Ueda, H., Kuriyama, W., & Uzawa, K. (2015). Mechanical and thermal properties of carbon fiber / polypropylene composite filled with nano-clay. *COMPOSITES PART B*, *69*, 94–100. https://doi.org/10.1016/j.compositesb.2014.09.033
32. Ganesh, S., Sathiyamurthy, S., Jayabal, S., & Chidambaram, K. (n.d.). Impact Behavior of Termite Mound Particulated Natural Fiber-Polymer Composites. *IOSR Journal of Mechanical and Civil Engineering*.
33. Gill, Y. Q., Jin, J., & Song, M. (2020). Comparative study of carbon-based nanofillers for improving the properties of HDPE for potential applications in food tray packaging. *Polymers and Polymer Composites*, *28*(8–9), 562–571. https://doi.org/10.1177/0967391119892091
34. Grujicic, M., Pandurangan, B., Koudela, K. L., & Cheeseman, B. A. (2006). A computational analysis of the ballistic performance of light-weight hybrid composite armors. *Applied Surface Science*, *253*(2), 730–745. https://doi.org/10.1016/j.apsusc.2006.01.016
35. Guo, Y., Wang, L., Wang, H., Chen, Y., Zhu, S., Chen, T., & Luo, P. (2020). Properties of bamboo flour/high-density polyethylene composites reinforced with ultrahigh molecular weight polyethylene. *Journal of Applied Polymer Science*, *137*(33), 48971. https://doi.org/10.1002/app.48971
36. Han, G., Lei, Y., Wu, Q., Kojima, Y., & Suzuki, S. (2008a). Bamboo–Fiber Filled High Density Polyethylene Composites: Effect of Coupling Treatment and Nanoclay. *Journal of Polymers and the Environment*, *16*(2), 123–130. https://doi.org/10.1007/s10924-008-0094-7
37. Han, G., Lei, Y., Wu, Q., Kojima, Y., & Suzuki, S. (2008b). Bamboo–Fiber Filled High Density Polyethylene Composites: Effect of Coupling Treatment and Nanoclay. *Journal of Polymers and the Environment*, *16*(2), 123–130. https://doi.org/10.1007/s10924-008-0094-7
38. Han, G., Lei, Y., Wu, Q., Kojima, Y., & Suzuki, S. (2008c). Bamboo–Fiber Filled High Density Polyethylene Composites: Effect of Coupling Treatment and Nanoclay. *Journal of*

Polymers and the Environment, *16*(2), 123–130. https://doi.org/10.1007/s10924-008-0094-7

39. Hani, A. R. A., Roslan, A., Mariatti, J., & Maziah, M. (2012). Body Armor Technology: A Review of Materials, Construction Techniques and Enhancement of Ballistic Energy Absorption. *Advanced Materials Research*, *488–489*, 806–812. https://doi.org/10.4028/www.scientific.net/AMR.488-489.806
40. Hao, X., Zhou, H., Mu, B., Chen, L., Guo, Q., Yi, X., Sun, L., Wang, Q., & Ou, R. (2020). Effects of fiber geometry and orientation distribution on the anisotropy of mechanical properties, creep behavior, and thermal expansion of natural fiber/HDPE composites. *Composites Part B: Engineering*, *185*, 107778. https://doi.org/10.1016/j.compositesb.2020.107778
41. Hein, P. R. G., & Brancheriau, L. (2018). Comparison between three-point and four-point flexural tests to determine wood strength of Eucalyptus specimens. *Maderas. Ciencia y Tecnología*, (ahead), 0–0. https://doi.org/10.4067/S0718-221X2018005003401
42. Hopewell, J., Dvorak, R., & Kosior, E. (2009). Plastics recycling: Challenges and opportunities. *Philosophical Transactions of the Royal Society B: Biological Sciences*, *364*(1526), 2115–2126. https://doi.org/10.1098/rstb.2008.0311
43. Hufenbach, W., Gude, M., Ebert, C., Zscheyge, M., & Hornig, A. (2011). Strain rate dependent low velocity impact response of layerwise 3D-reinforced composite structures. *International Journal of Impact Engineering*, *38*(5), 358–368. https://doi.org/10.1016/j.ijimpeng.2010.12.004
44. Ilinsky, A. G., Maslov, V. V., Nozenko, V. K., & Brovko, A. P. (n.d.). *On determination of volume fraction of crystalline phase in partially crystallized amorphous and nanocrystalline materials*.
45. Jacob, G. C., Starbuck, J. M., Fellers, J. F., Simunovic, S., & Boeman, R. G. (2004). Strain rate effects on the mechanical properties of polymer composite materials. *Journal of Applied Polymer Science*, *94*(1), 296–301. https://doi.org/10.1002/app.20901
46. Jayabal, S., & Bharathiraja, G. (2016). Statistical Analysis and Particle Swarm Based Optimization of Mechanical Properties of Rice Husk and Termite Mound Soil Impregnated

Coir–Polyester Composites. *Transactions of the Indian Institute of Metals*, *69*(4), 925–934. https://doi.org/10.1007/s12666-015-0582-0

47. Jo, C., & Naguib, H. E. (2008). Modeling the Effect of Strain Rate on the Mechanical Properties of HDPE/Clay Nanocomposite Foams. *Polymers and Polymer Composites*, *16*(8), 561–575. https://doi.org/10.1177/096739110801600810
48. Jollands, M., & Gupta, R. K. (2010). Effect of mixing conditions on mechanical properties of polylactide/montmorillonite clay nanocomposites. *Journal of Applied Polymer Science*, *118*(3), 1489–1493. https://doi.org/10.1002/app.32475
49. Jouquet, P., Tessier, D., & Lepage, M. (2004). The soil structural stability of termite nests: Role of clays in Macrotermes bellicosus (Isoptera, Macrotermitinae) mound soils. *European Journal of Soil Biology*, *40*(1), 23–29. https://doi.org/10.1016/j.ejsobi.2004.01.006
50. Jung, A., Pullen, A. D., & Proud, W. G. (2016). Strain-rate effects in Ni/Al composite metal foams from quasi-static to low-velocity impact behaviour. *Composites Part A: Applied Science and Manufacturing*, *85*, 1–11. https://doi.org/10.1016/j.compositesa.2016.02.031
51. Kanagaraj, S., Varanda, F. R., Zhil'tsova, T. V., Oliveira, M. S. A., & Simões, J. A. O. (2007). Mechanical properties of high density polyethylene/carbon nanotube composites. *Composites Science and Technology*, *67*(15–16), 3071–3077. https://doi.org/10.1016/j.compscitech.2007.04.024
52. Karmarkar, S., & Shashidhara, G. M. (2018). Thermal decomposition kinetics of jute fiber filled HDPE composites. *Journal of the Indian Academy of Wood Science*, *15*(1), 33–40. https://doi.org/10.1007/s13196-018-0205-6
53. Kaw, A. K., & Group, F. (2006). *Composite*.
54. Kiliç, E., Oliver-Ortega, H., Tarrés, Q., Delgado-Aguilar, M., Fullana-i-Palmer, P., & Puig, R. (2021). Valorization Strategy for Leather Waste as Filler for High-Density Polyethylene Composites: Analysis of the Thermal Stability, Insulation Properties and Chromium Leaching. *Polymers*, *13*(19), 3313. https://doi.org/10.3390/polym13193313

55. Kiliç, E., Tarrés, Q., Delgado-Aguilar, M., Espinach, X., Fullana-i-Palmer, P., & Puig, R. (2020). Leather Waste to Enhance Mechanical Performance of High-Density Polyethylene. *Polymers*, *12*(9), 2016. https://doi.org/10.3390/polym12092016
56. Kusuktham, B., & Teeranachaideekul, P. (2015). *Mechanical Properties of High Density Polyethylene / Modified Calcium Silicate Mechanical Properties of High Density Polyethylene / Modified Calcium Silicate Composites*. (July 2014). https://doi.org/10.1007/s12633-014-9204-4
57. Lee, Y. H., Park, C. B., Sain, M., Kontopoulou, M., & Zheng, W. (2007). Effects of clay dispersion and content on the rheological, mechanical properties, and flame retardance of HDPE/clay nanocomposites. *Journal of Applied Polymer Science*, *105*(4), 1993–1999. https://doi.org/10.1002/app.26403
58. Lei, Y., Wu, Q., Clemons, C. M., Yao, F., & Xu, Y. (2007). *Influence of Nanoclay on Properties of HDPE / Wood Composites*. https://doi.org/10.1002/app
59. Li, G., & Liu, D. (2015). Low Strain Rate Testing Based on Drop Weight Impact Tester. *Experimental Techniques*, *39*(5), 30–35. https://doi.org/10.1111/j.1747-1567.2012.00862.x
60. Mesbah, A., Zaïri, F., Naït-Abdelaziz, M., Gloaguen, J. M., Anoukou, K., Zaoui, A., Qu, Z., Boukharouba, T., & Lefebvre, J. M. (2014). Micromechanics-based constitutive modeling of plastic yielding and damage mechanisms in polymer–clay nanocomposites: Application to polyamide-6 and polypropylene-based nanocomposites. *Composites Science and Technology*, *101*, 71–78. https://doi.org/10.1016/j.compscitech.2014.05.032
61. Millogo, Y., Hajjaji, M., & Morel, J. C. (2011a). Physical properties, microstructure and mineralogy of termite mound material considered as construction materials. *Applied Clay Science*, *52*(1–2), 160–164. https://doi.org/10.1016/j.clay.2011.02.016
62. Millogo, Y., Hajjaji, M., & Morel, J. C. (2011b). Physical properties, microstructure and mineralogy of termite mound material considered as construction materials. *Applied Clay Science*, *52*(1–2), 160–164. https://doi.org/10.1016/j.clay.2011.02.016
63. Mokarizadeh Haghighi Shirazi, M., Khajouei-Nezhad, M., Zebarjad, S. M., & Ebrahimi, R. (2020). Evolution of the crystalline and amorphous phases of high-density polyethylene

subjected to equal-channel angular pressing. *Polymer Bulletin*, *77*(4), 1681–1694. https://doi.org/10.1007/s00289-019-02827-7

64. Mujinya, B. B., Mees, F., Erens, H., Dumon, M., Baert, G., Boeckx, P., Ngongo, M., & Van Ranst, E. (2013). Clay composition and properties in termite mounds of the Lubumbashi area, D.R. Congo. *Geoderma*, *192*, 304–315. https://doi.org/10.1016/j.geoderma.2012.08.010
65. Ngo, T.-D. (2020). Introduction to Composite Materials. In T.-D. Ngo (Ed.), *Composite and Nanocomposite Materials—From Knowledge to Industrial Applications*. IntechOpen. https://doi.org/10.5772/intechopen.91285
66. Ortiz, A. V., Teixeira, J. G., Gomes, M. G., Oliveira, R. R., Díaz, F. R. V., & Moura, E. A. B. (2014). Preparation and characterization of electron-beam treated HDPE composites reinforced with rice husk ash and Brazilian clay. *Applied Surface Science*, *310*, 331–335. https://doi.org/10.1016/j.apsusc.2014.03.075
67. Ou, R., Zhao, H., Sui, S., Song, Y., & Wang, Q. (2010). Reinforcing effects of Kevlar fiber on the mechanical properties of wood-flour/high-density-polyethylene composites. *Composites Part A: Applied Science and Manufacturing*, *41*(9), 1272–1278. https://doi.org/10.1016/j.compositesa.2010.05.011
68. Pan, B., Ning, N., Liu, J., Bai, L., & Fu, Q. (2009a). MECHANICAL PROPERTIES OF SMC WHISKER REINFORCED HIGH DENSITY POLYETHYLENE COMPOSITES. *Chinese Journal of Polymer Science*, *27*(02), 267. https://doi.org/10.1142/S0256767909003893
69. Pan, B., Ning, N., Liu, J., Bai, L., & Fu, Q. (2009b). MECHANICAL PROPERTIES OF SMC WHISKER REINFORCED HIGH DENSITY POLYETHYLENE COMPOSITES. *Chinese Journal of Polymer Science*, *27*(02), 267. https://doi.org/10.1142/S0256767909003893
70. Panthapulakkal, S., & Sain, M. (2007a). Agro-residue reinforced high-density polyethylene composites: Fiber characterization and analysis of composite properties. *Composites Part A: Applied Science and Manufacturing*, *38*(6), 1445–1454. https://doi.org/10.1016/j.compositesa.2007.01.015

71. Panthapulakkal, S., & Sain, M. (2007b). Agro-residue reinforced high-density polyethylene composites: Fiber characterization and analysis of composite properties. *Composites Part A: Applied Science and Manufacturing*, *38*(6), 1445–1454. https://doi.org/10.1016/j.compositesa.2007.01.015
72. Pickering, K. L., Efendy, M. G. A., & Le, T. M. (2016). A review of recent developments in natural fibre composites and their mechanical performance. *Composites Part A: Applied Science and Manufacturing*, *83*, 98–112. https://doi.org/10.1016/j.compositesa.2015.08.038
73. Polychronopoulos, N. D., & Vlachopoulos, J. (2019). Polymer Processing and Rheology. In Md. I. H. Mondal (Ed.), *Cellulose-Based Superabsorbent Hydrogels* (pp. 1–47). Springer International Publishing. https://doi.org/10.1007/978-3-319-92067-2_4-1
74. Prabowo, S., Ujianto, O., Wijaya, R., & Priyani, D. A. (2024). Effect of Clay, Mixing Speed, and Time on Mechanical Properties of Glass Fiber/Clay Reinforced Unsaturated Polyester Prepared by Vacuum Bag Technique. *Journal of The Institution of Engineers (India): Series D*, *105*(2), 923–928. https://doi.org/10.1007/s40033-023-00505-7
75. Ragaert, K., Delva, L., & Van Geem, K. (2017). Mechanical and chemical recycling of solid plastic waste. *Waste Management*, *69*, 24–58. https://doi.org/10.1016/j.wasman.2017.07.044
76. Rasib, S. Z. M., Mariatti, M., & Atay, H. Y. (2021). Effect of waste fillers addition on properties of high-density polyethylene composites: Mechanical properties, burning rate, and water absorption. *Polymer Bulletin*, *78*(12), 6777–6795. https://doi.org/10.1007/s00289-020-03454-3
77. Sadik, W. A., El-Demerdash, A.-G. M., Abokhateeb, A. E. A., & Elessawy, N. A. (2021). Innovative high-density polyethylene/waste glass powder composite with remarkable mechanical, thermal and recyclable properties for technical applications. *Heliyon*, *7*(4), e06627. https://doi.org/10.1016/j.heliyon.2021.e06627
78. Saeed, U., Al-Turaif, H., & Siddiqui, M. E. (2021). Stress relaxation performance of glass fiber-reinforced high-density polyethylene composite. *Polymers and Polymer Composites*, *29*(6), 705–713. https://doi.org/10.1177/0967391120932062

79. Shaari, N. Z. K., Rahman, N. A., Taha, A. R., Alauddin, S. M., & Akhbar, S. (2021). Enhancement of strength and flexibility of high-density polyethylene using rubber leaves. *IOP Conference Series: Materials Science and Engineering*, *1053*(1), 012029. https://doi.org/10.1088/1757-899X/1053/1/012029
80. Shebani, A., Elhrari, W., Klash, A., Aswei, A., Omran, K., & Rhab, A. (2016). *Effects of Libyan Kaolin Clay on the Impact Strength Properties of High Effects of Libyan Kaolin Clay on the Impact Strength Properties of High Density Polyethylene / Clay Nanocomposites*. (September). https://doi.org/10.5923/j.cmaterials.20160605.02
81. Sinha Ray, S., & Okamoto, M. (2003a). Polymer/layered silicate nanocomposites: A review from preparation to processing. *Progress in Polymer Science*, *28*(11), 1539–1641. https://doi.org/10.1016/j.progpolymsci.2003.08.002
82. Sinha Ray, S., & Okamoto, M. (2003b). Polymer/layered silicate nanocomposites: A review from preparation to processing. *Progress in Polymer Science*, *28*(11), 1539–1641. https://doi.org/10.1016/j.progpolymsci.2003.08.002
83. Sultana, R., Akter, R., & Alam, Z. (2013). *Preparation and Characterization of Sand Reinforced Polyester Composites*. (02).
84. Tanniru, M., Yuan, Q., & Misra, R. D. K. (2006). *On significant retention of impact strength in clay – reinforced high-density polyethylene (HDPE) nanocomposites*. *47*, 2133–2146. https://doi.org/10.1016/j.polymer.2006.01.063
85. Treesh, A. A., Elhrari, W., & Etmimi, H. (2023). *High-Density Polyethylene/Kaolin Clay Composites: Optimiztion of The Injec- tion Moulding Process Parameters Towards Minimum Shrinkage and Warpage*.
86. Wang, W., Ciselli, P., Kuznetsov, E., Peijs, T., & Barber, A. H. (2008). Effective reinforcement in carbon nanotube–polymer composites. *Philosophical Transactions of the Royal Society A: Mathematical, Physical and Engineering Sciences*, *366*(1870), 1613–1626. https://doi.org/10.1098/rsta.2007.2175
87. Wang, Z., Liu, Y., Liu, C., Yang, J., & Li, L. (2019). Understanding structure-mechanics relationship of high density polyethylene based on stress induced lattice distortion. *Polymer*, *160*, 170–180. https://doi.org/10.1016/j.polymer.2018.11.054

88. Wu, F., He, X., Zeng, Y., & Cheng, H.-M. (2006). Thermal transport enhancement of multi-walled carbon nanotubes/ high-density polyethylene composites. *Applied Physics A*, *85*(1), 25–28. https://doi.org/10.1007/s00339-006-3649-2
89. Xie, Y., Hill, C. A. S., Xiao, Z., Militz, H., & Mai, C. (2010). Silane coupling agents used for natural fiber/polymer composites: A review. *Composites Part A: Applied Science and Manufacturing*, *41*(7), 806–819. https://doi.org/10.1016/j.compositesa.2010.03.005
90. Xuen, F. Y., Hoe, K. W., & Munusamy, Y. (2021). Mechanical Performance of High-Density Polyethylene (HDPE) Composites Containing Quarry Dust Filler. *IOP Conference Series: Earth and Environmental Science*, *945*(1), 012075. https://doi.org/10.1088/1755-1315/945/1/012075
91. Yigit, A. S., & Christoforou, A. P. (2007). *Limits of asymptotic solutions in low-velocity impact of composite plates*. *81*, 568–574. https://doi.org/10.1016/j.compstruct.2006.10.006
92. Young, R. J. (n.d.). *Introduction to Polymers: Third Edition*.
93. Yuan, Q., & Misra, R. D. K. (2006). *Impact fracture behavior of clay – reinforced polypropylene nanocomposites*. *47*, 4421–4433. https://doi.org/10.1016/j.polymer.2006.03.105
94. Zeng, Q. H., Yu, A. B., Lu, G. Q. (Max), & Paul, D. R. (2005). Clay-Based Polymer Nanocomposites: Research and Commercial Development. *Journal of Nanoscience and Nanotechnology*, *5*(10), 1574–1592. https://doi.org/10.1166/jnn.2005.411
95. Zhang, Q., Cai, H., Ren, X., Kong, L., Liu, J., & Jiang, X. (2017). The Dynamic Mechanical Analysis of Highly Filled Rice Husk Biochar/High-Density Polyethylene Composites. *Polymers*, *9*(11), 628. https://doi.org/10.3390/polym9110628
96. Zhang, Q., Khan, M. U., Lin, X., Cai, H., & Lei, H. (2019). Temperature varied biochar as a reinforcing filler for high-density polyethylene composites. *Composites Part B: Engineering*, *175*, 107151. https://doi.org/10.1016/j.compositesb.2019.107151
97. Zheng, W., Lu, X., & Wong, S. (2003). *Electrical and Mechanical Properties of Expanded Graphite-Reinforced High-Density Polyethylene*.

APPENDEX

Delta Values of each property

Statistics

Variable	N	N*	Mean	SE Mean	StDev	Minimum	Q1	Median	Q3	Maximum
Delta_Den	9	0	0.347	0.106	0.318	0.000	0.091	0.269	0.556	1.000

Statistics

Variable	N	N*	Mean	SE Mean	StDev	Minimum	Q1	Median	Q3	Maximum
Delata_Water Ab	9	0	0.328	0.105	0.315	0.000	0.114	0.182	0.500	1.000

Statistics

Variable	N	N*	Mean	SE Mean	StDev	Minimum	Q1	Median	Q3	Maximum
Delata_Tensile	9	0	0.4022	0.0948	0.2843	0.0000	0.2100	0.3997	0.5202	1.0000

Statistics

Variable	N	N*	Mean	SE Mean	StDev	Minimum	Q1	Median	Q3	Maximum
Delata_Flexural	9	0	0.5466	0.0978	0.2935	0.0000	0.3447	0.5963	0.7360	1.0000

Statistics

Variable	N	N*	Mean	SE Mean	StDev	Minimum	Q1	Median	Q3	Maximum
Delata_Impact	9	0	0.5598	0.0989	0.2968	0.0000	0.4335	0.5255	0.7836	1.0000

Regression Equations for each Property

Regression Equation

Density = 1.276 + 0.00057 Plastic Amount - 0.00285 Mixing Time
- 0.00164 Particle Size

Regression Equation

percentage water = 0.223 - 0.00083 Plastic Amount
Absorption - 0.00500 Mixing Time
+ 0.000416 Particle Size

Regression Equation

Tensile = 14.1 + 0.116 Plastic Amount + 0.092 Mixing Time
- 0.0619 Particle Size

Regression Equation

Flexural = -85.4 + 1.598 Plastic Amount + 0.117 Mixing Time
+ 0.128 Particle Size

Regression Equation

Impact = 1.78 + 0.0945 Plastic Amount + 0.0518 Mixing Time
+ 0.0159 Particle Size

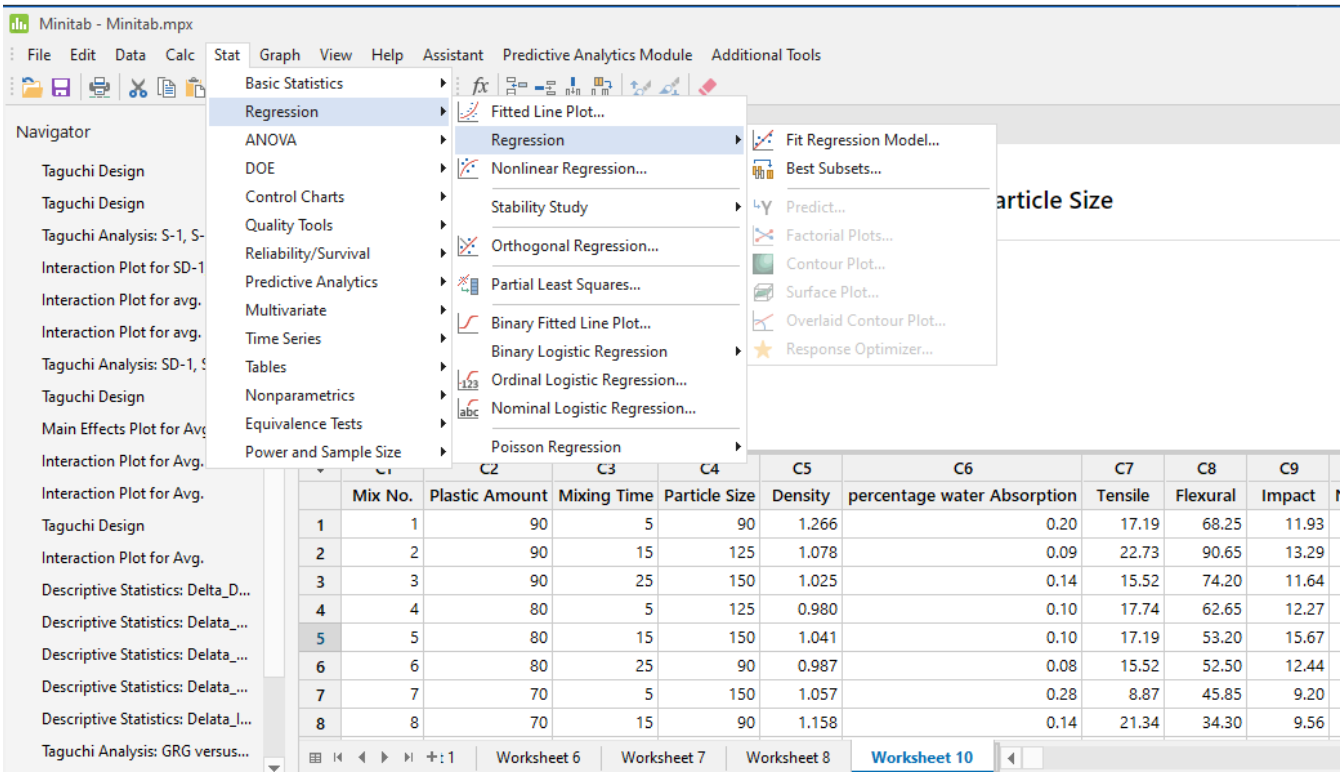

	C1	C2	C3	C4	C5	C6	C7	C8	C9
	Mix No.	Plastic Amount	Mixing Time	Particle Size	Density	percentage water Absorption	Tensile	Flexural	Impact
1	1	90	5	90	1.266	0.20	17.19	68.25	11.93
2	2	90	15	125	1.078	0.09	22.73	90.65	13.29
3	3	90	25	150	1.025	0.14	15.52	74.20	11.64
4	4	80	5	125	0.980	0.10	17.74	62.65	12.27
5	5	80	15	150	1.041	0.10	17.19	53.20	15.67
6	6	80	25	90	0.987	0.08	15.52	52.50	12.44
7	7	70	5	150	1.057	0.28	8.87	45.85	9.20
8	8	70	15	90	1.158	0.14	21.34	34.30	9.56

Figure 37 : Procedure for obtaining regression equation

Multiple Response Prediction

Variable	Setting
Plastic Amount	90
Mixing Time	7.0202
Particle Size	150

Response	Fit	SE Fit	95% CI	95% PI
Impact	13.03	1.50	(9.18, 16.88)	(6.49, 19.57)

Flexural	78.54	7.69	(58.77, 98.32)	(44.97, 112.11)
Tensile	15.82	3.10	(7.86, 23.78)	(2.31, 29.33)
percentage water Absorption	0.1756	0.0483	(0.0513, 0.2998)	(-0.0354, 0.3865)
Density	1.0611	0.0701	(0.8808, 1.2413)	(0.7550, 1.3671)

Response Optimization

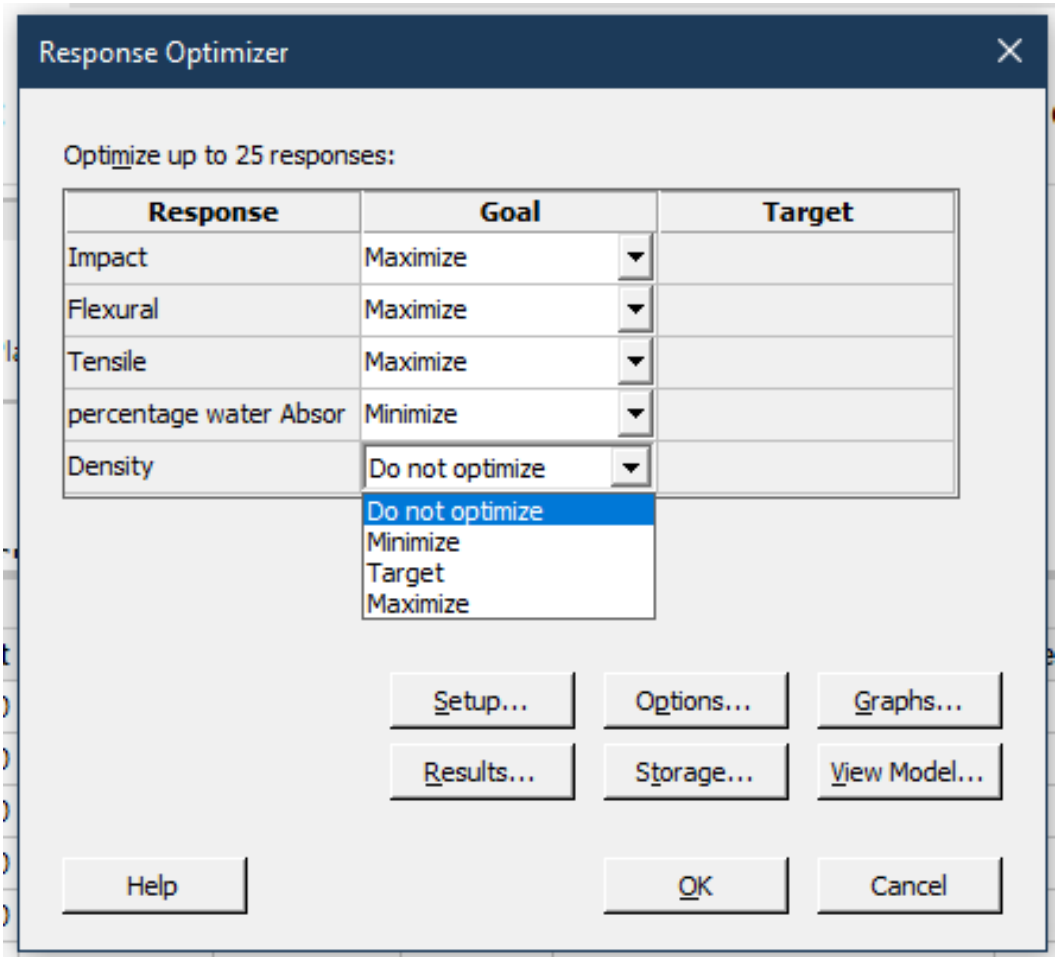

Figure 38 : Optimization goal of property

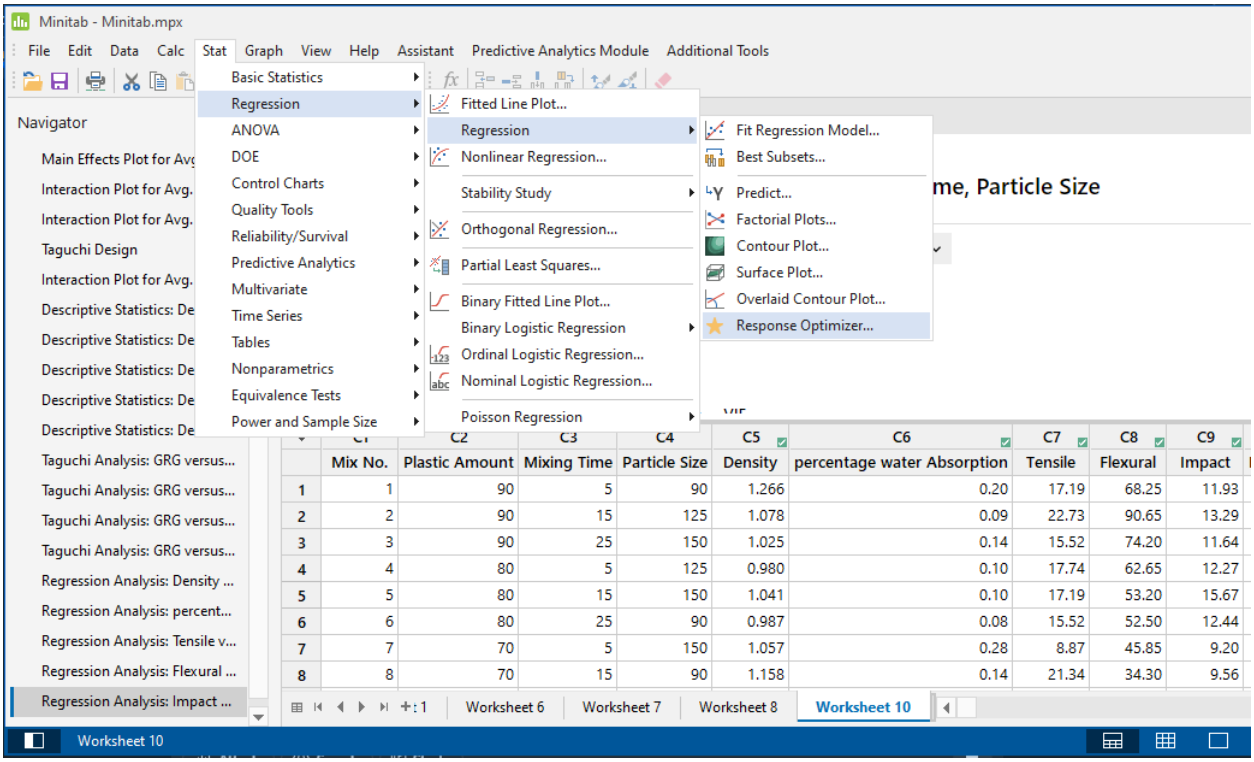

	C1	C2	C3	C4	C5	C6	C7	C8	C9
	Mix No.	Plastic Amount	Mixing Time	Particle Size	Density	percentage water Absorption	Tensile	Flexural	Impact
1	1	90	5	90	1.266	0.20	17.19	68.25	11.93
2	2	90	15	125	1.078	0.09	22.73	90.65	13.29
3	3	90	25	150	1.025	0.14	15.52	74.20	11.64
4	4	80	5	125	0.980	0.10	17.74	62.65	12.27
5	5	80	15	150	1.041	0.10	17.19	53.20	15.67
6	6	80	25	90	0.987	0.08	15.52	52.50	12.44
7	7	70	5	150	1.057	0.28	8.87	45.85	9.20
8	8	70	15	90	1.158	0.14	21.34	34.30	9.56

Figure 39 : Input values and procedure for response optimization

Response Optimization: Impact, Flexural, Tensile, percentage water Absorption, Density

Parameters

Response	Goal	Lower	Target	Upper	Weight	Importance
Impact	Maximum	9.20	15.67		1	1
Flexural	Maximum	34.30	90.65		1	1
Tensile	Maximum	8.87	22.73		1	1
percentage water Absorption	Target	0.06	0.30	0.330	1	1
Density	Minimum		0.98	1.266	1	1

Starting Values

Variable	Setting
Plastic Amount	70
Mixing Time	5
Particle Size	90

Solution

Solution	Plastic Amount	Mixing Time	Particle Size	Impact Fit	Flexural Fit	Tensile Fit	percentage water Absorption Fit	Density Fit
1	90	7.02020	150	13.0295	78.5415	15.8187	0.175572	1.06106

Solution	Composite Desirability
1	0.604010

Multiple Response Prediction

Variable	Setting
Plastic Amount	90
Mixing Time	7.0202

Particle Size	150

Response	Fit	SE Fit	95% CI	95% PI
Impact	13.03	1.50	(9.18, 16.88)	(6.49, 19.57)
Flexural	78.54	7.69	(58.77, 98.32)	(44.97, 112.11)
Tensile	15.82	3.10	(7.86, 23.78)	(2.31, 29.33)
percentage water Absorption	0.1756	0.0483	(0.0513, 0.2998)	(-0.0354, 0.3865)
Density	1.0611	0.0701	(0.8808, 1.2413)	(0.7550, 1.3671)